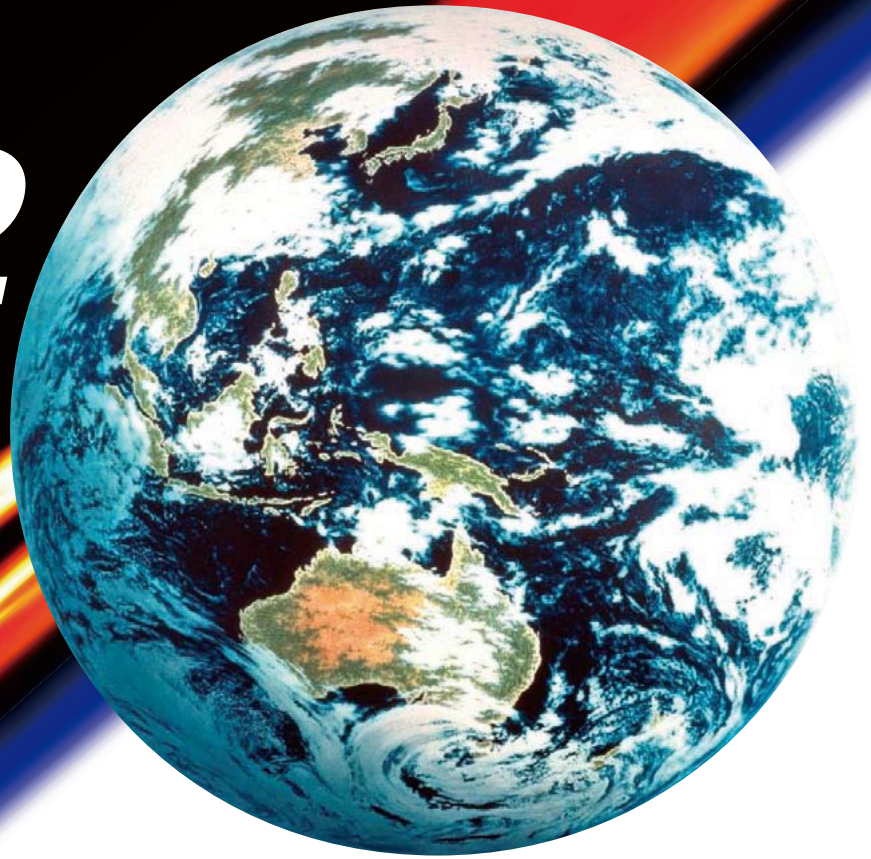


**EORC Bulletin**

ISSN 1349-113X  
JAXA-SP-09-017E

*Annual Report*  
**2008**  
**No.12**  
*March 2009*



**JAXA** **EORC**

## CONTENTS

Foreword	iii
1. OUTLINE OF THE EARTH OBSERVATION RESEARCH CENTER (EORC)	
1.1 Objectives	1-1
1.2 Organization	1-2
1.3 Science Projects	1-4
1.4 Individual Research Activities	1-4
2. RESEARCH ACTIVITIES	
2.1 Research Programs and Projects	2-1
2.1.1 ALOS	2-1
2.1.2 TRMM and GPM	2-25
2.1.3 EarthCARE/CPR	2-30
2.1.4 GCOM	2-31
2.1.5 GOSAT	2-42
2.2 Cross-Cutting / interdisciplinary science	2-49
2.2.1 The Water Cycle Research Group	2-49
2.2.2 Ecology Research Group	2-55
2.2.3 Disaster Research Group	2-61
3. RESEARCH AND DEVELOPMENT ON INSTRUMENTATION	
3.1 Overview	3-1
3.2 Large-diameter Mirror	3-1
3.2.1 Manufacturing Components of All C/SiC Optics Models	3-2
3.2.2 Preparation for Large-scale Optics Test	3-2
3.2.3 Low Temperature Test for Main Mirror	3-4
3.2.4 Stitching Test Method	3-4
3.3 Geostationary Meteorology and Atmospheric Chemistry Mission	3-6
3.3.1 Mission	3-6
3.3.2 Target of Measurement	3-7
3.3.3 Sensor Specification	3-7
3.3.4 IR Sensor Overview	3-8
3.4 Compact Infrared Camera (CIRC) for Earth Observation	3-9
3.4.1 The Compact Infrared Camera (CIRC)	3-9
3.4.2 Feasibility Study of Wildfire Detection	3-10
3.5 Calibration of Optical Sensors	3-12
3.5.1 Introduction	3-12
3.5.2 Calibration System	3-12
3.5.3 Gold-coated Integrating Sphere	3-14

---

4. DEVELOPMENT ON GROUND SYSTEMS	
4.1 Overview	4-1
4.2 GPM Mission Operation System	4-1
4.3 GCOM Mission Operation System	4-2
4.3.1 Status of the GCOM-W1 Mission Operation System	4-2
4.3.2 Status of the GCOM-C1 Mission Operation System	4-3
4.4 EarthCARE Mission Operation System	4-4
4.5 GOSAT Mission Operation System	4-4
4.5.1 System Overview	4-4
4.5.2 MOS Preparation for GOSAT Launch	4-6
4.5.3 GOSAT Initial Checkout Operation and the MOS Evaluation in Initial Operation	4-6
4.5.4 Products Release plan	4-7
4.6 Research and Development for Data Utilization	4-7
5. GROUND SYSTEM OF OPERATIONS	
5.1 The EOC (Earth Observation Center)	5-1
5.1.1 History and Current Operations	5-1
5.1.2 System Overview	5-12
5.2 Data Analysis System	5-14
5.2.1 History and Current Operations	5-14
5.2.2 System Overview	5-16
6. DATA OF EORC ACTIVITIES	
6.1 Publicity	6-1
6.2 Data Delivery Statistics	6-2
6.3 International Collaboration	6-3
6.3.1 International Meetings	6-3
6.3.2 International Collaboration Research	6-3
6.3.3 Foreign Guest Researchers	6-3
6.3.4 International Arctic Research Center (IARC)	6-3
6.3.5 Space Applications For Environment (SAFE)	6-4
6.4 Affiliated Graduate School	6-6
6.5 List of Scientific Contributions (January-December 2008)	6-7
6.5.1 Journal Articles	6-7
6.5.2 Conference Proceedings	6-7
6.5.3 Oral Presentations	6-9
6.6 Budget and Personnel	6-12
6.6.1 Budget	6-12
6.6.2 Number of Personnel	6-12
6.7 History of EORC	6-13
6.8 Acronyms and Abbreviations	6-22

### *Foreword*

The Earth Observation Research Center (EORC) at the Japan Aerospace Exploration Agency (JAXA) provides the following services:

- (1) Earth-observing satellite data acquisition, processing, preservation, and provision
- (2) Development of ground systems for Earth-observing satellite data
- (3) Development of algorithms to calibrate and validate satellite data
- (4) Research and development of satellite data application
- (5) Research on sensors for Earth observation missions in the future

JAXA started its Earth Observation Program in 1978. The Earth Observation Center (EOC) was established in the same year to receive and process U.S. Landsat satellites data. The Marine Observation Satellite, “MoMo 1” (MOS-1), Japan’s first Earth observation satellite, was put into operation in 1987. Since then, the EOC has been conducting all tasks including data acquisition, processing, preservation, and provision for all JAXA’s Earth observation satellites and directly received foreign satellites data.

In its early stages, the EOC was considered a factory for performing data processing based on established algorithms, creating standard processing data, and providing data to users. However, with the appearance of satellites, such as MOS-1 and the Japanese Earth Resources Satellite, “Fuyo 1” (JERS-1), the importance of calibration and validation of sensor data, which determines the algorithms of processing and data quality became better recognized. In addition, the Advanced Earth Observation Satellite (ADEOS), “Midori”, a new generation project, was created with achieving significant scientific and physical outcomes as its main objective.

Close cooperation with the scientific community is essential in developing leading algorithms and JAXA was determined to improve its research ability. This led to the founding of the EORC, a research center that conducts calibration/validation, research, acquisition, processing, data archiving, and distribution of data. The EOC was integrated as a division of the EORC.

The EORC has since conducted a variety of tasks. Its most fundamental tasks are calibrating/validating data for quality assurance and developing useful information for multiple users. Moreover, the final purpose of our research is to contribute to society. The EORC promotes crosscutting research of satellite data in the fields of meteorology, forestry and fisheries resources, and disaster prevention, among others, by bringing together satellite/sensor research teams.

We hope this document gives you an idea of the various strategic activities that the EORC performs.

Autumn 2009

Toru Fukuda, EORC Director  
Katumi Musiake, Technical Counselor



***1. OUTLINE OF THE  
EARTH OBSERVATION  
RESEARCH CENTER (EORC)***

## 1. OUTLINE OF THE EARTH OBSERVATION RESEARCH CENTER (EORC)

### 1.1 Objectives

The Earth Observation Research Center (EORC) has been developing continuously as the core organization covering the full spectrum of Earth-observation activities in JAXA, i.e., mission planning, R&D of sensors, algorithms, calibration, validation, data products, ground segments, operations of mission data handling, research coordination, promotion of applications, support of administrative and strategic matters, and so on. At EORC, we analyze observation data acquired by Earth-observation satellites, develop algorithms to derive geophysical parameters and to calibrate and validate satellite data, and try to maintain the quality of the data. We also promote research and application of satellite data in the fields of meteorology, control of forestry and fisheries resources, disaster prevention and national land use, and global environmental changes. To conduct these activities smoothly, we employ new Earth-observation instruments, and develop and operate the ground system for Earth-observation satellite data. As part of this task, we operate the Earth Observation Center (EOC) to receive, process, and distribute satellite data.

EORC was founded to conduct Earth-observation satellite data acquisition, processing, and research in April 1995, and has three major goals of data utilization: climate change, disaster monitoring, and resource management. After the October 2003 integration of three space institutions in Japan, NASDA, ISAS, and NAL, all Earth-observation projects were defined as enterprises of the Office of Space Applications (OSA). In 2006, EORC (formerly the Earth Observation Research and application Center) was divided in two centers. One is the Earth Observation Research Center (EORC), which is the core for analysis and research of Earth-observation satellite data. The other is the Satellite Applications and Promotion Center (SAPC), which is responsible for promoting satellite data and products. The new EORC moved from Tokyo to Tsukuba Space Center in 2006 and has since started to communicate with institutions and agencies in Tsukuba.

The biggest event for us in FY 2008 was the successful launch of “Tbuki” (GOSAT: Greenhouse Gases Observing Satellite) on January 23, 2009. GOSAT is a satellite that observes the concentration distribution of greenhouse gases from space, and its purpose is to contribute to the international effort toward prevention of global warming, including monitoring the greenhouse gas absorption and emission state. The initial checkout of the instruments confirmed they are functioning properly and the instrument will proceed to routine operation.

The global climate and environment changes in recent years are of great concern and even threaten the continuation of the Earth system. Global change may even menace people's daily lives by generating frequent storms and flood damage, such as mighty typhoons. The Global Earth Observation System of Systems (GEOSS), a cooperative project for international Earth observation, was started in 2006 to cope with such changes. In concert with these international activities, the Earth Observation and Ocean Exploration System, including Earth-observation satellite systems, was selected as a national key technology by the Council for Science and Technology Policy (CSTP) in March 2006.

JAXA has been establishing Earth-observation systems to contribute to Earth observation and ocean exploration systems and GEOSS. “Daichi” (ALOS) and “Ibuki” (GOSAT) participate in the system together with the ongoing TRMM and AMSR-E programs. GCOM-W, the successor of ADEOS-II and AMSR-E aboard EOS-Aqua, and the Dual-frequency Precipitation Radar (DPR) on board the GPM core satellite are now in phase C/D and are expected to participate in the system. In addition, GCOM-C as the successor of ADEOS-II, the Cloud Profiling Radar (CPR) aboard EarthCARE, and ALOS-2/3 as successors of ALOS are now in phase A/B.

As Japan's core organization for Earth observation, EORC contributes to building a safe and secure society through the development of these satellite systems.

## **1.2 Organization**

EORC is a center for research related to Earth-observation satellite data and is a department of the Space Applications Mission Directorate of JAXA. Mr. Toru Fukuda, Director of EORC, is in charge of all organizational activities and reports to the Executive Director of the Space Applications Mission Directorate, Dr. Yasushi Horikawa, and Deputy Executive Director, Dr. Masanori Homma. Prof. Katumi Mushiake is leading research activities as Technical Counselor.

Research activities are conducted in a matrix organization, i.e., researchers of atmosphere, ocean, and land disciplines work on their own research themes, such as disaster monitoring, water cycle, eco-system, and global warming, as well as working on satellite projects. Senior Researchers lead their scientist groups, and Project Coordinators manage the projects. The System and Information group supports development and operations of computers and network systems. This group also develops and operates ground systems in EOC. The Instrumentation group conducts research on future spaceborne sensors. The Planning and Coordination group coordinates and supports all activities from the management side.

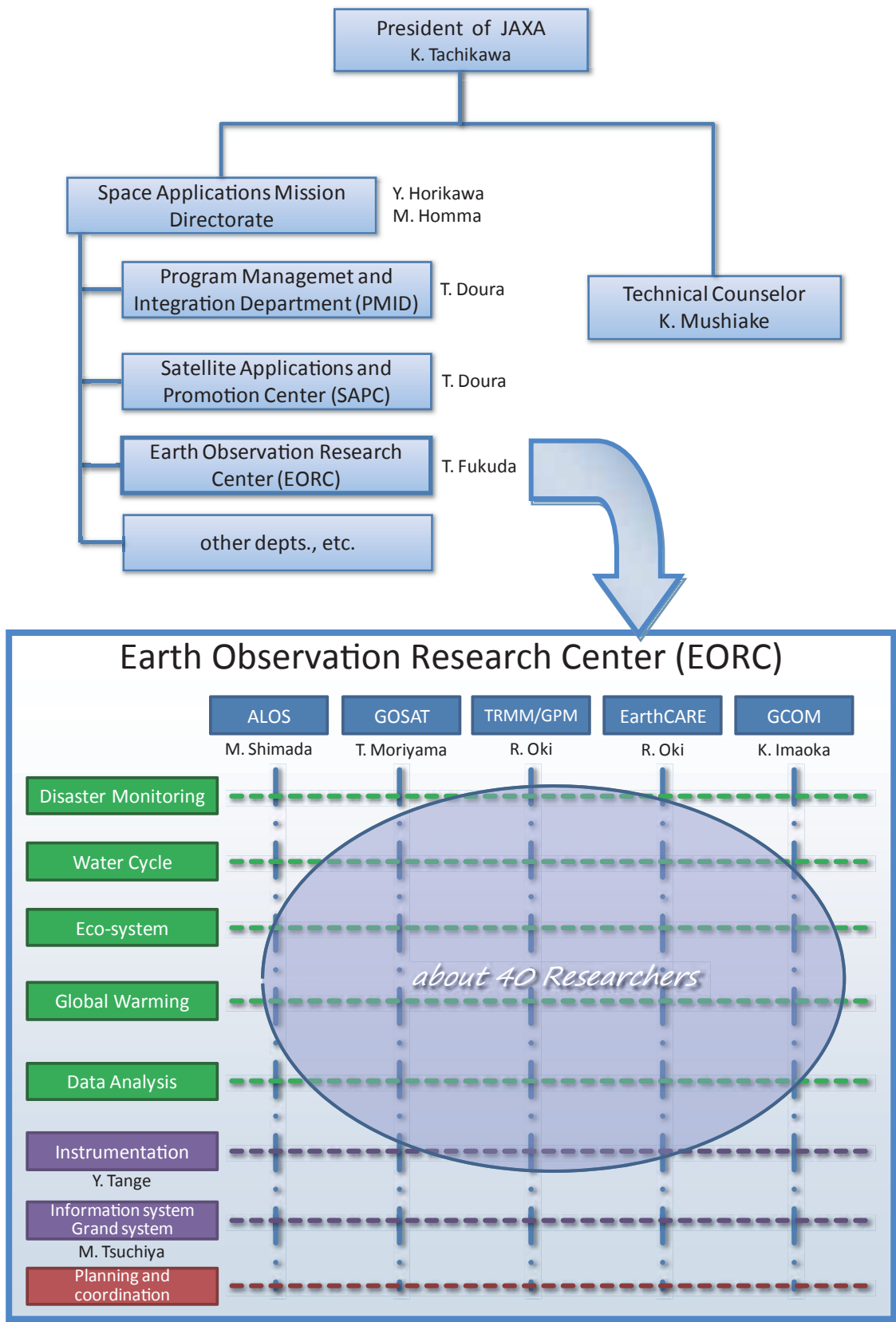


Fig. 1-1 Organization of the Space Applications Mission Directorate and EORC as of March 2008

1. OUTLINE OF THE EARTH OBSERVATION RESEARCH CENTER (EORC)

### 1.3 Science Projects

EORC coordinates several satellite projects and Earth science/application projects.

The JERS-1 science project, led by Dr. Masanobu Shimada, Senior Researcher at EORC, continues to process its L-band Synthetic-Aperture Radar (SAR) data to create global forest mapping and to develop analysis technology for applications to detect crustal deformation.

The ADEOS science project, led by Prof. Haruhisa Shimoda, Invited Researcher from Tokai University, continues to process OCTS and AVNIR data mainly for global change study.

The TRMM science project, led by Dr. Tetsuo Nakazawa, Senior Researcher at the Meteorological Research Institute, continues to process PR, TMI, VIRS, and LIS data mainly for global change study and improvement of weather forecasting.

The ADEOS-II science project, led by Prof. Akimasa Sumi and Prof. Yoshifumi Yasuoka, Invited Researchers from the University of Tokyo, are improving algorithms to retrieve geophysical parameters from AMSR and GLI, as well as studying a variety of science applications.

The ALOS science project, led by Prof. Ryosuke Shibasaki, Invited Researcher from the University of Tokyo, developed algorithms for orthographic mapping and DEM applications from PRISM, AVNIR, and PALSAR. It also carried out the CAL/VAL of PRISM, AVNIR-2, and PALSAR.

The Greenhouse Gas Observing Satellite (GOSAT) was launched successfully on January 23, 2009. The augmented follow-on mission as a part of AMSR, GLI, and SeaWinds aboard ADEOS-II, called the "Global Change Observation Mission (GCOM)" as well as the Global Precipitation Mission (GPM) are being studied in phase A/B.

The Global Energy and Water Cycle Experiment (GEWEX) project, led by Prof. Akimasa Sumi, is primarily studying TRMM, ADEOS-II, and AMSR-E data validation and applications for Asian Monsoon study and for data assimilation.

### 1.4 Individual Research Activities

About 40 researchers, including invited and post-doctoral researchers, conduct their own research as well as project activities as stated above. There were six reviewed papers and letters and over 50 oral and poster presentations in calendar year 2008.



## ***2. RESEARCH ACTIVITIES***

## 2. RESEARCH ACTIVITIES

### 2.1 Research Programs and Projects

#### 2.1.1 ALOS

##### 1) Overview

ALOS was launched on January 24, 2006, in a sun-synchronous polar orbit of 691-km height with a 46-day recurrence cycle. It carried three high-resolution imaging sensors, highly accurate attitude sensors, and dual-frequency GPS receivers. The initial mission check and calibration were performed soon after orbit insertion. The ALOS research activities also started at the same time.

- Data simulation

We compiled observation requests for ALOS calibration/validation and basic observation scenarios. Using the mission simulation software and the satellite orbit data after the launch, we optimized the operation scenario and evaluated success rates for each observation request submitted by ALOS users. The simulation results help us modify the observation plan to achieve higher data acquisition rates.

- Data utilization system

The ALOS Geoscience and Application Processor (AGAP) generates ALOS products for the ALOS science activities. It demonstrates that a computing system consisting of 64 Intel Pentium machines is suitable for data conversion from Level 0 to Level 1.0; image processing of PALSAR data; high-level processing of PALSAR, PRISM, and AVNIR-2 data; data archiving; and distribution of these data. Computing power is essential for processing the PALSAR data on a continental scale so it can be adapted for the Kyoto and Carbon Initiative project. In the year 2007, AGAP was being upgraded to AGAP2. AGAP2 will become operational September 2008 after pre-operation and the software update.

- Calibration/validation (CAL/VAL)

The three sensors were calibrated and validated using the CAL/VAL sites deployed worldwide. Calibration and validation of the three ALOS sensors were concluded. PRISM and AVNIR-2 exhibited improved radiometric and geometric accuracy. PALSAR showed no change or degradation of performance as measured in the initial calibration phase.

- Algorithm development

We have tuned the routines of the PRISM DEM/ORTHO algorithm, which generates a DEM through a pixel-matching technique and a coarse-to-fine iterative technique. JERS-1 OPS data was used to verify the method and to demonstrate that the algorithm could generate a DEM within a theoretical error limit. We have developed basic routines of the PALSAR DEM/ORTHO algorithm and confirmed the functions using the JERS-1 SAR data. The current version of the software can generate a DEM corrected for atmospheric delay using meteorological analysis data.

- Kyoto and Carbon Initiative (K&C Initiative)

The ALOS Kyoto & Carbon Initiative is supported by the Global Forest Mapping program of JERS-1 SAR in the area of ALOS and ADEOS-II GLI. Using PALSAR as a principal data source, it

organizes four themes (i.e., forestry, wetlands, desert and water, and SAR mosaic products) to support regional- to continental-scale data and information requirements for terrestrial carbon researchers (GTOS TCO Panel, IGOS-P GCO, and IGOL themes), environmental conventions (the UNFCCC Kyoto Protocol and the Ramsar Convention), and nature conservation. The K&C Science Advisory Panel/Science Team, consisting of some 20 scientists from 13 countries, met twice (at the EORC at the end of June 2008 and at RESTEC at the beginning of 2009) to focus on defining high-level prototype products and the ALOS data acquisition plan. During the first 3 years after the ALOS launch, the Science Team, along with the EORC, is to develop and subsequently generate verified, regional-scale prototype products, including forest and deforestation maps in four continents, flood duration maps in major river basins, subsurface desert geomorphology maps in Africa, and 50-meter-resolution PALSAR mosaics of all land areas of the Earth.

- PI activities

After the initial calibration phase was completed on October 24, 2006, JAXA started releasing calibrated ALOS standard products to the public, including PIs. PI research agreements covering 101 of the 124 existing PIs (excluding JAXA PIs, and resigned or disagreeing PIs) were completed in 2006. JAXA issued the second ALOS Research Announcement (RA) on December 8, 2006, for researchers in Asian and Russian countries, based on the ALOS Data Node (ADN) concept that came into effect in 2006. The second ALOS node PI meeting was held at the Hilton, Rhodes Island, Greece, organized by the ESA.

- An IEEE special issue for ALOS sensor CALVAL and application was planned for publication in Nov. 2009. Paper submissions were solicited widely for ALOS PI and related researchers.

## 2) Calibration and validation of PRISM and AVNIR-2

CAL/VAL during the initial calibration phase (May 16, 2006 to Oct. 23, 2006) resulted in the sensor characterizations and radiometric accuracies of PRISM and AVNIR-2 almost meeting their goal (except for Band 4 of AVNIR-2). However, the geometric accuracies were inadequate because the satellite attitude was not precise or the offset components (i.e., sensor alignments) were not evaluated. In the operational phase after Oct. 23, 2006, we continued to improve the absolute accuracies of PRISM and AVNIR-2. We also continued to evaluate their stabilities.

### a. Geometric calibration

PRISM and AVNIR-2 were geometrically calibrated in two steps, i.e., relative calibration and absolute calibration. The relative geometric calibration was done by evaluating and correcting parameters for band-to-band registration of AVNIR-2, and relative CCD alignments for PRISM. The absolute geometric calibration was done by evaluating the sensor alignments for both AVNIR-2 and PRISM.

#### AVNIR-2

The uncalibrated band-to-band registration, which is referred to as Band 3, was measured as -0.3 to +0.4 pixels errors, but was improved to less than 0.2 pixels (Fig. 2.1.3-1) by tuning the band-to-band registration parameters. Pointing-angle dependency of the error was also improved using the GCPs as seen in Fig. 2.1.3-2.

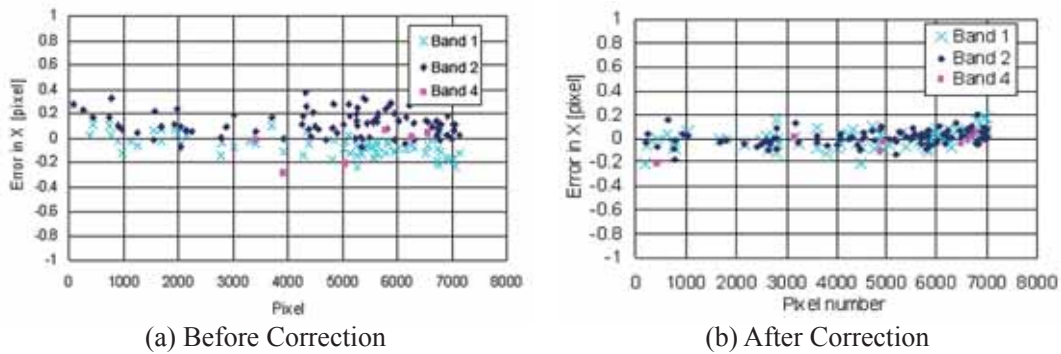


Fig. 2.1.3-1 Improved Band-to-Band Registration for AVNIR-2  
(0 degree pointing angle, X direction)

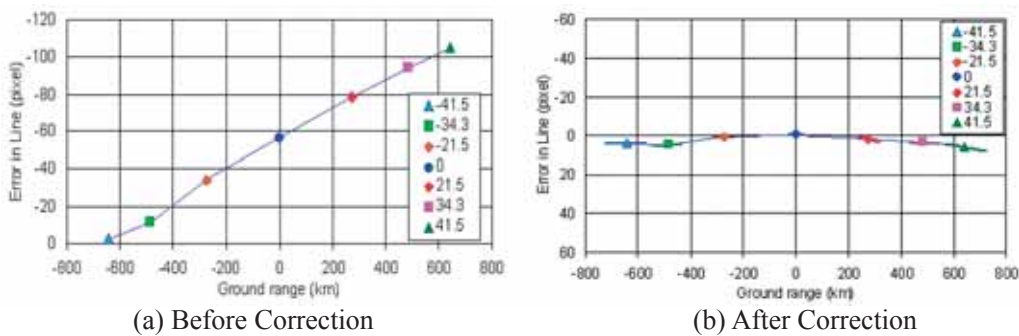
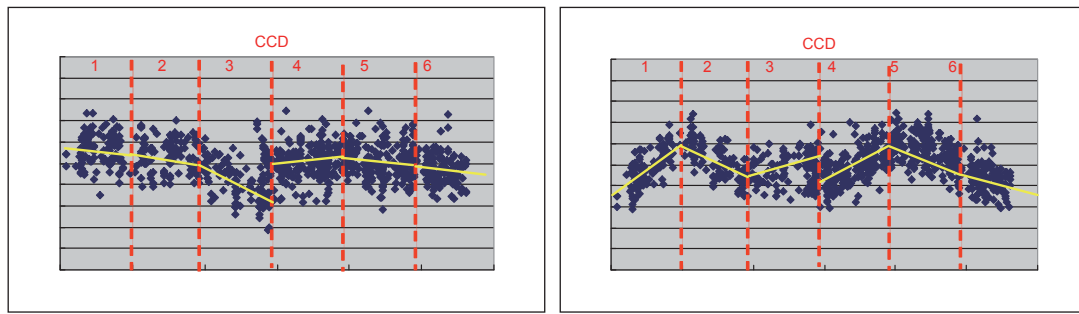


Fig. 2.1.3-2 Improved Sensor Alignments for AVNIR-2 (Y direction)

PRISM

While the nadir radiometer has six CCD units to cover a 70 km swath, the forward and backward radiometers have eight CCD units to cover the area viewed at nadir with time gaps of about 46 seconds as the Earth rotates. Alignments were measured on the ground before launch, but they might be changed due to vibrations of the launch and changes of thermal conditions in space. Residuals of exterior orientations using 706, 943, and 734 GCPs were used to measure the on-orbit alignment. GCP residuals of exterior orientations, which are back-projected on the image space of the nadir with uncalibrated CCD alignment models, are depicted in Fig. 2.1.3-3. Linear regression was applied to govern the deviation at each CCD unit in each sensor. We will continue monitoring its accuracy and variation with each season and update them if necessary.



(a) X Direction

(b) Y Direction

Fig. 2.1.3-3 Relative CCD Alignments for PRISM

#### b. Radiometric calibration

Stripe noise needs to be eliminated during standard-product processing. The power spectrum of the PRISM image in Fig. 2.1.3-4 indicates that a high correlation appears at 1/2 cycle (sample number 2048) and a low correlation at 1/4 cycle (sample number 512). This means that stripe noises appears at every pixel or every other pixel. Zero filling and inverse FFT resolves this problem. Some images were recovered successfully (no stripes), but some were not. Additionally, we implement the averaging DN method to correct the odd-even DN difference.

Cross-calibration using the calibrated satellite data was adopted. We used two types of existing satellite data: a moderate-spatial resolution sensor and a high-resolution sensor. Moderate-spatial-resolution sensors (MODIS on TERRA and AQUA) are used to increase the number of evaluations; high-spatial-resolution sensors (ASTER, SPOT-5, and Landsat) are used to evaluate their pixel scale. Simultaneous observations with ALOS are difficult. We collected many test areas whose images look homogeneous and stable (White Sands, Lunar Lake, Rail Road Valley, and Ivanpah Playa) and which were observed by ALOS and the other satellites within a 1-day time difference and a 5-degree difference of incidence angle as the line of sight.

Figure 2.1.3-5 presents evaluation points for AVNIR-2 and MODIS. The left image is Arizaro Salt Lake, Argentina, where the altitude is about 4,000 m and the atmosphere is stable. Arizaro was used for calibrating EO-1/Hyperion with the AVIRIS airborne sensor, and the surface reflectance was investigated during the campaigns. The right image is Rab Khali Desert, Saudi Arabia. The yellow dots indicate the evaluation points. The AVNIR-2 data were averaged over a 500 m x 500 m area. The variance of digital number (DN) is within 3 percent, indicating a stable target. Figure 2.1.3-6 compares radiance ( $W/m^2/str/micro-m$ ) for each band without atmospheric correction between MODIS (x-axis) and AVNIR-2 (y-axis); the upper figure is a comparison with TERRA/MODIS, and the lower, a comparison with AQUA/MODIS. Figure 2.1.3-6 indicates good agreement between MODIS and AVNIR-2 except for Band 4. The reflectance of Band 4 of AVNIR-2 is below the estimate for MODIS. Table 2.1.3-1 summarizes the initial results of cross-calibration with MODIS, as derived from Fig. 2.1.3-6. The radiometric accuracies of AVNIR-2 are less than 4.6 percent for Bands 1 to 3, and 15.6 percent for Band 4.

Absolute calibration of PRISM involves AVNIR-2 using simultaneous images over Arizaro (Fig. 2.1.3-7) and exhibits good agreement.

## c. Summary of calibration

Table 2.1.3-2 summarizes the calibration results of standard products (Level 1B2) as of September 28, 2007. The satellite position and attitude are precisely determined. The relative geometric accuracies almost meet design requirements. The absolute geometric accuracy of AVNIR-2 has been improved. The absolute accuracy of PRISM depends on that of the pointing alignment parameter that will be continuously updated. The radiometric accuracies generally meet requirements, except for stripe noise in PRISM.

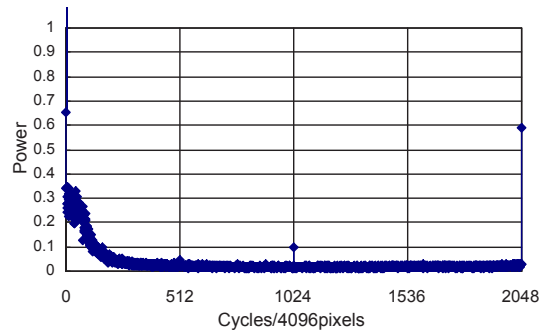


Fig. 2.1.3-4 Power Spectrum of PRISM Nadir Image (CCD #4)

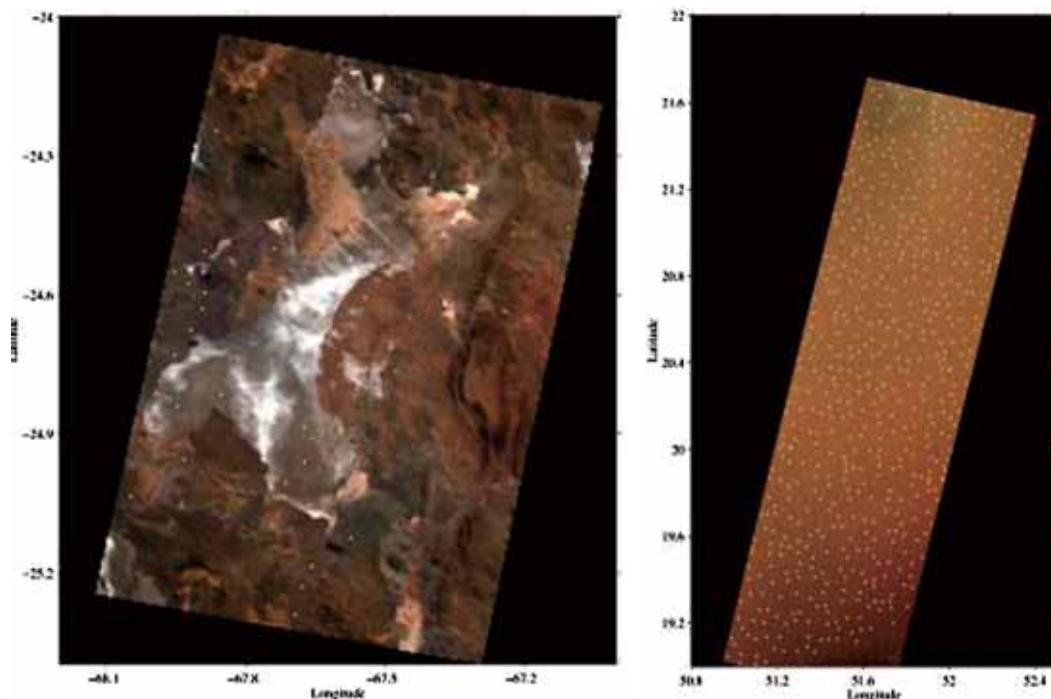


Fig. 2.1.3-5 AVNIR-2 Image Cross-calibrated with MODIS (Yellow dots denote evaluation points. Left: Arizaro, Argentina; Right: Rab Khali Desert, Saudi Arabia.)

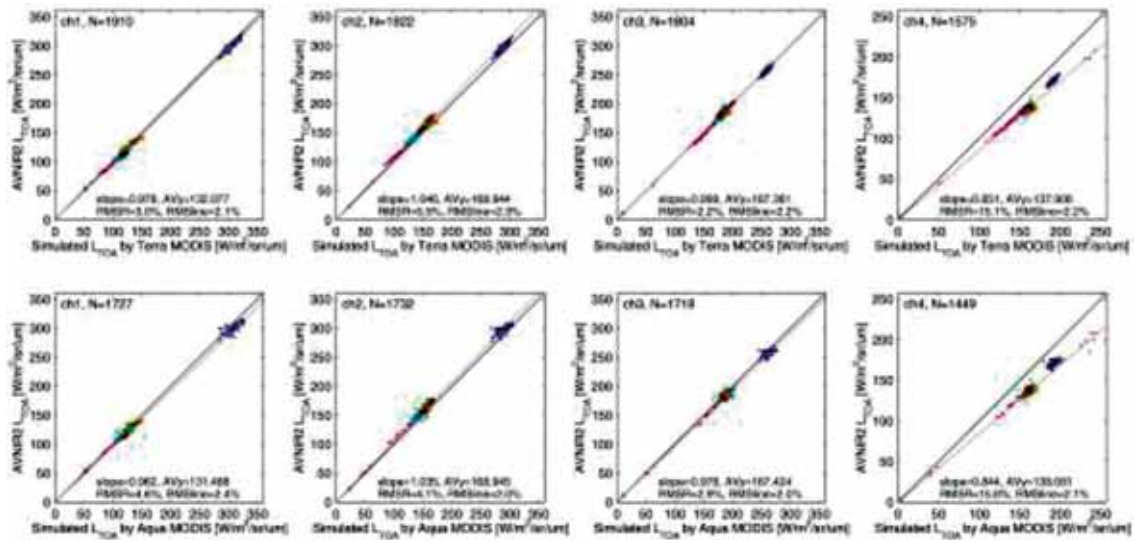


Fig. 2.1.3-6 Comparison of Radiances Between MODIS (TERRA (upper) and AQUA (lower)) and AVNIR-2 (Left to right: Bands 1 to 4. Plots include results for six AVNIR-2 scenes.)

Table 2.1.3-1 Results of Radiometric Cross-calibration of AVNIR-2 and MODIS (as of March 29, 2007)

AVNIR-2 Band	TERRA/MODIS			AQUA/MODIS		
	Number	Slope	RMSR	Number	Slope	RMSR
1	1910	0.978	2.2 %	1727	0.962	3.8 %
2	1922	1.046	4.6 %	1732	1.035	3.5 %
3	1804	0.999	0.1 %	1718	0.978	2.2 %
4	1575	0.851	14.9 %	1449	0.844	15.6 %

\* Number: Number of evaluation points. Slope: Radiance ratio of AVNIR-2/MODIS. Ave: average of AVNIR-2's radiance (W/m<sup>2</sup>/str/micro-m). RMSR: root mean square of residual.

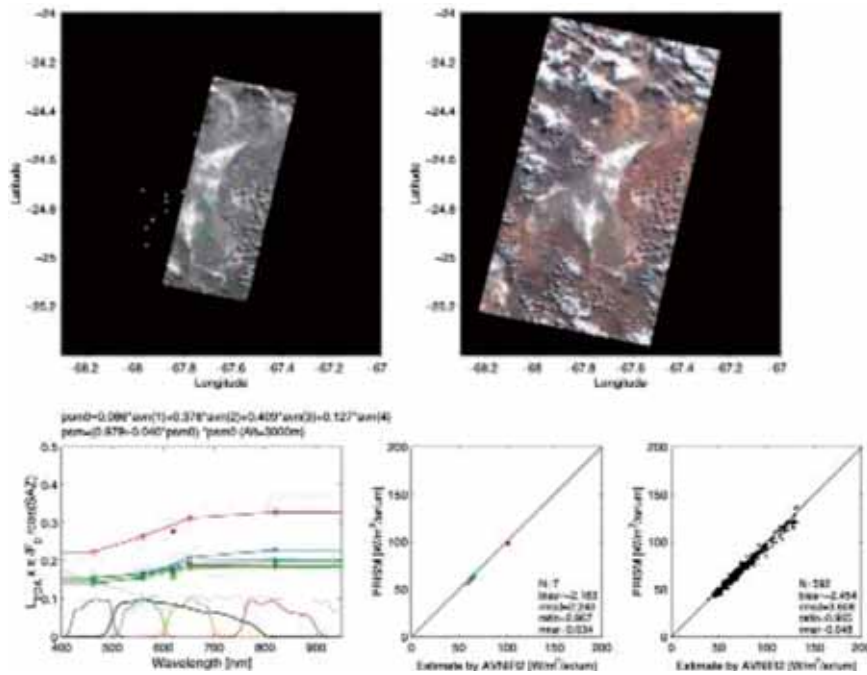


Fig. 2.1.3-7 Cross-calibration of PRISM (upper left) with AVNIR-2 (upper right) over Arizaro, Argentina and Comparison of Radiances Between PRISM and AVNIR-2 (lower center and right)

Table 2.1.3-2 Calibration Summary of Standard Products (September 28, 2007)

Sensor	Accuracy (as of September 28, 2007)
PRISM (L1B2)	Geometry (m):
	Absolute X (Pixel) Y (Line) distance (RMS)
	Nadir 6.5 7.3 9.8
	Forward 8.0 14.7 16.7
	Backward 7.4 16.6 18.1
Relative 1.9 2.3 3.0 (3 radiometers, 1σ)	
Radiometry (%):	Relative 0.4 (stripe noise sometimes appears)
	Absolute 4.6 (1σ)
AVNIR-2 (L1B2)	Geometry (m):
	Absolute X (Pixel) Y (Line) distance
	-41.5 to +41.5 deg. pointing 106 19 108 (RMS)
	Relative 4 4 6 (1σ)
	Radiometry (%):
Relative 0.4 (less than 1 DN, 1σ)	
Absolute 3.8 (B1), 4.6 (B2), 2.2 (B3), 15.6 (B4) (1σ)	

d. Validation of generated digital surface model (DSM) by PRISM

The digital surface model (DSM) generating algorithm is a correlation-based triplet of stereo image matching algorithms exclusively developed for PRISM. The major characteristics of the

algorithm are as follows:

- Area-based grid matching with cross-correlations
- Epipolar geometry constraints for simultaneous triplet-image 1-D matching
- Cross-correlation patch size dynamic optimization
- Coarse-to-fine image pyramid

DSM generation software only estimates the bias errors of roll and pitch angles as the exterior orientation parameters because the yaw angles of pointing elements given by Star Tracker (STT) and PRISM sensor alignments are accurate enough. The triplet triangulation accuracies of exterior orientations are evaluated with 1, 9, 25, and all GCPs. To evaluate the capability of automatic determination of exterior orientation parameters, the relative orientations are performed without GCP registration (0-GCP). The absolute accuracies of relative orientations with Tie Points (TPs) are attributed to accuracies of the on board GPS receiver (GPSR), STT data, and trend-compensating sensor alignment parameters. Here, the stereo images are listed in Table 2.1.3-3, and the characteristics of the reference DSM are given in Table 2.1.3-4 and Fig. 2.1.3-8.

The accuracies of those orientations are presented in Tables 2.1.3-5 to 2.1.3-7 for scene 1 to 3. The GCP residuals are the standard deviations of registered GCPs, and the RMSEs are the errors of independent checkpoints (ICPs), which were not used as the registering GCPs. The results indicate that the triangulation accuracies are 6.4 and 6.2 m RMSE for planimetry (xy) and 8.7 and 23.1 m RMSE for height (z) without GCPs. The height errors are correlated to the relative pitch errors of forward and backward images against nadir. These height errors are nearly consistent with the absolute pointing pitch errors estimated during sensor alignment trend analysis. Just one GCP registration can improve the absolute accuracies to 1.9 to 2.3 m RMSE for planimetry and 2.1 to 3.4 m RMSE for height.

An example of generated DSMs spaced at 10 m and 0.3 arcsec is depicted in Fig. 2.1.3-9. Cloud and land water (i.e., large rivers or lakes) areas are masked by manual editing. The standard deviations (SD) are almost the same even though the GCP numbers differ. This implies that the planimetric accuracies of 0.3 arcsec DSM are almost the same among those different numbers of GCP models including 0-GCP. In the flat Saitama site, which includes paddies and urban terrain, the height accuracy is 4.74 m ( $1\sigma$ ); in Okazaki, Thun, SW, and Bern sites, which include various terrains, i.e., mountains, farms, and cities, the height accuracies are 5.36 to 7.80 m ( $1\sigma$ ). Figures 2.1.3-10 present bird's-eye views over the glacier area of Bhutan using PRISM/DSM as a high-level product of the EORC.

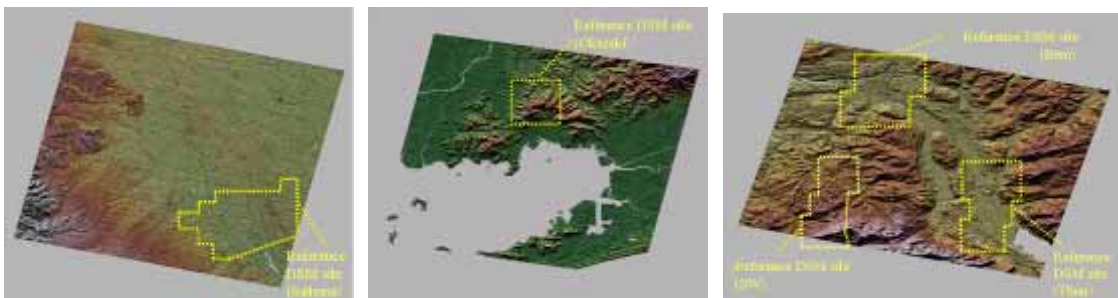


Fig. 2.1.3-9 Color-shaded PRISM-DSM (Left: Scene 1; Center: Scene 2; Right: Scene 3)

Table 2.1.3-8 Height Accuracies of Generated DSM

Site	Terrain	Model	Points	Bias [m]	SD [m]	RMSE [m]	Max [m]	Min [m]
Saitama	Flat & Urban	0-GCP	1505339	0.64	5.12	5.16	74	-200
		213-GCP	1505512	1.50	4.74	4.97	78	-195
Okazaki	Mountainous	0-GCP	548352	-16.08	6.14	17.21	85	-98
		17-GCP	548352	-0.48	6.00	6.02	99	-85
Thun	Various	0-GCP	1672554	-1.69	5.49	5.74	94	-79
		54-GCP	1672584	-1.40	5.36	5.54	94	-77
SW	Steep	0-GCP	1205609	-1.22	7.88	7.97	87	-105
		54-GCP	1205923	-1.12	7.80	7.88	86	-103
Bern	Various	0-GCP	2034946	-2.37	6.70	7.11	71	-57
		54-GCP	2034642	-2.08	6.68	6.99	76	-58

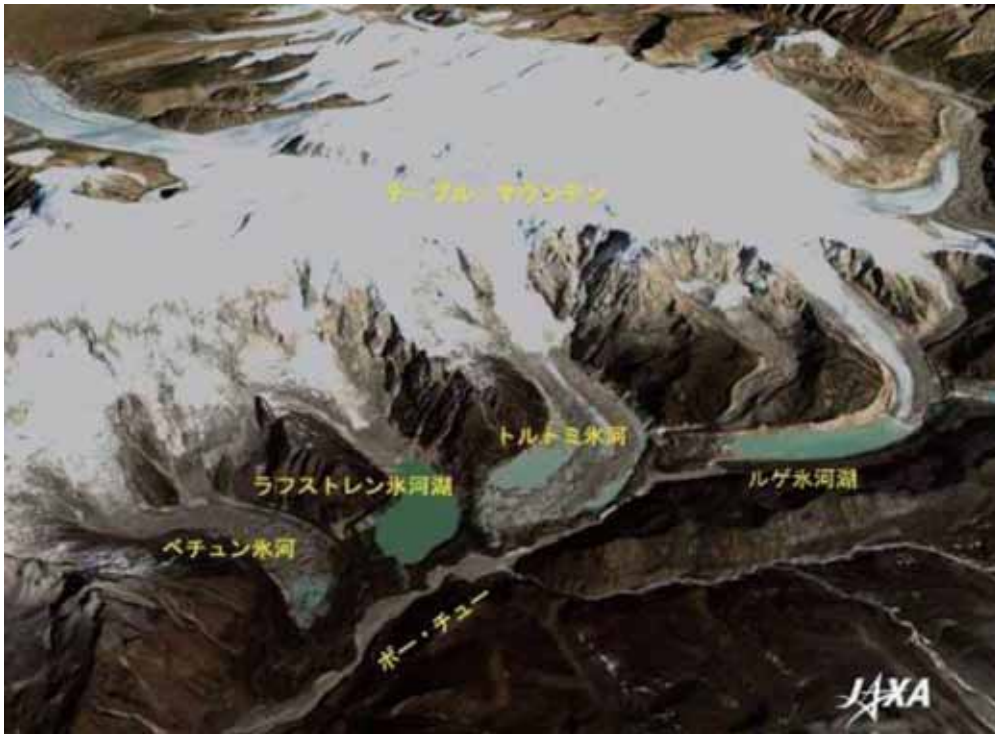


Fig. 2.1.3-10 Bird's-eye View of Glacier Area in Bhutan Using a Pan-sharpened Image with DSM Generated by PRISM

### 3) Calibration and validation of PALSAR

#### a. General

We will summarize the PALSAR geometric and radiometric calibration results achieved during the ALOS initial calibration phase, which covered 5 months between May 16, 2006, and October 23, 2006, and the half-year of the operational phase. All the PALSAR modes, FBS (fine beam single), FBD (Fine beam dual), SCANSAR, DSN (band-limited SAR), and POL (Full polarimetry) were

calibrated and validated using a total of 500 calibration points collected worldwide and distributed target data from the Amazon. While characterizing PALSAR, determining the antenna pattern, and conducting polarimetric calibration, we adjusted the PALSAR radiometric and geometric model installed on the SAR processor (SIGMA-SAR). Using the reference points, we confirmed that the geometric accuracy of the FBS, FBD, DSN, and POL modes is 9.3 m; that of SCANSAR mode is 70 m; and the radiometric accuracy is 0.64 dB. Polarimetric calibration was successful; the amplitude balance of VV/HH is 0.025 dB, and the phase balance is 0.32 degrees.

## b. CAL/VAL

### b-1) Stability of the chirp data

PALSAR has only three chirp rates even though it has six modes, i.e., FBS, FBD, DSN, SCAN-WB1, SCAN-WB2, and polarimetry. The temporal variations of these chirp rates were measured and plotted in Fig. 2.1.3-12. All the chirp rates are very stable (normalized standard deviation, standard deviation divided by an average) varying less than  $1.0 \times 10^{-4}$  during the 1-year monitoring period after the ALOS launch. This variation produces only a 1.0-degree maximum disagreement at the pulse end and does not cause compression errors in the range-compression step.

$$2\pi \frac{\Delta k}{2} \left( \frac{\tau}{2} \right)^2 \leq \frac{\pi}{180} \quad (1)$$

Here,  $\Delta k$  is the deviation in the chirp rate, and  $\tau$  is the pulse width.  $\Delta k$ , which causes phase disagreements of 1 degree at the pulse end, is  $3.0 \times 10^7$  for FBS,  $3.0 \times 10^7$  for FBD, and  $8.7 \times 10^7$  for polarimetry. The measurements are always below this. This means that the chirp rate can be made constant.

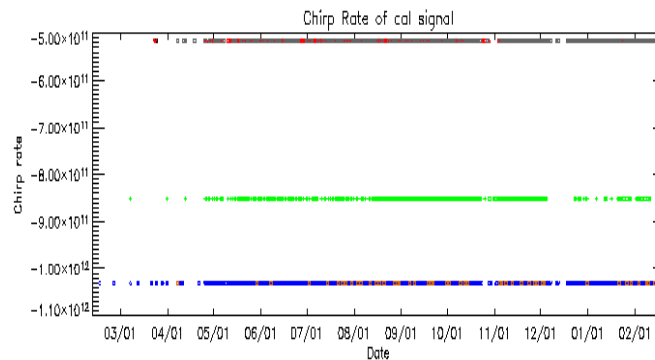


Fig. 2.1.3-12 Temporal stabilities of the three chirp rates observed from the PALSAR calibration data. Here, black indicates the chirp rate of FBS, SCAN-WB2, blue represents that for FBD, DSN, and SCAN-WB1, and the green for polarimetry.

### b-2) Raw data summary

Table 2.1.3-9 summarizes the raw data characterization obtained from all the PALSAR data. This result was acquired at the end of the CAL/VAL phase and was slightly improved. The SNR of the natural target is improved for FBD because the FBD with an off-nadir angle of 34.3 degrees is included and in the total worse SNR of only 4.15 was improved. The saturation rate was measured and found to be less than 3 percent. This is a significant improvement over the previous report and results

from the attenuators for all the modes optimized on Aug. 7, 2006. Additional updates will be provided for SCANSAR SCANS 2 to 5. Interference did not change very much. In total, PALSAR exhibited better raw data characteristics than did JERS-1 SAR.

b-3) Stabilities of the azimuth antenna pattern

In the previous report, we noted that the PALSAR azimuth antenna pattern (AAP) is almost the same as the pre-launch AAP (exactly the same in the main lobe and only slightly different in the side lobes). The temporal change was evaluated by drawing all the AAPs in the same plane (Fig. 2.1.3-13). The AAP can be obtained by converting the azimuth time to the angle between the satellite and the target, and the orbital deviation (height, shift from the nominal orbit) needs exact conversion of the coordinate system. For simplicity, we evaluate the time variation of the AAP's main lobe only. This figure demonstrates that the main lobe does not change over six flights. The other AAPs at different off-nadir angles and different modes, seven cases in total, do not exhibit any differences either. AAP is thus time invariant.

Table 2.1.3-9 Summary of the PALSAR Raw Data Characteristics

	FBS	FBD	PLR	WB1	WB2
I	16.049	16.188	16.254	16.245	16.041
Q	15.850	15.973	16.078	15.950	15.835
Gain Ratio I/Q	1.007	1.010	1.001	1.015	1.008
Phase Diff. of I/Q (deg)	1.598	1.579	1.577	1.581	1.597
SNR (dB)	8.6698	6.9575	8.5104	9.4869	8.3310
Chirp Rate (Hz/s)	-1.03158 x E12	-0.515923 x E12	-0.850977 x E12	-0.515903 x E12	-1.03159 x E12
Chirp Rate Std	2.5e7	2.2e7	4.0e7	1.2e7	5.1e7
Saturation	Saturation rate dropped to 3% after August 7, 2006.				
Interference	In general, the interference is less than that of JERS-1 SAR (because it has four times greater transmission power) except for occasional greater bandwidth noise.				

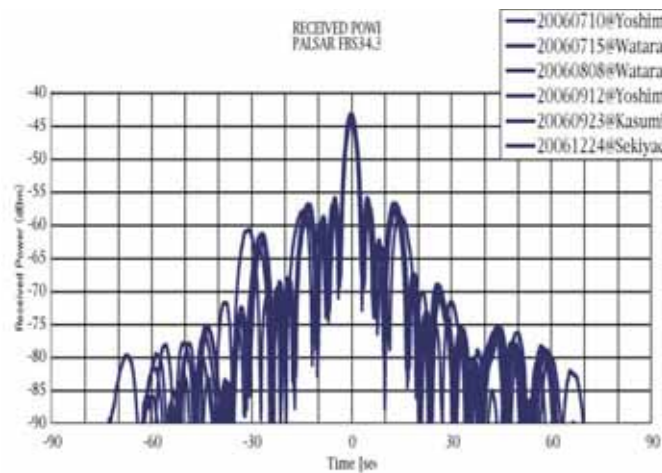


Fig. 2.1.3-13 Measured Azimuth Antenna Pattern (in HH pol) The red curve is the real measurement, and the blue curve is the ground measurement.

#### b-4) Elevation Antenna Pattern

Elevation Antenna Patterns (EAPs) were measured using the Amazon data. For off-nadir angles of less than 40 degrees, the EAPs were almost the same as the on-ground measurements. At greater off-nadir angles, EAPs were degraded due to the range ambiguities (see Fig. 2.1.3-14; the small circles at 41.5 of FBS and FBD indicate that EAP deviates due to the azimuth ambiguity). Thus, the 34.3-degree and 21.5-degree off-nadir angles are being used for standard operation.

#### c. Image quality and summary

c-1) Resolution: After calibrating the PALSAR data, we measured the image quality of the PALSAR data using all the corner-reflector responses. The results are summarized in Table 2.1.3-10. The representative impulse response function (IRF) is presented in Fig. 2.1.3-15 for two cases.

c-2) Geometric accuracy: A geometric accuracy of 9.2 m RMS was achieved (Fig. 2.1.3-16).

c-3) Radiometric accuracy: See Fig. 2.1.3-17 for the distribution of the calibration factor using all the CRs.

c-4) Disturbances of VV/HH in phase and amplitude: Figure 2.1.3-18 plots these two parameters measured from the CRs.

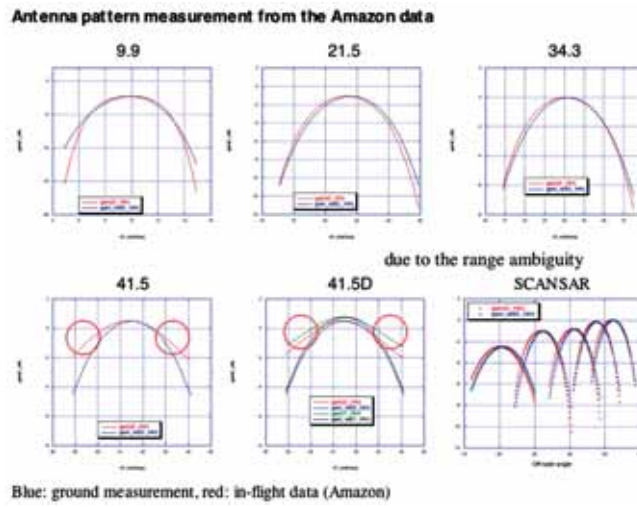


Fig. 2.1.3-14 EAPs Before and after Launch. Small circles on the shoulders of the 41.5 case represent the range ambiguities.

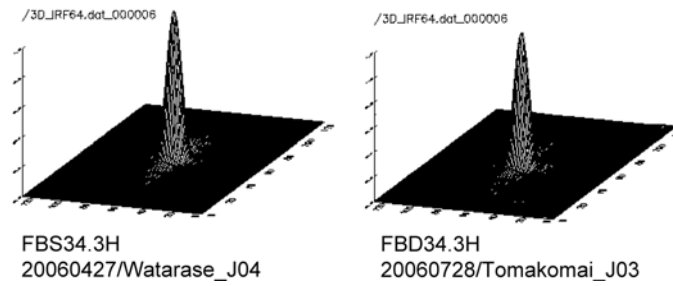


Fig. 2.1.3-15 3D Responses (Left: FBS; Right: FBD.)

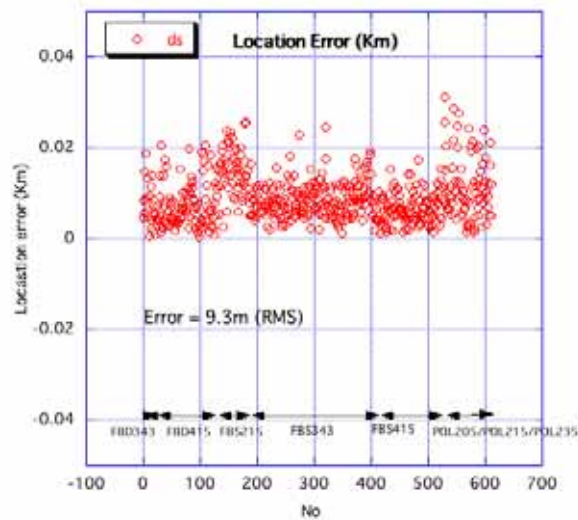


Fig. 2.1.3-16 Geometric Error Distribution

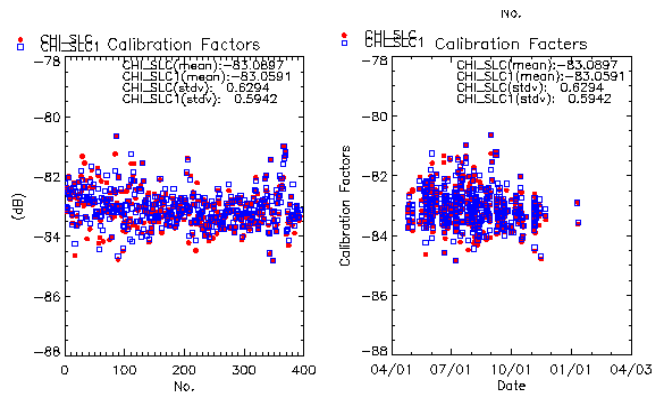


Fig. 2.1.3-17 Distribution of the Calibration Factors (Left: All modes; Right: Ordered in time.)

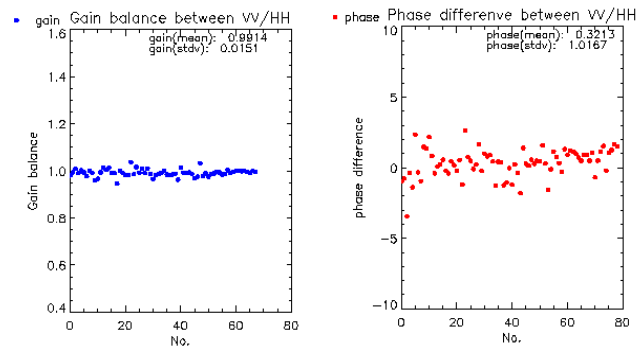


Fig. 2.1.3-18 Amplitude and Phase Disturbances of the Polarimetrically Calibrated PALSAR Data (Left: Gain difference; Right: Phase difference.) Here, the distortion matrices were calculated using the Amazon corner reflector.

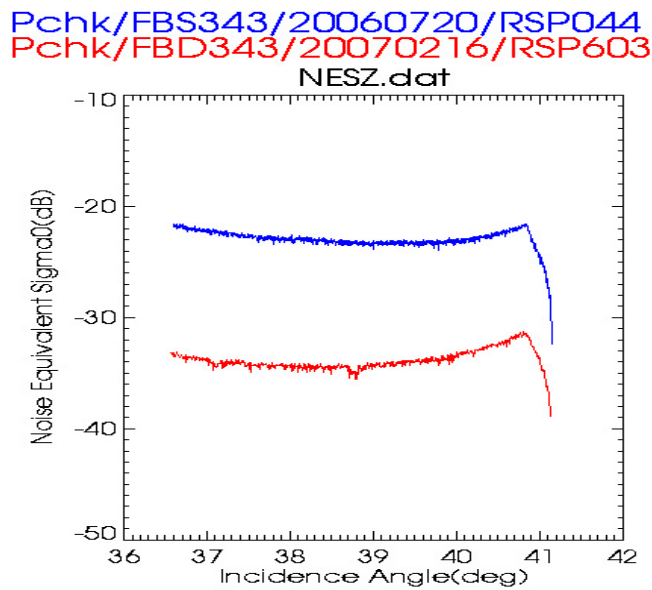


Fig. 2.1.3-19 Noise Equivalent Sigma-naught vs. Incidence Angle (Blue: Greenland by FBSHH; Red: Hawaii by FBD-HV)

c-5) Noise equivalent sigma-naught: The noise equivalent sigma-naught parameter expresses how well dark targets can be observed. The value is determined by searching for the minimum from the browse strip data generated by cataloging all the PALSAR images at the EORC. Browse processing is possible by combining range compression and the azimuth SPECAN. The minimum value is sought in the azimuth direction in every range bin. Figure 2.1.3-19 presents two cases: (a) from the FBS over Greenland ice and (b) from HV polarization of the image path over the Hawaiian Islands. Both curves resemble the inverse of the range antenna pattern, and the correct values seem to have been obtained. The noise-equivalent sigma-zero is -34 dB, which is 10 dB better than the other spaceborne sensors and 13 dB better than JERS-1 SAR.

c-6) Stability evaluation of the gamma-zero using the Amazon Rainforest: The Amazon Rainforest is a uniform reference target for relative (range and azimuth antenna pattern determination) and absolute calibration. Statistical analysis demonstrates that the seasonal variation is only 0.25 dB. Thus, the Amazon can be used for calibration. A multiple-beam SAR like PALSAR has many modes for calibration. The limited conditions for deploying corner reflectors require including Amazon-based calibration for both relative and absolute calibration. At the beginning of the PALSAR CAL/VAL, we used the following for determining the gain offset among the beams, so that the gamma-naught could be constant over the incidence angle:

$$\gamma^0 = \sigma^0 / \cos \theta = \text{constant}. \quad (2)$$

Here,  $\theta$  is the incidence angle. We confirmed the validity of this assumption using the ten Amazon data points for the strip mode and two data points for the SCANSAR. Figure 2.1.3-20 indicates the stability of the PALSAR Amazon data. This suggests that the Amazon data is not always seasonally and spatially stable. The difference is between 0.5 dB to 1.0 dB. We need to investigate this variation further. It appears that the Amazon can be used for relative calibration but not for absolute calibration. Independently, calibration sites, including corner reflectors, were established worldwide, and more than 600 matched data sets were collected. Calibration, which actually means determining the calibration factor, should rely on the CRs. However, in general, gamma-naught is found to be -6.5 dB with a standard deviation of 0.5 dB.

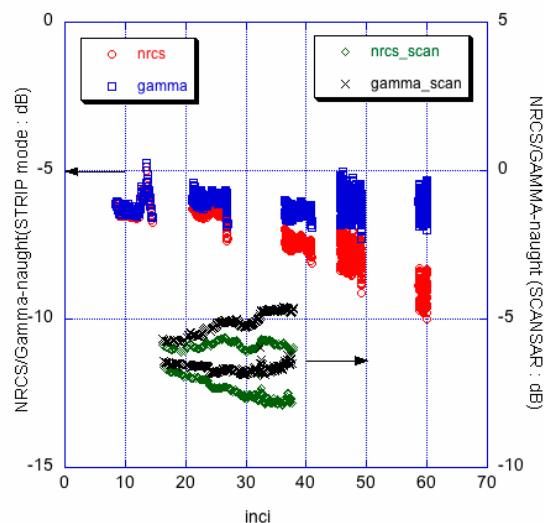


Fig. 2.1.3-20 Measured Gamma-naught vs. Incidence Angle (a. Strip modes; b. ScanSAR)

## d. Conversion formula

Standard products (Level 1.1 or 1.5) that JAXA produces can be converted to normalized radar cross-section by

$$\sigma_{\text{sigma-sar},Q16}^0 = 10 \cdot \log_{10} \langle DN^2 \rangle + CF_1 \quad (3-1)$$

$$\sigma_{\text{sigma-sar},slc}^0 = 10 \cdot \log_{10} \langle I^2 + Q^2 \rangle + CF_1 - A \quad (3-2)$$

where, I (Q) is the real (imaginary) part of SLC (Single Look Complex, process level is 1.1), and DN is the digital number of the amplitude image (1.5). The conversion factor, CF1, is -83.0, and its standard deviation is 0.64 dB. An additional factor (A) of 32.0 exists when the SLC is considered. A standard deviation of 0.64 is obtained by using all the CRs deployed worldwide. The CRs are trihedral corner reflectors, and their responses might vary since their characteristics and test site conditions might differ at the times of the overflights. When we used only the Swedish CRs, the largest CRs with a 5-mleaf size, the standard deviation became minimum at 0.17 dB. The PALSAR radiometric performance can thus be estimated to be 0.17 dB.

Table 2.1.3-10 PALSAR Calibration Accuracy (summary)

Item	Measured Value		Data	Spec.
Geometric Accuracy	9.3m (RMS): Strip mode		615	100 m
	70 m (RMS): SCANSAR			
Radiometric Accuracy	0.64 dB (1 sigma)		478	1.5 dB
	0.17 dB (1sigma: Sweden)		16	1.5 dB
	-34 dB(Noise equivalent NRCS)			-23 dB
Polarimetric Calibration	VV/HH ratio	0.02 dB (0.04)	79	0.2 dB
	VV/HH phase diff	0.32deg(1.01)		5 deg.
	Crosstalk	31~40 dB		30 dB
Resolution	Azimuth	4.49m (0.1) 9.6m	478	4.5m
	Range (14M)	(0.1m) 4.7m		10.7m
	Range (28M)	(0.1m)		5.4m
Side Lobe	PSLR (azimuth)	-16 dB	478	-10 dB
	PSLR (range)	-12.5 dB		-10 dB
	ISLR	-8.6 dB		-8 dB
Ambiguity	Azimuth	None		16 dB
	Range	23 dB		16 dB

## e. High-level products and research products

High-level products and research products are being generated. Two examples are introduced below.

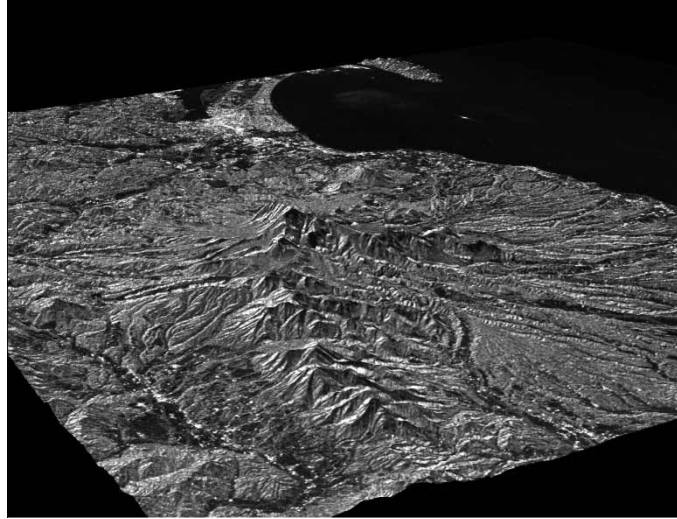


Fig. 2.1.3-21 Bird's-eye View of Mt. Daisen Using the InSAR DEM and Ortho-rectified PALSAR Image

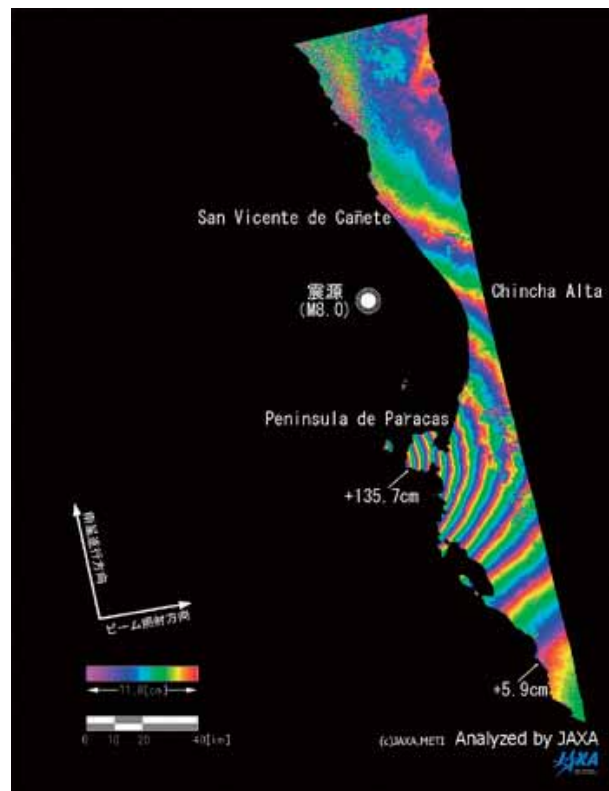


Fig. 2.1.3-22 Surface Deformation Pattern of Peru by PALSAR DinSAR

e. Potential applicability of L-band SAR in disasters (Disaster-Monitoring Experiments using Pi-SAR Data)

Pi-SAR is a high-resolution, full-polarimetric airborne SAR system developed in order to calibrate and validate satellites for the next generation SAR system. Pi-SAR flight experiments have recently been conducted for a variety of purposes, particularly disaster-monitoring experiments. Ground-based investigation or experiments are often conducted simultaneously with Pi-SAR flights.

Figure 2.1.3-25 presents the result of an experiment for evaluating the effectiveness of SAR data in monitoring disaster-affected areas. In this experiment, two flights are flown within a week in January 2008. The ground-experiment team flooded a fallow field simultaneously with the second flight to imitate inundation. We developed a change-detection algorithm to detect the difference between the first flight (not flooded) and the second flight (flooded) images. The result demonstrates that the pseudo-inundated area was successfully detected. Additionally, a change in the Nagara River was also detected (Fig. 2.1.3-26). The river width decreased here because of the lowered water level.

The change-detection methods we are developing will be applied to actual disaster data to identify inundation areas, landslides, collapsed buildings, etc.

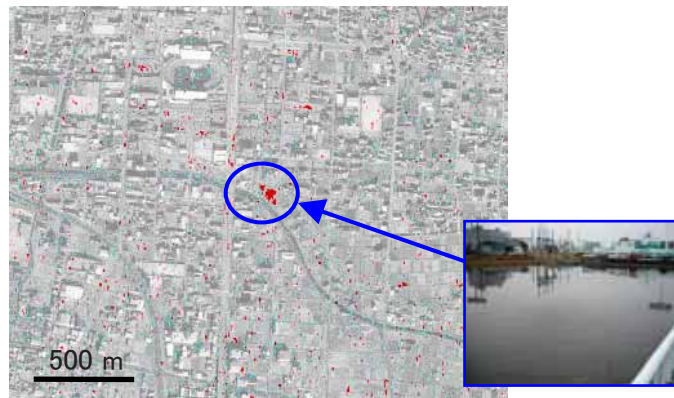


Fig. 2.1.3-25 Change-detection Result Derived from Pi-SAR Flooded and not Flooded Images (Jan. 6 and 13, 2008, respectively) The background image is a low-contrasted image acquired by ALOS optical sensors.

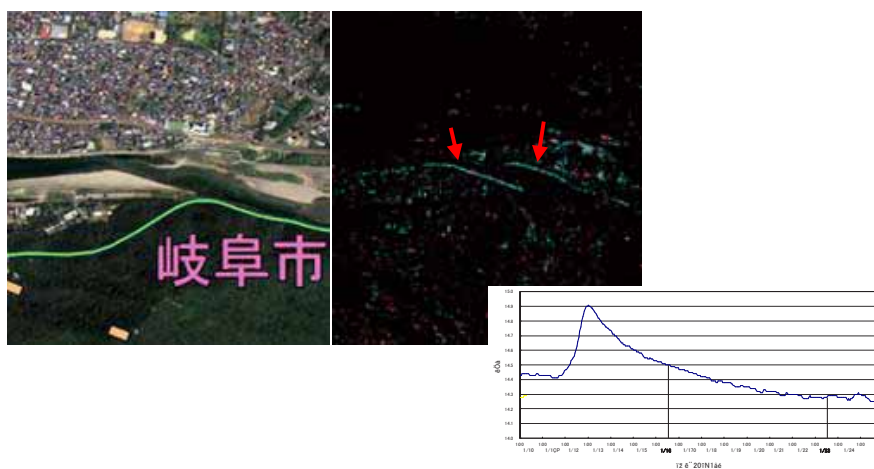


Fig. 2.1.3-26 Detected Change in River Width Due to Reduced Water Level. The line plot represents the corresponding water-level measurement.

#### 5) ALOS observation plans

To achieve a good success rate for requests from major users, i.e., Japanese government agencies, ALOS data nodes, and researchers (PI), we created a basic observation scenario and revised it to achieve better success rates. Negotiations started with major users with higher request priority, such as Japanese government users and ALOS data nodes.

#### 6) ALOS www

We currently maintain two web sites:

- 1) General ALOS information      <http://www.eorc.jaxa.jp/ALOS/index.htm>
- 2) Principal Investigators (PIs)      <http://www.eorc.jaxa.jp/ALOS/ForPI/index.htm>

The general ALOS site was established January 6, 2006, with the sample top page in Fig. 2.1.3-30, and its Image Gallery was updated with 16 images during FY 2007. The site also contains the science plan, research announcement (RA), project and symposium information, as well as characteristics of the satellite and sensors. We maintain the site for the CAL/VAL and Science Team (CVST) to facilitate sharing information on CAL/VAL test sites, data acquisition plans, technical information, and meeting information.

The site for RA PIs presents information on PIs, i.e., the PI list including names, organizations, research titles, e-mail addresses, telephone numbers, PI workshops, ALOS simulation data for research activities, and research agreement related documents.

#### 6) ALOS Kyoto and Carbon Initiative

The ALOS Kyoto and Carbon Initiative (K&C Initiative) initiated by the EORC in 2000 is based on the conviction that ALOS has the potential to play a significant role in supporting certain environmental conventions, carbon-cycle science, and natural conservation with information that cannot feasibly be obtained by any other means. In this context, the L-band SAR sensitivity to vegetation structure and inundation, together with the microwave cloud-penetrating capacity to ensure global observations, is relevant.

##### a. Project organization

The K&C Initiative is organized as an international collaborative effort based on the experience and project structure developed for the JERS-1 SAR Global Forest Mapping project. The initiative is led by the EORC, which is responsible for the overall management and implementation of the ALOS systematic acquisition strategy, as well as processing and distribution of all ALOS data. Product development is undertaken jointly by the EORC and the international K&C Science Team, which involves universities and research organizations from 14 countries.

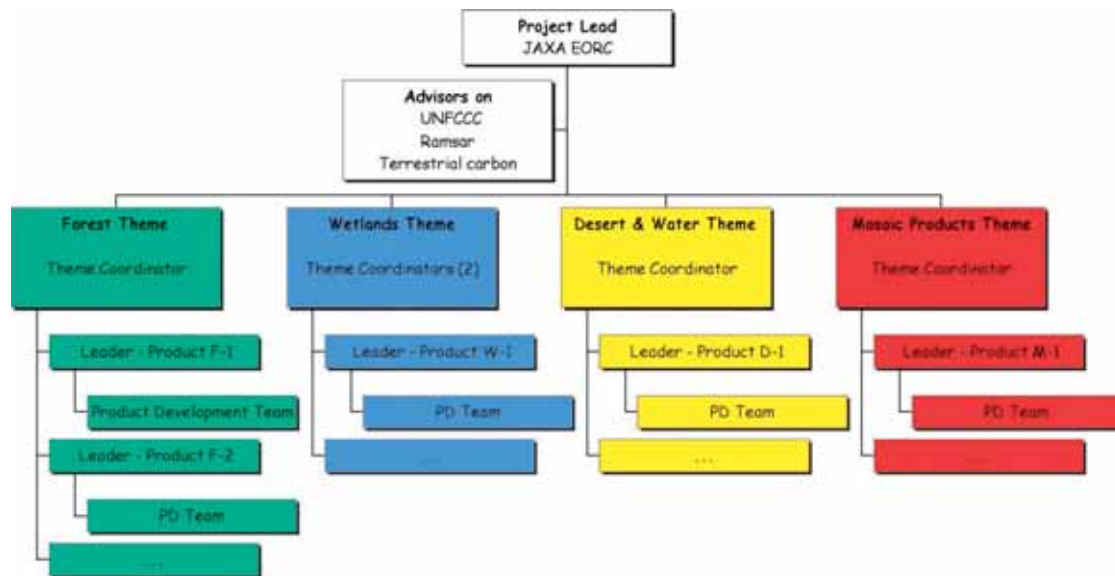


Fig. 2.1.3-29 Structure of the K&C Initiative Project

The Initiative is structured around three main thematic areas: Forest, Wetlands and Desert, and Water, in which each relates uniquely to one or more of the project drivers (International Conventions, Carbon Science and Environmental Conservation), as well as a data-oriented theme (Mosaic Products) to support the three other themes with image data products. Each theme has a Theme Coordinator and a number of Product Development (PD) Teams.

The Forest Theme focuses on supporting the UNFCCC Kyoto Protocol and some of the carbon research community concerned with CO<sub>2</sub> fluxes from terrestrial sinks and sources. Key areas considered include land-cover (forest) mapping, forest-change mapping, and biomass and structure. The Wetlands Theme aims to serve information needs of the Ramsar Wetlands Convention and the Convention on Biological Diversity, as well as the significance of wetlands as sources of tropospheric carbon. Key areas considered include regional wetland inventories, seasonal inundation monitoring, and specific inventories of mangroves and peat-swamp forests. The Desert and Water Theme addresses issues relevant to water supply and land degradation in arid and semi-arid areas. Key areas considered include freshwater supply and desertification. The Mosaic Products Theme is a semi-independent unit within the Initiative, which largely constitutes a global-scale extension of the JERS-1 SAR Global Forest Mapping project in terms of member composition and scope. The principal objective of this theme is to generate continental-scale

PALSAR mosaics, to be used both as intermediate input data to the other three themes, as well as stand-alone image products to be made available to the public.

#### b. Implementation

The K&C Initiative is implemented in a number of steps to assure validated development of thematic products from local to global scales.

c. Project output

All data products generated within the K&C Initiative, both thematic products as well as PALSAR mosaics, will be made available free of charge for public users. For updated information about the K&C Initiative, please refer to the K&C homepage at the EORC www site:

[http://www.eorc.jaxa.jp/ALOS/kyoto/kyoto\\_index.htm](http://www.eorc.jaxa.jp/ALOS/kyoto/kyoto_index.htm)

d. Mosaic data sets were generated, and distribution has begun. Below is the first 50 m spaced mosaic data generated for Southeast Asia (Fig. 2.1.3-30).

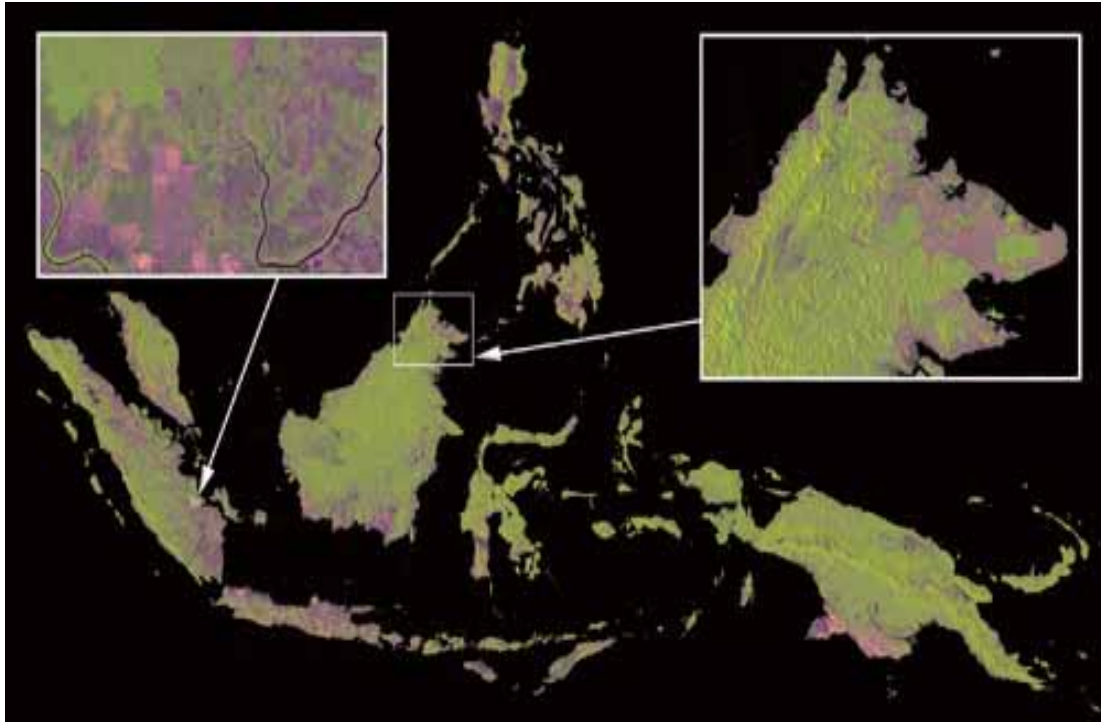


Fig. 2.1.3-30 First Mosaic Generated for the K&C Initiative

7) PI activities

Since the ALOS Data Node (ADN) concept came into effect in 2006, JAXA issued the second Research Announcements (RA) only for researchers living in the Asian Node area for which JAXA is responsible. One hundred and twenty eight effective research proposals were submitted by the March 2007 deadline. Through evaluations by experts from the scientific community and JAXA's internal Evaluation Board, JAXA selected one hundred and three Principal Investigators (PIs) on May 31, 2007.

Other ALOS Data Node organizations, the European Space Agency (ESA), Alaska Satellite Facility (ASF) of the University of Alaska Fairbanks, and Geoscience Australia (GA), launched PI research programs in their respective Node areas.

JAXA hosted the First Joint PI Symposium of ALOS Data Nodes for the ALOS Science Program from November 19 to 22, 2007, at the Kyoto International Conference Center in Kyoto. This was the

first symposium attended by PIs from all the ADN PI programs and supported by all the ADN organizations. About 170 attendees, excluding symposium secretariat staff, attended and made oral presentations or active discussions throughout the 14 technical sessions. The second Joint PI Symposium was hosted by ESA in November 2008 in Rhodes Island, Greece.

JAXA conducted an interim evaluation of JAXA PI activities from February to March 2008 to check the progress of PI activities selected in both JAXA's first and second RA. Successful PIs can extend their PI research until the end of July 2009.

PIs were requested to submit their interim report by the end of January 2008, and the reports together with their original research proposal documents were evaluated by an independent expert group contracted with JAXA.

After the evaluation by the experts, the JAXA RA Evaluation Board re-evaluated the results and decided which PIs could continue their research. One hundred and ninety two PIs in total passed the interim evaluation (see the table below for more details).

Table 2.1.3-11 Results of Interim Evaluation (as of June 30, 2008)

PI category	Passed	Failed	Resigned
PIs Selected in RA #1 (127 PIs)	97	25	5
PIs Selected in RA #2 (101 PIs)	95	6	0
Total (228 PIs)	192	31	5

Most of the failed PIs did not submit their reports. Such PIs in the RA #1 category may not have intended to participate in this RA research because they were selected a long time ago (in 2000).

#### 8) ALOS www

We previously maintained two web sites:

- 1) General ALOS information <http://www.eorc.jaxa.jp/ALOS/index.htm>
- 2) Principal Investigators (PIs) <http://www.eorc.jaxa.jp/ALOS/ForPI/index.htm>

The general ALOS site, established on January 6, 2006, with the sample top page in Fig. 2.1.3-31, has an "Image Gallery" with 60 images. The site also contains the science plan, research announcement (RA), project and symposium information as well as satellite and sensor characteristics. We maintained the site for the CAL/VAL and Science Team (CVST) to facilitate sharing information on CAL/VAL test sites, data acquisition plans, technical information, and meeting information.

The site for RA PIs presents information on PIs, i.e., the PI list including names, organizations, research titles, e-mail addresses, telephone numbers, PI workshop, ALOS simulation data for research activities, and research agreement related documents.



Fig. 2.1.3.8-31 Top Page of ALOS@EORC Website

## 9) Satellite data utilization for disaster monitoring

Responding to emergency calls, quick actions on data acquisition, extraction of the disaster area, and dissemination of data and analysis results, are requirements of ALOS for disaster mitigation applications. The International Disaster Charter, Sentinel Asia, and JAXA's internal and external efforts are the main body and drivers for this purpose. During the past few years, a number of large-scale disasters have occurred, such as the Solomon M 8.2 earthquake on April 10, 2007, the Wenchuan earthquake on May 12, 2008, and the large-scale cyclone (Nergis) in Burma, and the number of emergency actions JAXA has responded to have increased to a total of 94 events (as of Feb. 2, 2009). According to statistics, flooding, hurricanes, earthquakes, volcano eruptions, mountain fires, landslides, and oil spills represent the main classes of disasters. Samples of images distributed by JAXA are presented in Fig. 2.1.3.8-32.

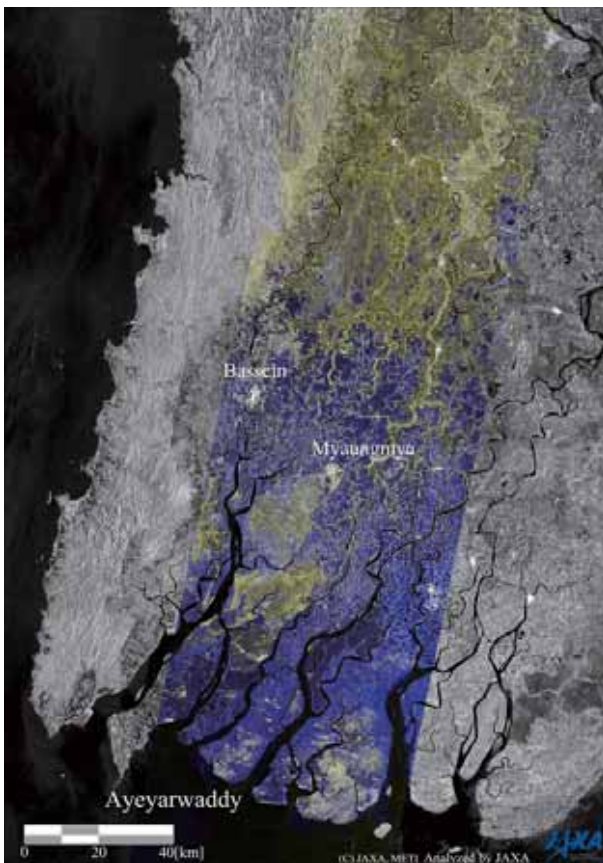
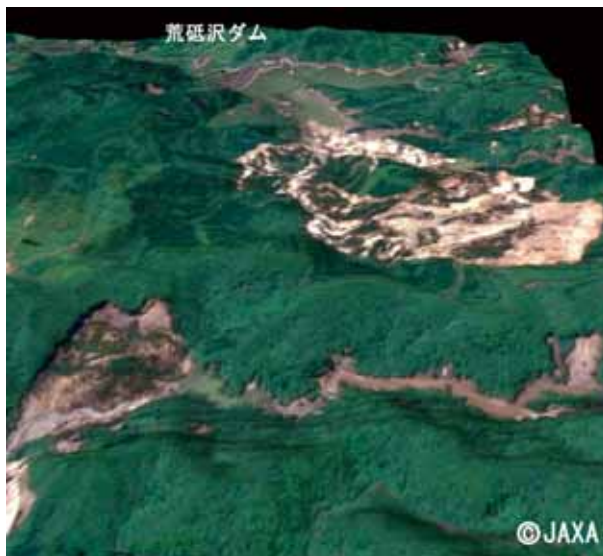


Fig. 2.1.3.8-32 Images for Disaster Mitigation. The top image shows the landslide of the Iwate-Miyagi earthquake observed by PRISM/AVNIR-2, and the bottom image is of the flooded regions of the Irrawaddy, obtained from two-season PALSAR data.

## 2.1.2 TRMM and GPM

### 1) Overview

The Tropical Rainfall Measuring Mission (TRMM) is entering its twelfth year of operation. NASA evaluates all operating missions every 2 years and TRMM was evaluated last in 2007. They decided that the TRMM satellite will continue operation through FY 2009, and is warranted to extend through FY 2011, depending upon spacecraft/instrument health. There is no significant change of satellite operation from the previous year. Based on accumulated data, we have compiled an 11-year rainfall record in the tropics.

A Phase C study of the Global Precipitation Measurement (GPM) mission has been conducted. The GPM algorithm development team has continued developing advanced retrieval algorithms for precipitation using GPM/Dual-frequency Precipitation Radar (DPR) and constellation satellites since last year.

The science team for precipitation study that consists of Principal Investigators (PIs) of the fifth Research Announcement (RA) and algorithm developers of TRMM and GPM/DPR on cooperative/contract research was established in 2007 and continues its activities.

We are contributing to studies of changes to the water cycle through those activities.

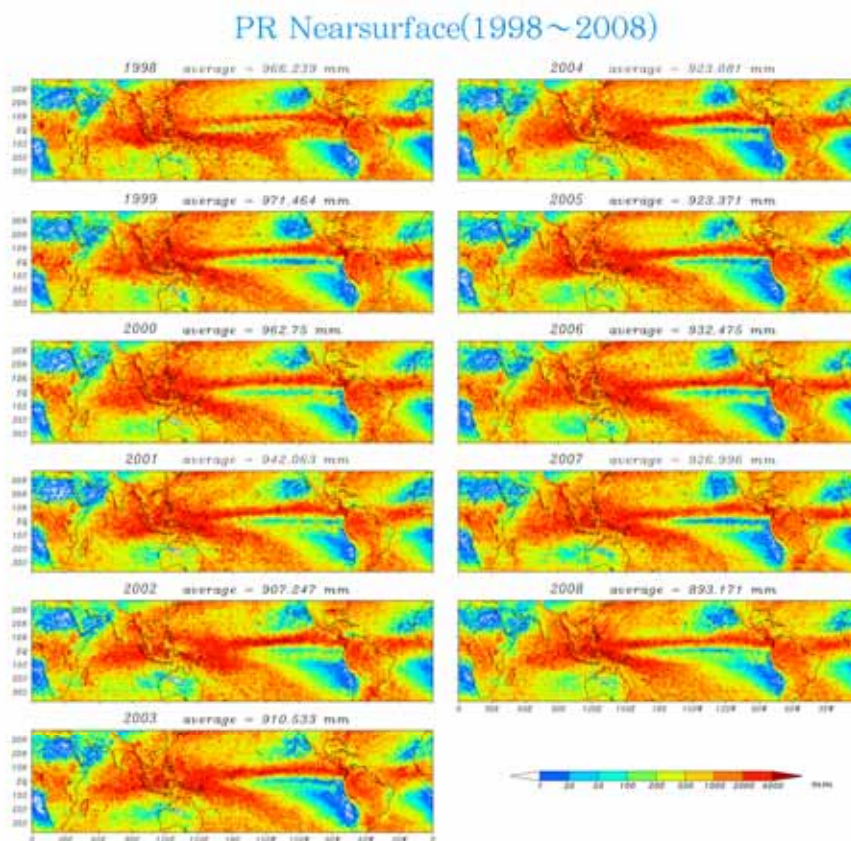


Fig. 2.1.1-1 Annual accumulated rainfall from 1998 to 2008 measured by PR

## 2) Eleven-year record of rainfall by TRMM Precipitation Radar (PR)

We have been evaluating monthly rainfall in the tropics from 1998 to the present. The primary data of PR is the monthly rainfall map covering 35°N to 35°S. The observation area covers half of the Earth. We can clearly identify the regional features of rainfall such as those in the Intertropical Convergence Zone (ITCZ), the arid desert, and the monsoon region as well as their interannual variations. Climatological statistics of precipitation are becoming reliable by long observations of TRMM satellites.

## 3) Research highlights

### a. Analyses of the tropical cyclone using the near real-time global satellite rainfall map

Tropical cyclone “Nargis” directly hit the coastal area of Myanmar on May 2-3, 2008, and caused severe social losses. JAXA/EORC has developed and operated a near real-time data processing system and distributed the global rainfall product (GSMaP\_NRT) via the Internet (<http://sharaku.eorc.jaxa.jp/GSMaP/>) as a prototype of the GPM product. Using the GSMaP\_NRT data, we can compare Cyclone Nargis and Cyclone Sidr, which hit the coastal area of southern Bangladesh during November 10-16, 2007, in terms of accumulated rainfall amount and see differences of rainfall distributions between both tropical cyclones. In the case of Sidr, heavy rainfall was distributed along the cyclone track. On the other hand, heavy rainfall spread over the Bay of Bengal in the case of Cyclone Nargis, which suggests that the atmosphere there at that time was unstable.

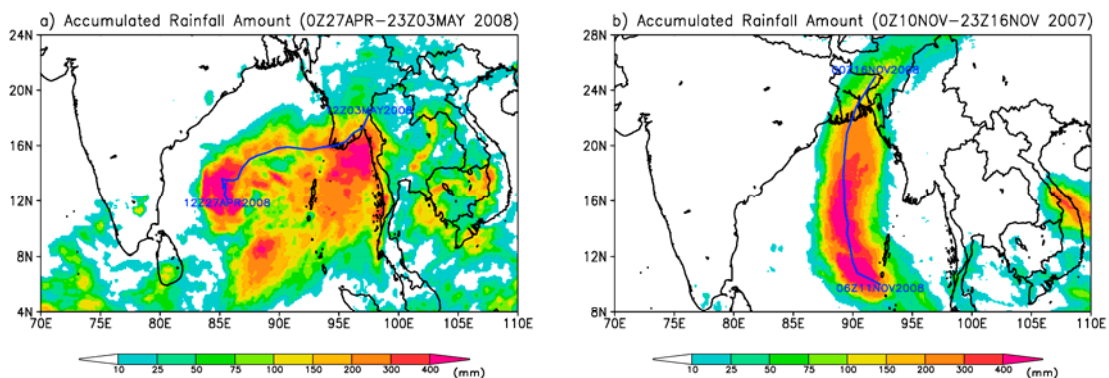


Fig. 2.1.1-2 Accumulated rainfall amount, calculated by the GSMaP\_NRT (mm)

The analyzed period is during a) April 27 and May 3, 2008, for Cyclone Nargis, and b) November 10-16, 2007, for Cyclone Sidr. Blue lines in the figures indicate center positions of the cyclones.

### b. Latent heat research product released on May 16, 2008

The retrieval algorithm of latent heating profile from TRMM three-dimensional precipitation data is developed in joint research with Prof. Takayabu of the Univ. of Tokyo. The estimation of latent heat release from precipitation is an important objective of TRMM. It is essential information to study the global water and energy cycle. The products are expected to contribute to improvement of the global circulation model and other research for global changes.

The latent heat research product based on the Spectral Latent Heating (SLH) algorithm (Shige, Takayabu et al. 2004, 2007) released on May 16, 2008. The algorithm uses TRMM/PR information (convective/stratiform classification, precipitation top height (PTH), precipitation rates at the surface, melting level, etc.) to retrieve heating profiles utilizing lookup tables. Heating profile lookup tables for the three rain types —convective, shallow stratiform, and anvil rain (deep stratiform with a melting level)—were derived from numerical simulations of tropical clouds utilizing a cloud-resolving model (CRM). For convective and shallow stratiform regions, the lookup table is based on the PTH. However, PR cannot observe PTH accurately enough for the anvil regions because of its insensitivity to the small ice-phase hydrometeors. Thus, for the anvil region, the lookup table refers to the precipitation rate at the melting level instead of PTH.

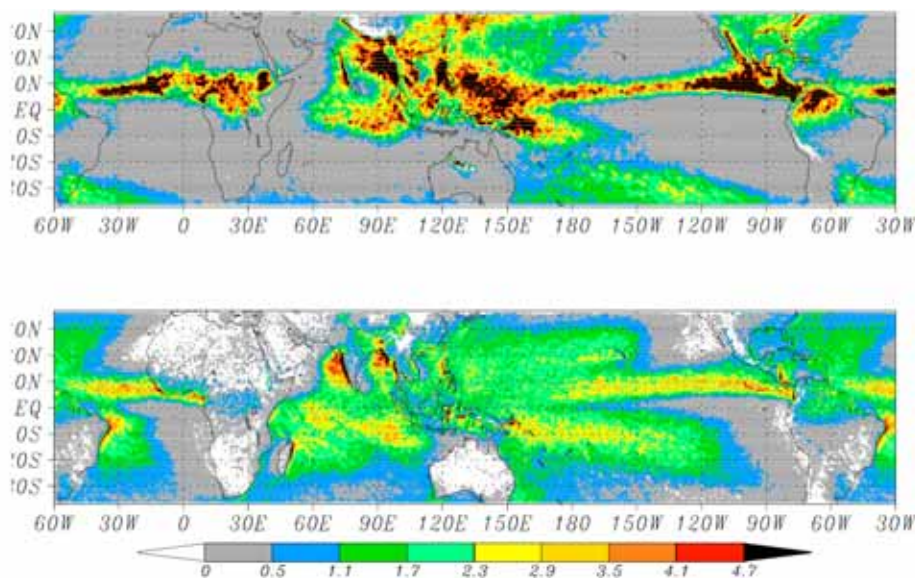


Fig. 2.1.1-3 Estimated amount of climatological latent heat release from precipitation by the TRMM/PR during December-February (a) Altitude 7.5 km, (b) Altitude 2 km. The data were averaged during 1998-2007.

#### 4) Outreach

##### a. EORC/Web pages for drawing TRMM data using Google Earth

We have started providing Web pages for drawing TRMM data using Google Earth. Users can easily make figures by combining the TRMM real-time monitoring for tropical cyclones, TRMM Sea Surface Temperature (SST), Global Rainfall Map in Near Real Time (GSMaP\_NRT), Radar, and Precipitation Nowcast over Japan, and Typhoon Images and Information on Google Earth. We attached information on Google Earth Training and the introduction of the TRMM. The pages are available from the following Web page:

[http://www.eorc.jaxa.jp/TRMM/data/trmmxge/google\\_earth\\_e.html](http://www.eorc.jaxa.jp/TRMM/data/trmmxge/google_earth_e.html).

**TRMM X Google Earth Lab.**  
 What happens when you combine Google Earth and TRMM? [Japanese]

Let's enjoy TRMM data by using "GoogleEarth"  
 You will see new collaboration between TRMM and GoogleEarth from our laboratory.

**Google Earth Training**  
 Getting the information for using Google Earth with Earth Observation Satellite Images

**What's TRMM**  
 Introducing you to TRMM, where does it move? What can be observed?

**Chase the Typhoon**  
 Viewing the birth and death of Typhoons on Google Earth

**How to download Google Earth KML files**  
 1) Check contents you want from below  
 2) Click the [Generate KML - Download] button.

Contents	No content is added		
	1 Look for 1. baby	2 Forecast 2. Route	3 Observation 3.
<input type="checkbox"/> TRMM real-time monitoring for tropical cyclones <a href="http://www.eorc.jaxa.jp/TRMM/TC/typhoon/">http://www.eorc.jaxa.jp/TRMM/TC/typhoon/</a>		●	●
<input type="checkbox"/> TRMM Sea Surface Temperature (SST) <a href="http://www.eorc.jaxa.jp/TRMM/data/monitoring/day_or_night/_a.htm">http://www.eorc.jaxa.jp/TRMM/data/monitoring/day_or_night/_a.htm</a>	●	●	
<input type="checkbox"/> Global Rainfall Map in Near Real Time <a href="http://www.eorc.jaxa.jp/GSMAP/">http://www.eorc.jaxa.jp/GSMAP/</a>	●		
<input type="checkbox"/> Radar and Precipitation Nowcast: Japan <a href="http://www.jma.go.jp/jma/techres/300/">http://www.jma.go.jp/jma/techres/300/</a>			●
<input type="checkbox"/> Digital Typhoon: Typhoon images and information <a href="http://www.cgd.cma.gov.cn/digital/typhoon/">http://www.cgd.cma.gov.cn/digital/typhoon/</a>			●
<input type="checkbox"/> Google Earth Blog : Hurricanes - Live positions (Forecast route) <a href="http://www.gsemlab.org/">http://www.gsemlab.org/</a>		●	●

[Generate KML - Download]

Fig. 2.1.1-4 Example of the TRMM X Google Earth Laboratory

b. TRMM observation of Cyclone Nargis

We reported the TRMM observation results of Cyclone Nargis causing severe social losses in Myanmar to the press on May 8, 2008.

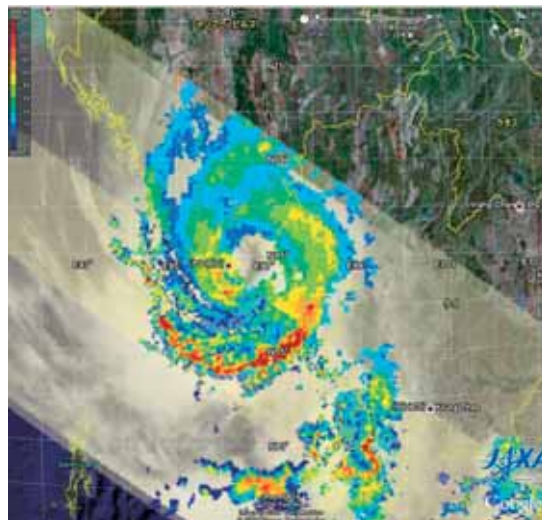


Fig. 2.1.1-5 Surface rain rate by TRMM/PR and TMI on 0:44Z May 3, 2008, around Myanmar (Orbit number: 59618)

## 5) Activities for science

## a. Japanese Precipitation Measurement Missions (PMM) Science Team

Japanese PMM Science Team has continued TRMM/GPM research since last year. The team is organized by fourteen PIs selected through the fifth Precipitation Science Mission Research Announcement (RA), three TRMM/PR standard algorithm developers on cooperative/contract research, and one DPR/GMI combined algorithm developer on contract research. The annual meeting was held on Jan. 26-27, 2009, as a JAXA-NASA joint PMM team meeting.

## b. The first GPM Japan-U.S. joint algorithm meeting

The first GPM Japan-U.S. joint algorithm meeting was held on Jan. 28-29, 2009, continuing from the PMM Science Team meeting. There was a plenary session and three splinter sessions corresponding to DPR, DPR/GMI combined and Radiometer/GSMaP algorithm sub groups.

## c. The second Global Precipitation Measurement (GPM) Asia Workshop

The second Global Precipitation Measurement (GPM) Asia Workshop was held in Hamamatsu City, Japan on June 2-4, 2008. There were 45 participants, including 14 participants from 10 countries/13 agencies of Asia, that discussed possible cooperation in application of satellite precipitation data and ground validation.

### 2.1.3 EarthCARE/CPR

#### 1) Background and significance

JAXA and the National Institute of Information and Communications Technology (NICT) are conducting a Phase B study of the Earth Clouds, Aerosols and Radiation Explorer (EarthCARE), together with the European Space Agency (ESA). A new project team was established to start the development phase in the latter half of FY 2008. EarthCARE has been selected as the sixth Earth Explorer mission of ESA and it is planned to be launched in 2013 for a 3-year mission.

#### 2) Overview of the instrument

The objectives of EarthCARE are to observe the three-dimensional distribution and microphysical characteristics of aerosols and clouds while simultaneously measuring the precise Earth radiation budget. The observation will reveal the interaction of aerosols and clouds, and their radiative effects on the climate, which is a significant process in the climate system.

JAXA and NICT are to provide the Cloud Profiling Radar (CPR), which is one of two core sensors on EarthCARE. The CPR is a 94-GHz radar with a Doppler measurement mode that employs a 2.5-m-diameter carbon fiber reinforced plastic (CFRP) core/skin reflector to achieve a high sensitivity of -35 dBZ. The horizontal resolution is 500 m and the vertical resolution is also 500 m with 100-m over-sampling. The pulse repetition frequency is variable between 6100 and 7500 Hz. Peak power of a radar pulse is 1.5 kW (@ End of Life).

#### 3) Study in FY 2008

A full-size antenna (2.5-m diameter with CFRP core/skin) was manufactured and tested to confirm its high surface accuracy.

Study results of the CPR in the pre-development phase were summarized and verified at the system definition review. The project approval review was held in the first quarter of FY 2008. Subsequently, the EarthCARE/CPR project team was organized. The development phase was started and the series of preliminary design reviews have begun. The memorandum of understanding (MOU) with cooperating organizations (i.e., ESA and NICT) was detailed and prepared for authorization.



Fig. 2.3.3-1 EarthCARE satellite configuration



Fig. 2.3.3-2 CPR configuration

The EarthCARE science team, mainly consisting of algorithm development researchers, was organized. The CPR, CPR+ATLID, ATLID, and MSI algorithms have been studied by the team. The science team drafted the first version of the JAXA EarthCARE Science Plan document as a complement to the Algorithm Theoretical Basis Document (ATBD), which had been drafted the previous year.

### 2.1.4 GCOM

In addition to conducting continuous research using ADEOS-II and AMSR-E data, we have been defining the mission objectives, examining appropriate sensor capabilities and performance, and investigating the feasibility of new products and algorithms of the Global Change Observation Mission (GCOM) based on ADEOS-II experience and are going to use “GCOM” to cover all ADEOS-II and GCOM activities. Japanese fiscal year 2008 was the first year of research activities solicited via the GCOM 1<sup>st</sup> research announcement (RA). The activities covered algorithm development, validation preparation, and data application for the GCOM-W1, which is the first satellite of the GCOM series. From January 13 to 15 of 2009 in Yokohama, we held the public GCOM Symposium followed by the first GCOM-W1 Principal Investigator (PI) Workshop and the briefing session for the GCOM-C1, which will be the second satellite of GCOM series. The GCOM-W1 PI workshop was the first opportunity to gather the selected PIs and discuss the research direction. The GCOM-C1 briefing session was to explain the GCOM 2<sup>nd</sup> RA, which was devoted to the development of retrieval algorithms, fundamental data acquisition and validation preparation, and application research directly connected to the GCOM-C1 data.



Fig. 2.1.4-1 Photos of GCOM symposium (left) and GCOM-W1 PI workshop (right)

GCOM consists of two satellite series: GCOM-W (Water) and GCOM-C (Climate). Each series will have multiple generations (e.g., three generations) with a 1-year overlap to obtain long-term and consistent data records. GCOM-W1 and GCOM-C1 are the first generation of satellites in the GCOM series. The Advanced Microwave Scanning Radiometer-2 (AMSR2) and the Second-generation Global Imager (SGLI) will be the respective mission instruments of GCOM-W1 and GCOM-C1. Following the GCOM-W1, the GCOM-C1 project was initiated in the middle of Japanese fiscal year 2008. Development of GCOM-W1 proceeded to Phase-C after the preliminary design review (PDR).

In January 2009, the special issue for GLI and AMSR research was published in the Journal of the Remote Sensing Society of Japan. The special issue summarized the related research activities of GLI, AMSR, and AMSR-E, as well as provided a basis of reference for the GCOM mission. The issue contained 35 papers contributed by domestic and international authors.

**1) Research and data analysis for AMSR, AMSR-E, and AMSR2**

The AMSR-E instrument successfully completed its 3-year mission life in 2005. It is continuing to perform global observation today. As of May 2008, 6 years of global observation records have been acquired. Data products are being used by a wide variety of scientific programs and communities, including the Coordinated Enhanced Observing Period (CEOP). All the operational users, including the Japan Meteorological Agency (JMA), the Japan Fisheries Information Service Center (JAFIC), the National Oceanic and Atmospheric Administration (NOAA), and the Canadian Ice Service, use the AMSR-E products continuously. The antenna motor torque of the instrument has been gradually increasing since the summer of 2006, and sometimes has rapid increasing peaks. The operation team at JAXA's Earth Observation Center is carefully monitoring this phenomenon with NASA's Aqua operation team, but actual observation data (i.e., brightness temperatures) are not affected. All other Aqua mission instruments, except the Humidity Sounder for Brazil (HSB), are still performing global observations.

Although we have not revised the standard retrieval algorithms for AMSR and AMSR-E in this fiscal year, continuous updates of the dynamic parameters for sea surface temperature (SST) retrieval were performed.

**a. Calibration and data evaluation**

Although post-launch calibration activities to improve the quality of brightness temperature ( $T_b$ ) products were continued, we have not updated the  $T_b$  product version this year as we have identified issues in the current calibration procedure. In addition, we have been continuously working on geometric calibration issues. In this year, we have almost identified the appropriate offset values in the instrument alignment and off-nadir angles for both AMSR and AMSR-E. Also related to calibration activities, we have been collaboratively working with the Global Precipitation Measurement (GPM) community for inter-sensor calibration among multiple microwave radiometers. As preparation for AMSR2 on GCOM-W1, we have been prototyping the AMSR-E spatially consistent brightness temperatures among different frequency channels. For AMSR2 processing, this will be defined as a new Level-1 product.

**b. Algorithm development and validation**

PIs and EORC researchers have updated retrieval algorithms for AMSR and AMSR-E on the EORC processing system. These include algorithms for retrieving SST, soil-moisture, and sea ice concentration. For the soil moisture algorithm, global applicability was improved by carefully considering the effects of vegetation and surface roughness. Regarding algorithm development for GCOM-W1, the selection or integration procedure was discussed and agreed at the PI workshop. For the sea ice concentration, it was proposed to unify the two major algorithms. For the precipitation algorithm, there was only one candidate that was able to retrieve global precipitation over land and ocean. For other geophysical parameters, algorithm comparison studies were proposed. The comparison results will be presented and discussed at the next PI workshop.

**c. Field campaigns**

Two monitoring activities have been underway: the ADEOS-II Mongolian Plateau Experiment for Ground Truth (AMPEX) and snow-depth measurement on the Yakutsuk and Tibetan Plateaus. The former is being led by Professor I. Kaihotsu of Hiroshima University, and the latter, by Professor T.

Koike of the University of Tokyo, both as AMSR2 PIs. Since the monitoring sites of these parameters are quite sparse worldwide, the measurements are valuable and are decided to be maintained as a GCOM-W1 activity.

#### d. Other activities

JMA is currently using microwave radiometer data including AMSR-E for the mesoscale numerical prediction model (used for small-scale weather forecasting around Japan) and the global numerical prediction model (e.g., used for better forecasting of typhoon movement). In April 2008, JMA started to use the maximum wind speed from microwave radiometers including AMSR-E for typhoon analysis. The maximum wind speed from microwave radiometers is being used to help in correcting analysis based on infrared measurements from geostationary satellites. We are continuing development of an all-weather wind-speed algorithm that uses the AMSR-E low-frequency channels of 6.9- and 10.65-GHz bands. The RSMC Tokyo-Typhoon Center of JMA is testing the product for their operational applications. The Numerical Prediction Division of JMA also performed research on using the product to complement the lack of assimilation data under cloudy conditions. Figure 2.1.4-2 shows the improvement of maximum wind speed forecasting using the AMSR-E all-weather wind speed as the information under cloudy conditions.

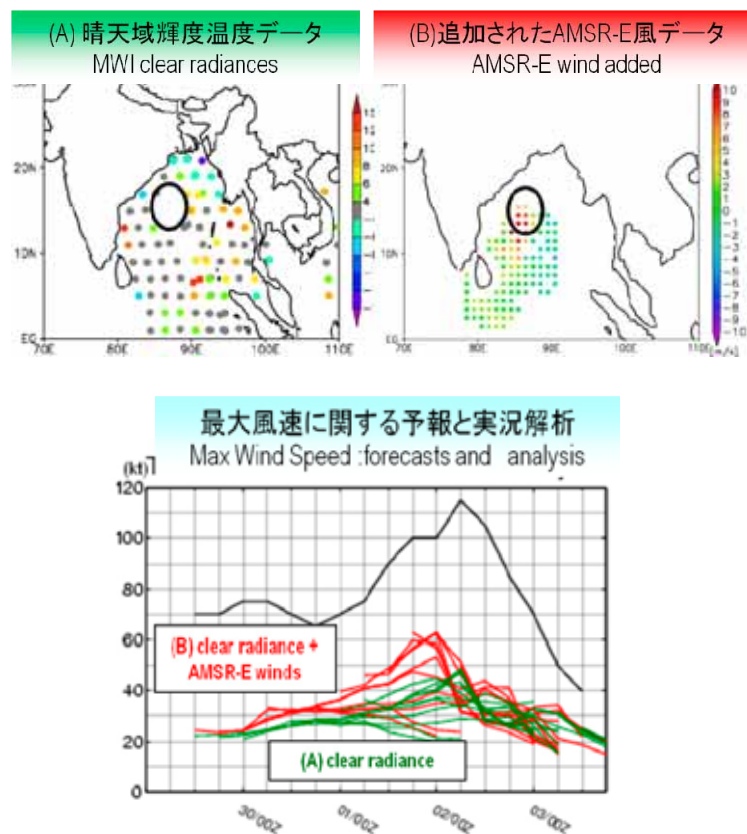


Fig. 2.1.4-2 Example of improvement in maximum wind speed forecasting using AMSR-E all-weather wind speed for Cyclone Nargis passing over the Indian Ocean in May 2008. Upper-left and -right panels show microwave radiances under a clear sky, which is usually used for forecasting, and AMSR-E all-weather wind speed. The lower panel shows analysis (black), a forecast using just clear microwave radiance (green), and a forecast using AMSR-E winds in addition (courtesy of the Numerical Prediction Division, Forecast Department, JMA).

Initially responding to the AMSR-E torque increase, we have started work on geophysical parameter retrieval using Tb from the TRMM Microwave Imager (TMI) and WindSat radiometer aboard the Coriolis satellite. From the importance in operational applications and advantages and uniqueness of the C/X-band channels, SST and soil moisture products were selected to begin with the algorithm development initiate algorithm development. The prototype product of SST was made available to JMA and JAFIC for their testing. We also started the processing of sea ice concentration from WindSat and the Special Sensor Microwave/Imager (SSM/I) radiometers.

Various AMSR-E images and data have been continuously updated on website pages, including SST anomalies in the northern high-latitude ocean, AMSR-E El-Nino Watch, All-weather and sea-surface wind speed. In addition, AMSR-E data have been used in other EORC websites including the real-time global rainfall map maintained by the GPM research project and the AMSR-E sea ice monitor maintained by the International Arctic Research Center (IARC, see the website at <http://www.ijis.iarc.uaf.edu/cgi-bin/seaice-monitor.cgi>). The sea ice extent in the summer of 2008 in the Arctic Ocean, which did not underrun the value in 2007, was monitored continuously by the AMSR-E sea ice-monitoring site. In addition to the homepages shown above, several monitoring activities using AMSR-E data are also continuing. An example of soil moisture monitoring over northeast Argentina is shown in Fig. 2.1.4-3. It was reported that a spell of low rainfall over northeast Argentina during 2008 through 2009 influenced the serious crop damage. Soil moisture trends observed by AMSR-E captured this phenomenon well. Please visit our website “<http://www.eorc.jaxa.jp/AMSR/>” for more information and images.

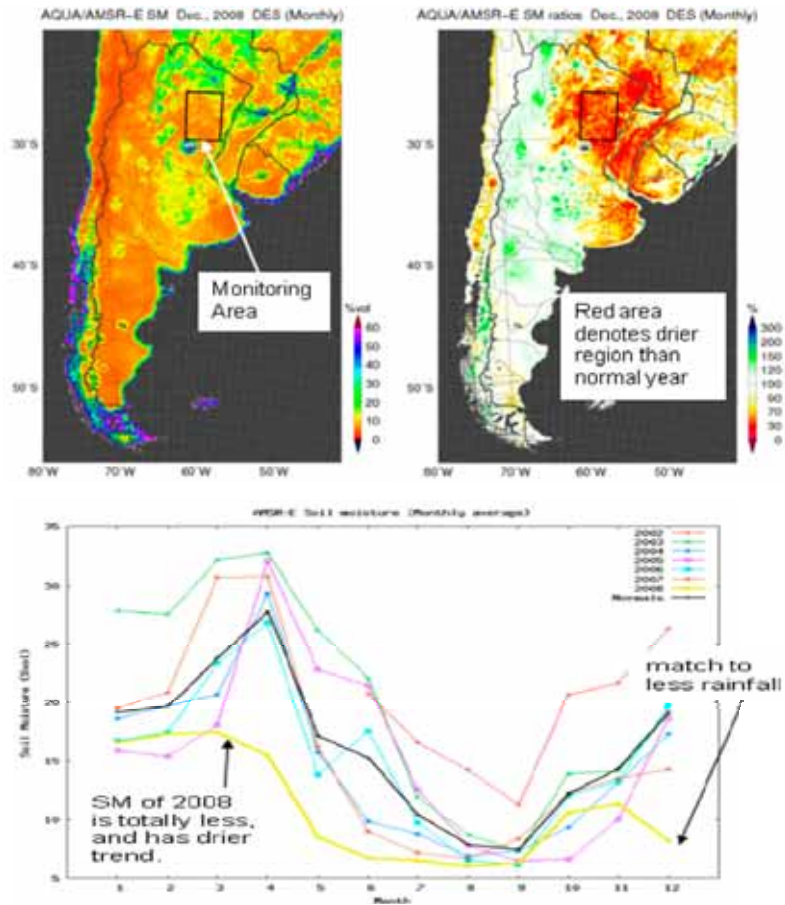


Fig. 2.1.4-3 Example of soil moisture monitoring over northeast Argentina. Upper panels show monthly average of soil moisture in volumetric percentage (left) and its ratio to a normal year (right) for December 2008. The lower panel shows seasonal changes in soil moisture for each year from 2002 to 2008.

## 2) Research and development of Global Imager (GLI) and Second Generation GLI (SGLI)

GLI/SGLI group researchers at EORC continued to analyze MODIS data using standard and/or research algorithms. This year (FY 2008), we conducted the following activities:

- a. Estimation and validation of photosynthetically available radiation (PAR) using MODIS data
- b. Evaluation of atmospheric circulation models outputs, generally used for atmospheric properties retrievals
- c. Development and validation of wildfire detection algorithm using MODIS data
- d. Development of vegetation indices
- e. Evaluation of NASA's Land Long Term Data Record (LTDR) data set
- f. Expansion of the data providing service using MODIS data received at EOC
- g. Data simulation service using radiative transfer

### a. Estimation and validation of photosynthetically available radiation (PAR) using MODIS data

PAR was derived using data from two MODIS on the Terra and Aqua satellites. The derived PAR was evaluated using ground truth observations, which were obtained from Japan Flux, CEOP, AERONET, etc. Figure 2.1.4-4 depicts the MODIS-derived semi-monthly averaged PAR around Japan. A fine structure of the spatial pattern of PAR in summer was successfully captured using MODIS data with a high spatial resolution of 1 km. Also depicted well is the high contrast of PAR between winter and summer seasons.

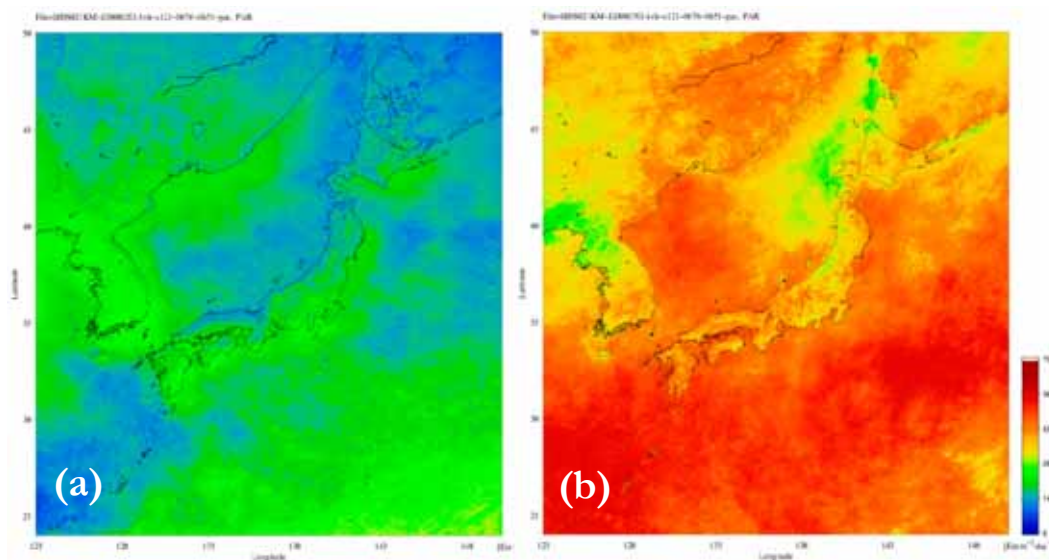


Fig. 2.1.4-4 MODIS-derived semi-monthly averaged photosynthetically available radiation of (a) Feb. 2008 and (b) July 2008.

Comparison results are presented in Fig. 2.1.4-5. It is apparent that MODIS-derived PAR are consistent with those from ground stations, although there are still slight biases in the data from desert and snow covered areas.

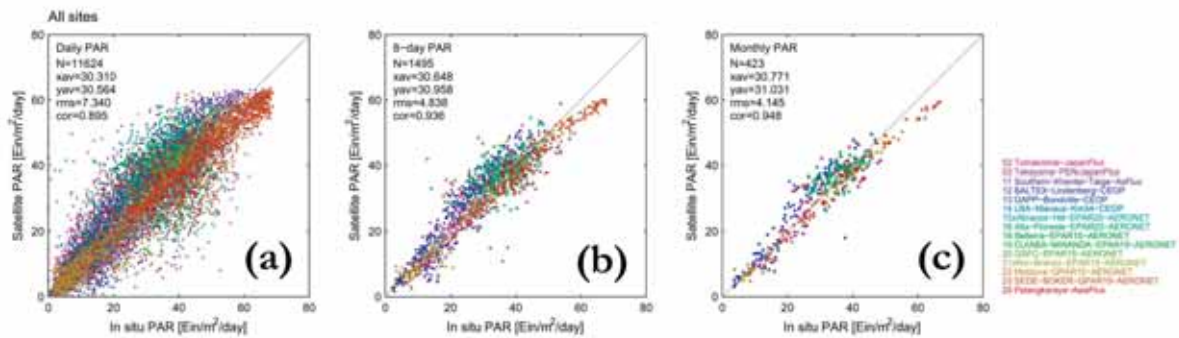


Fig. 2.1.4-5 Comparison of MODIS-derived PAR with those observed at ground station sites (Japan Flux, CEOP, AERONET) (a) daily average, (b) 8-day average, (c) monthly average

### b. Evaluation of atmospheric circulation models outputs, generally used for atmospheric properties retrievals

The accuracy of the atmospheric products obtained from satellite retrievals depends on the capacity of the climate models outputs considered for the algorithms to reproduce properly actual field observations. In addition, as model data can also help to generate some products that may not be generated by satellite data only, it is necessary to verify the degree of reliability of these atmospheric models. Then, the performance of two models outputs (the National center for Environmental protection/Department Of Energy (NCEP/DOE) reanalysis-2 data and the Nonhydrostatic Icosahedral Atmospheric Model (NICAM)) to simulate atmospheric radiances in the upper troposphere is investigated.

To conduct this evaluation, simulated satellite atmospheric properties such as the upper tropospheric brightness temperature (UTBT) and the relative humidity (UTRH) are compared with observations of the Terra/Moderate Resolution Imaging Spectrometer (Terra/MODIS) satellite, which has many spectral characteristics close to GCOM-C/SGLI). Results of these comparisons are interpreted in terms of the influences of atmospheric stability, cloud emitting properties, and cloud convection processes.

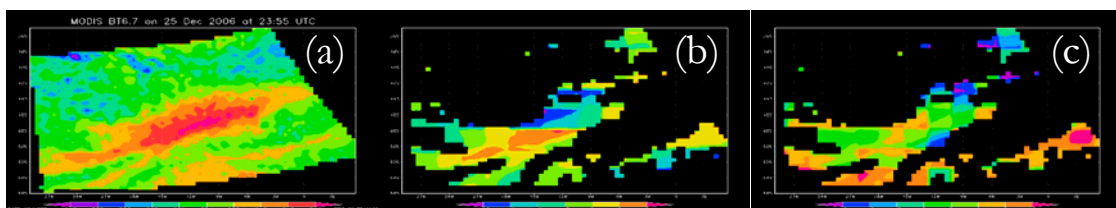


Fig. 2.1.4-6 (a) MODIS observed brightness temperature at water vapor channel (6.7um), (b) brightness temperature difference between MODIS observation and simulation with NCEP/DOE, (c) same as (b) with NICAM.

The study shows that the depiction of water vapor properties in the upper troposphere is relatively close between the NICAM and the NCEP/DOE results. NCEP/DOE appears to show lesser discrepancies with satellite observations than NICAM simulations (Fig. 2.1.4-6). Differences tend to be high (NICAM and NCEP/DOE UTBT are underestimated and UTRH are overestimated) in unstable atmospheres. NICAM and NCEP/DOE fail to depict properly the degree of atmospheric instability. This implies low values of UTBT. Heat distribution due to clouds, is analyzed through

the cloud effective emissivity. Discrepancies are high in areas of relatively low effective emissivity. More often model UTBT is underestimated. These low effective emissivity areas are zones of reduced cloud fractions. NCEP/DOE fails more often than NICAM to capture the energy variation due to small clouds. NICAM large cloud expansion seems to be limited. Cloud type distribution analyses show that the existence of deep convective clouds creates disturbances, and unstable atmospheres. Large discrepancies are noticed around these areas. As we move away from these areas, model and observations show better agreement. Convection processes are insufficiently enhanced in the model data compared to observations. Simulation results may be improved with the adjustment of cloud resolving parameters such as the cloud amount and types.

### c. Development and validation of wildfire detection algorithm using MODIS data

An algorithm for detecting wildfire has been developed using MODIS data. We made an improvement to the algorithm by adjusting the threshold values for detecting fire spots and taking into account the snow mask, etc. The accuracy of the improved algorithm was evaluated using ASTER high-resolution images. Fig. 2.1.4-7 indicates hot spot distribution detected using the MOD14 algorithm (NASA standard) and the improved algorithm. Analysis results show that our improved algorithm can detect not only small and weak fire spots but also strong smoky fires, most of which cannot be detected with MOD14. As a result, the number of hot spots correctly detected by the improved algorithm increased significantly, by about 80%, while that of false detections decreased by 10% compared with MOD14 results.

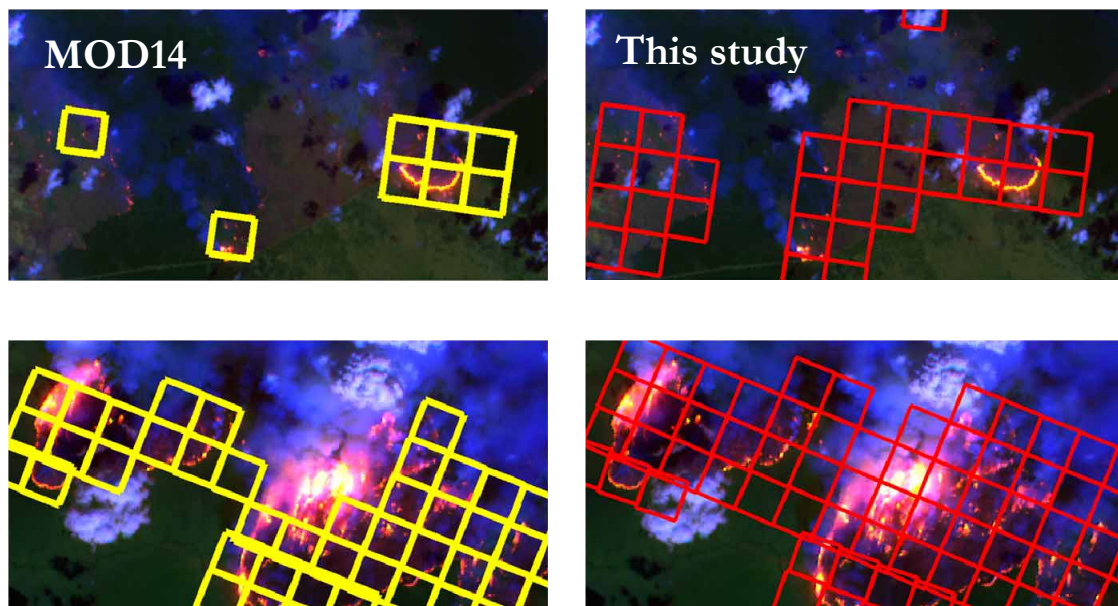


Fig. 2.1.4-7 Spatial distribution of hot spots detected using the MOD14 algorithm (yellow boxes) and the improved algorithm (red boxes). Upper images are weak and small fires and lower ones are strong smoky fires.

### d. Development of vegetation indices

An algorithm for retrieving shadow index (SI) and water stress trend (WST) has been developed for the coming GCOM-C1/SGLI mission. This year the algorithm was applied to global and

long-term satellite data sets, such as MODIS and LTDR (NASA's Land Long Term Data Record using AVHRR data). Figure 2.1.4-8 illustrates a retrieved global map of shadow index indicating that the shadow index is low over forest areas in the cold season in the Northern Hemisphere and becomes high in the hot summer season when leaf volumes are expected to increase.

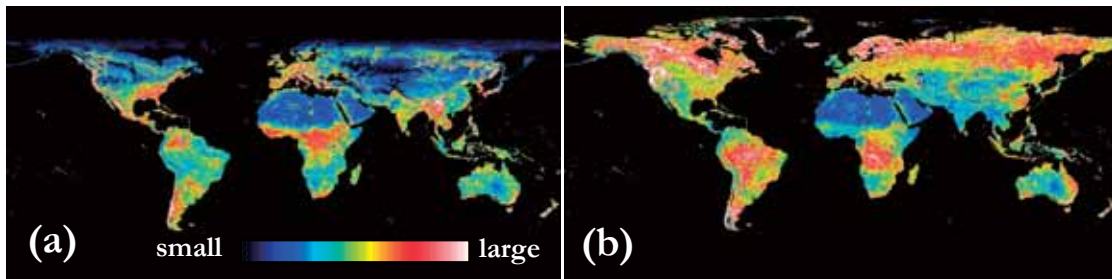


Fig. 2.1.4-8 Spatial distribution of shadow index derived from MODIS data of (a) January 2008 and (b) July 2008.

Figure 2.1.4-9 illustrates spatial distribution of 9-year averaged WST in August (2000-2008) and anomalies of 2002, 2003, and 2004. WST is large at arid regions such as the Sahara Desert and the western United States, etc., while WST is low at humid regions, such as forest areas. Anomaly maps of WST clearly indicate that heavy water stress occurred in Australia in 2002 when an El Nino event occurred. Europe and Alaska also had great stress in 2003 (when attacked by a severe heat wave) and 2004 (when severe wildfires occurred), respectively.

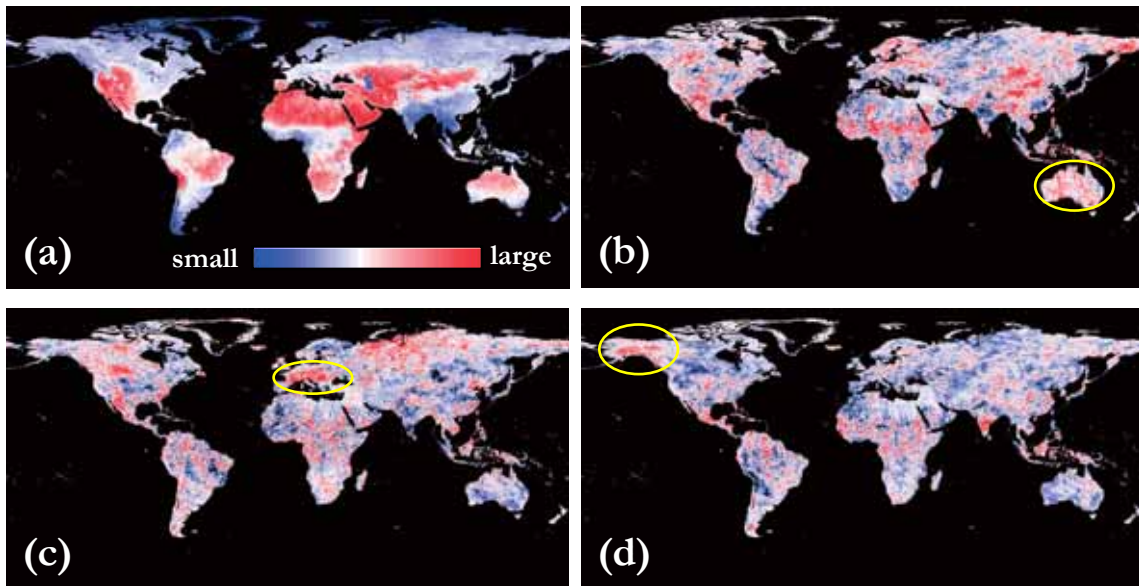


Fig. 2.1.4-9 (a) Spatial distribution of 9-year averaged water stress trend (WST) derived from MODIS data during 2000 to 2008 (August). (b)-(d) spatial distribution of WST anomaly of (b) August 2002, (c) August 2003, and (d) August 2004.

### e. Evaluation of NASA's Land Long Term Data Record (LTDR) data set for cryosphere use

Land Long Term Data Record (LTDR) is a global satellite data set prepared by NASA using AVHRR series data for the studies of land applications such as long-term analysis of vegetation etc. Toward the GCOM-C1 mission, LTDR was obtained from NASA's data archive and evaluated for the cryospheric application, such as the analysis of snow cover extent and cloud cover over the Polar Regions. It is apparent that there are several deficits in the current version of LTDR (ver.2) as the followings; 1) data of both Polar Regions during May 1993 to June 1996 are lost, 2) high latitude area of the Northern Hemisphere are covered with off-nadir data (high sensor zenith angle). In particular, the latter off-nadir data for the Polar Regions will make the quality of snow and cloud cover retrievals poorer because of the much larger footprint at off-nadir angle within a satellite image. Preliminary analysis of LTDR, however, shows there is a slight negative trend of snow cover extent during the last 30 years (Fig. 2.1.4-10), which indicate the validity of the long-term record of the original AVHRR data itself. Thus, we will obtain original AVHRR GAC data for studying long-term trend of various geophysical parameters including snow and cloud covers next year toward the coming GCOM-C1/SGLI mission.

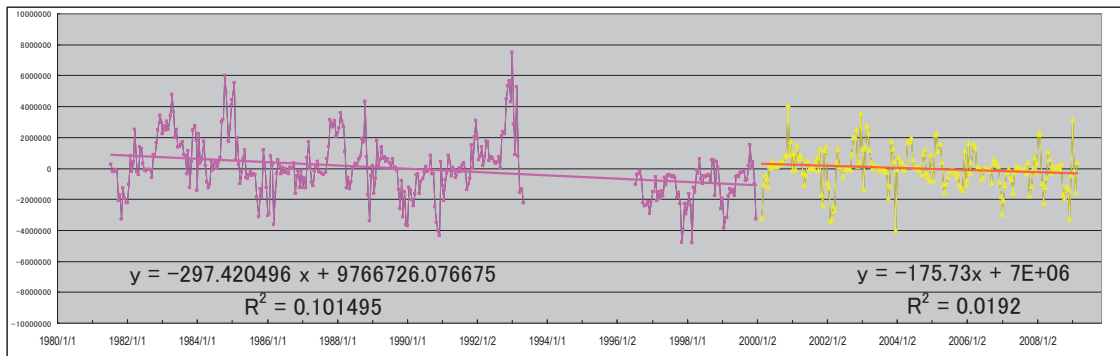


Fig. 2.1.4-10 Long-term trend of snow cover extent (anomaly) in the Northern Hemisphere from 1981 to 2009. The first 20-year (1981-1999) results (pink line) were obtained from LTDR and the later 10-year (2000-2009) results (yellow line) are from MODIS.

### f. Expansion of the data providing service using MODIS data received at EOC

Data from MODIS on NASA's Terra and Aqua satellites data have been received at the Earth Observation Center (EOC) since 2004. Those data have been analyzed to produce ocean color and related products mainly for fishery application uses. This year we expanded the processing system to be able to produce data of photosynthetically available radiation (PAR) and snow cover around the islands of Japan every half month and made the data open to the public through an EORC web site called JAXA Satellite Monitoring for Environmental Studies (JASMES) (Fig.2.1.4-11).

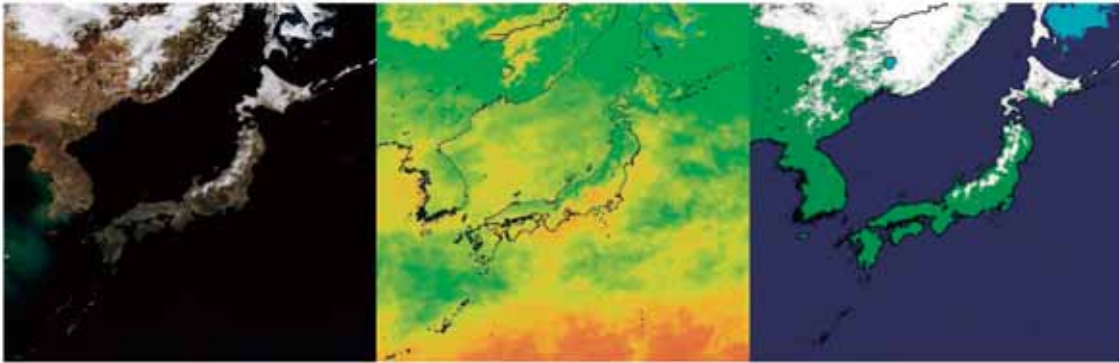


Fig. 2.1.4-11 (a) True color RGB composite image of MODIS data around the Japanese islands in the period of March 16-31, 2009. (b) spatial distribution of photosynthetically available radiation (PAR) of the same period, and (c) the same as (b) except with snow cover. Not only browse images but also binary data of the PAR and snow cover every half month are available at JASMES web (<http://kuroshio.eorc.jaxa.jp/JASMES/index.html>).

#### **g. Data simulation service using radiative transfer**

The GLI Signal Simulator (GSS) is a useful tool for the science and engineering community of Earth observation satellites to simulate top-of-atmosphere radiance. Any scientist, engineer, or general user can use it (<http://bishamon.eorc.jaxa.jp/ENTGSS/index.html>). GSS version 6.8 was released this year. Revisions of GSS from Ver.6.7 to Ver.6.8 include: 1) updating the graph of aerosol volume concentration vertical profile (relative value [no unit]), 2) adding data & graph of the phase function of each aerosol model in each atmospheric layer, and 3) adding relating comments for the above reasons.

## 2.1.5 GOSAT

### 1) Overview

GOSAT seeks to observe greenhouse gases, such as carbon dioxide (CO<sub>2</sub>) and methane (CH<sub>4</sub>), from space through collaboration of the Ministry of the Environment (MOE), the National Institute for Environmental Studies (NIES), and JAXA. The GOSAT satellite carries the Thermal and Near Infrared Sensor for Carbon Observation (TANSO). TANSO is composed of two instruments, a Fourier Transform Spectrometer (FTS) with shortwave infrared (SWIR) and thermal infrared (TIR) bands and a Cloud and Aerosol Imager (CAI) with UV-SWIR bands. JAXA is primarily responsible for instrument and satellite development, launching, operational L0/L1 processing, and post-launch calibration; NIES and MOE are responsible for data utilization of L2 processing and further CO<sub>2</sub> data applications of source and sink inversion under the Kyoto protocol requirements.

The EORC research project is responsible for (1) post-launch calibration and (2) data utilization of the TIR band.

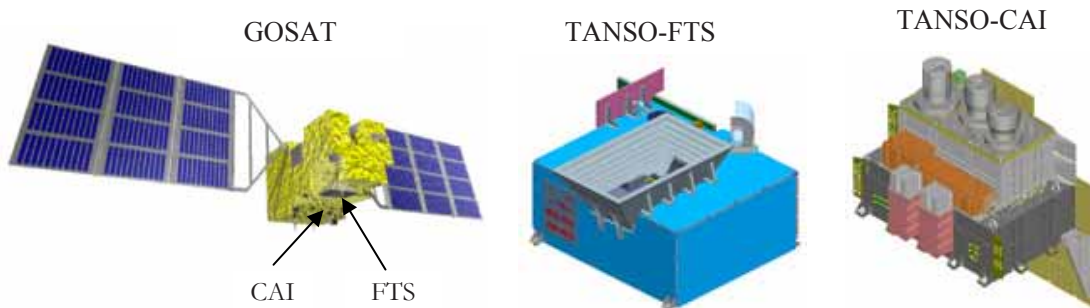


Fig. 2.1.5-1 GOSAT Satellite and TANSO Instruments: GOSAT Satellite (left), Fourier Transform Spectrometer (center), and Cloud and Aerosol Imager (right)

### 2) First data from TANSO-FTS

The Greenhouse gases Observing SATellite (GOSAT) “IBUKI” was launched by HII-A Launch Vehicle No. 15 at 3:54 (UT) on January 23, 2009 from the Tanegashima Space Center and injected into its prescribed orbit about 16 minutes later. The First SWIR and Thermal Infrared (TIR) spectra from the Thermal And Near infrared Sensor for carbon Observation-Fourier Transform Spectrometer (TANSO-FTS) were acquired successfully during its initial functional check.

The observations by the TANSO-FTS and TANSO-CAI when IBUKI passed over Japan at around 1:00 p.m. on February 7, 2009 (JST) are shown in Figures 2.1.5-2~3. The observation points of the TANSO-FTS, which are overlaid on the TANSO-CAI false color composite image, the interferogram taken by the TANSO-FTS, and the light intensity of each wavelength obtained from data from the interferogram are shown in Figure 2.1.5-2. Greenhouse gases (carbon dioxide and methane) absorb infrared signal at specific wavelengths. When Greenhouse gases are concentrated in greater volumes, absorption becomes stronger and light intensity becomes weaker. This figure shows that each absorption line is clearly separated and identified. This data is virtually identical to the simulation data by the National Institute for Environmental Studies (NIES). This shows that the functions of the TANSO-FTS were confirmed nominal as designed.

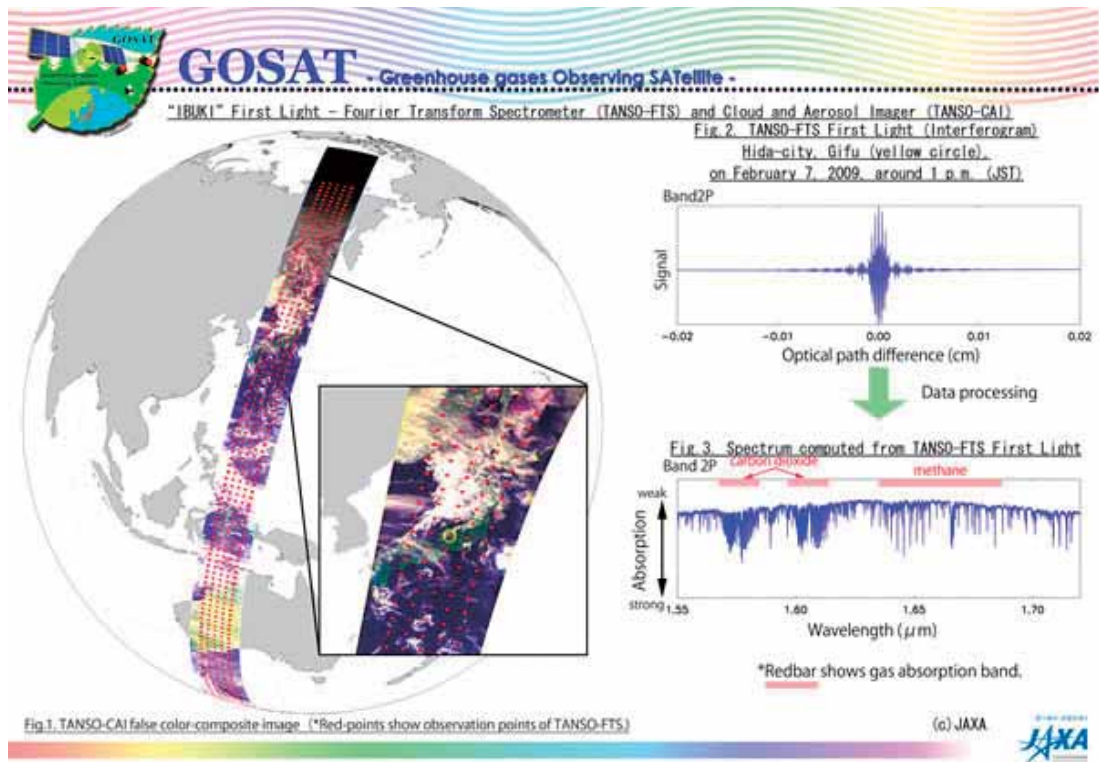


Fig. 2.1.5-2 IBUKI's Observation Data: Spectra and Images from the TANSO-FTS and TANSO-CAI

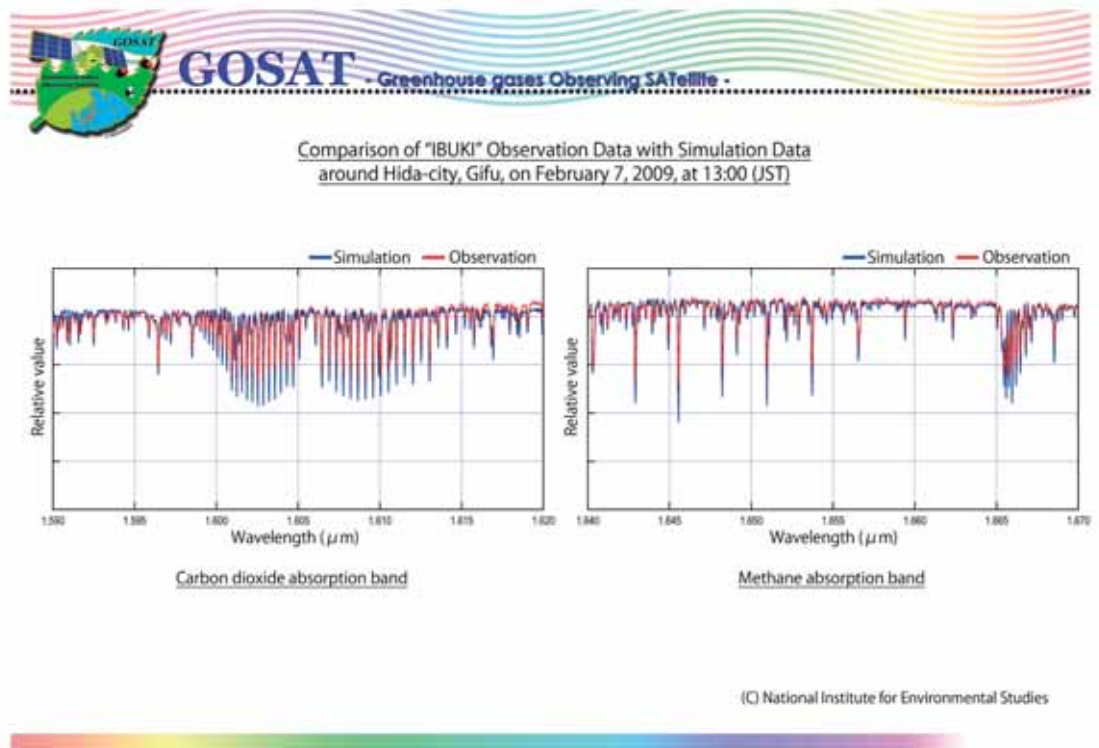


Fig. 2.1.5-3 Comparison of IBUKI Observation Data with Simulation Data

The observation results achieved by the TANSO-FTS thermal infrared band (Band 4) when IBUKI passed over the southern Pacific Ocean at around 7:30 a.m. and Egypt around 8:20 a.m. on March 12, 2009 (JST) are shown in Figures 2.1.5-4~5.

Greenhouse gases, such as carbon dioxide and methane, absorb infrared light at specific wavelengths. Figure 2.1.5-4 depicts the light intensity of each wavelength (spectrum) obtained from data of the TANSO-FTS TIR band. The data for point 1 were acquired over the Pacific Ocean in the daytime, and that of point 2 were acquired over Egypt in the nighttime. The SWIR bands mainly observe in the daytime because they measure the solar spectra reflected from the Earth's surface. However, the TIR band is able to observe in both the nighttime and daytime because it measures the spectra of Earth radiation. This figure demonstrates that each absorption line is clearly visible. We confirmed that the TIR band could observe absorption spectra of carbon dioxide and methane during both the day and night.

Figure 2.1.5-5 shows the observation data and the simulation results. The simulation data was calculated using the radiative transfer model (LBLRTM), sea surface temperature data from the NOAA, and temperature and water vapor profiles from Grid Point Value data of the Japan Meteorological Agency. The comparison demonstrated that the absorption line positions are in good agreement. We could thus confirm that the spectroscope performed as designed.

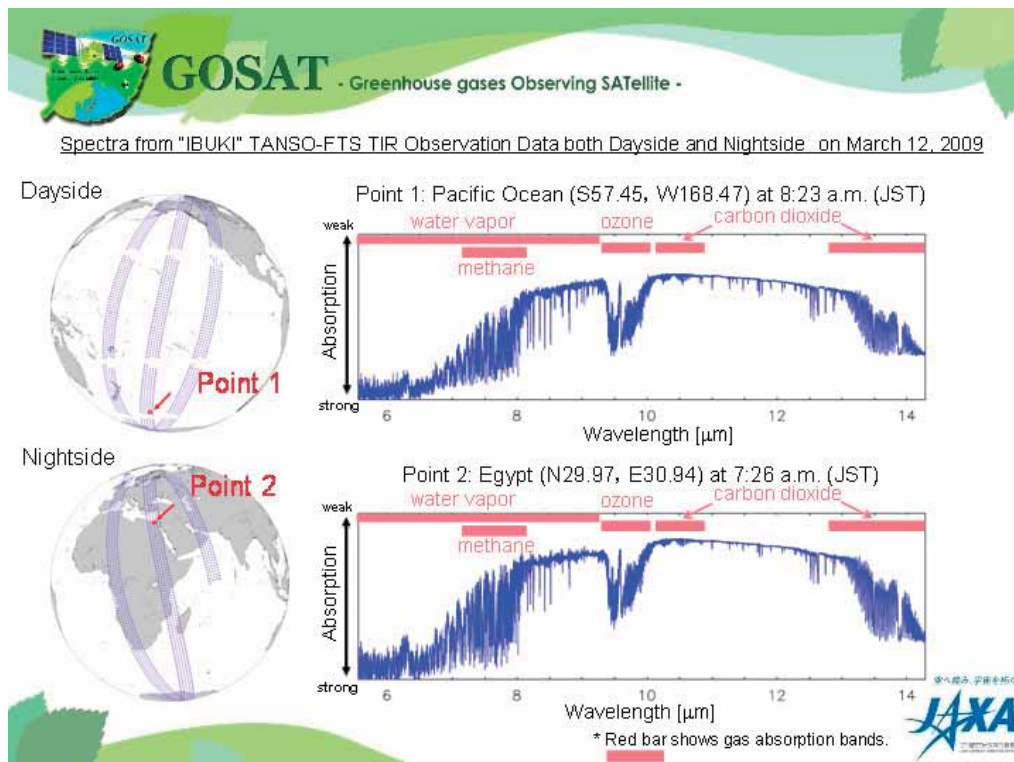


Fig. 2.1.5-4 Light Intensity of Each Wavelength (spectrum) Obtained from Data of the TANSO-FTS TIR Band

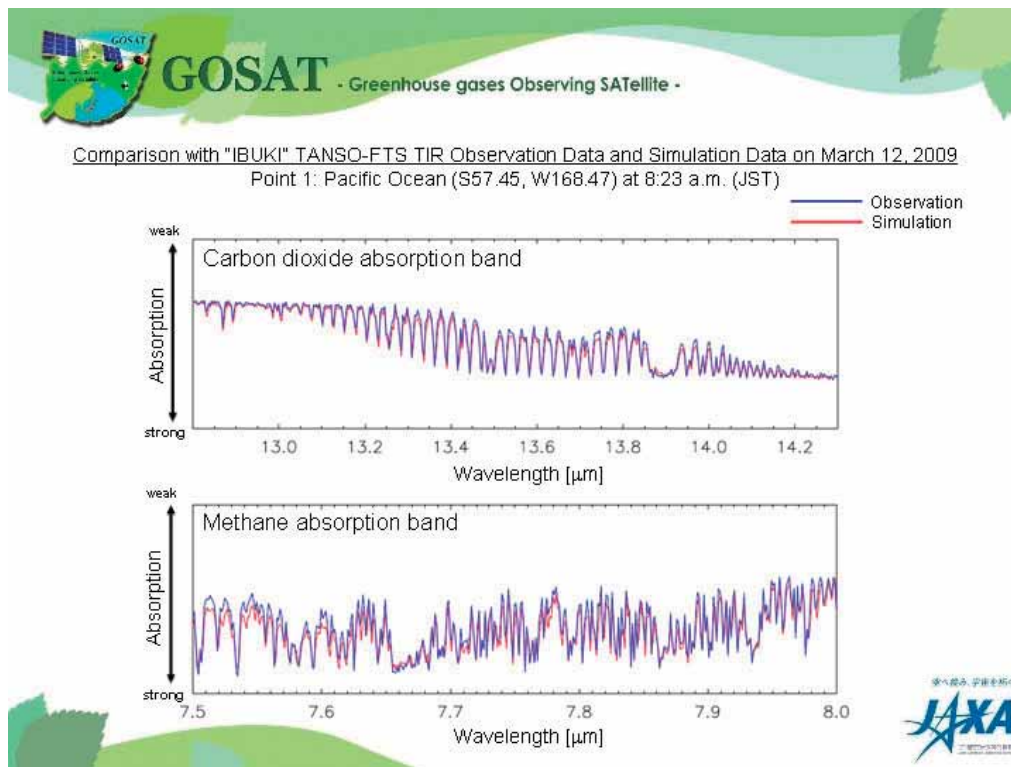


Fig. 2.1.5-5 Observation Data and the Simulation Results

### 3) Calibration

Post-launch calibration of TANSO will be carried out through onboard calibration and vicarious calibration. The FTS-observed radiances are calibrated using high- and low-radiance targets, such as solar irradiance and deep space for the SWIR band and a blackbody and deep space for the TIR band. Lunar calibration will be performed once a year to monitor the stability of sensor sensitivity. CAI onboard calibration data is obtained by nightside observation for noise level. Lunar calibration will also be performed once a year. The CAI observed radiances are calibrated using pre-launch test data and a post-launch vicarious method.

The EORC research project mainly studies the vicarious calibration method and its planning. Vicarious calibration is important because it will be the only way to evaluate sensor characterization other than using onboard calibration systems.

#### a. Calibration sites for ground-based measurements

We are investigating appropriate calibration sites in preparation for the FTS-SWIR. The FTS has a large (10 km) footprint. The calibration sites are preferably twice as large as the footprint due to the pointing accuracy of the FTS. The calibration sites are selected to satisfy the following conditions: (1) large area with homogeneity, (2) high reflectance with small BRDF, and (3) low aerosol and humidity. Both 1.6 and 2.0  $\mu\text{m}$  SWIR signals are absorbed under wet conditions. Figure 2.1.5-2 illustrates the investigation of calibration sites using satellite data. AQUA/MODIS data are suitable for preliminary study of GOSAT because it corresponds to TANSO-FTS observation bands and observation local time. Candidate sites include Tinga Tingana in the Strzelecki Desert, South Australia and Railroad Valley in Nevada. The figures present MODIS radiances for the 2.1  $\mu\text{m}$  band.

The red circle indicates the 10 km FTS footprint. We investigate the homogeneity, robustness against registration error, and time series variation at the candidate sites. The clear sky rate throughout the year is also significant information for field experiments.

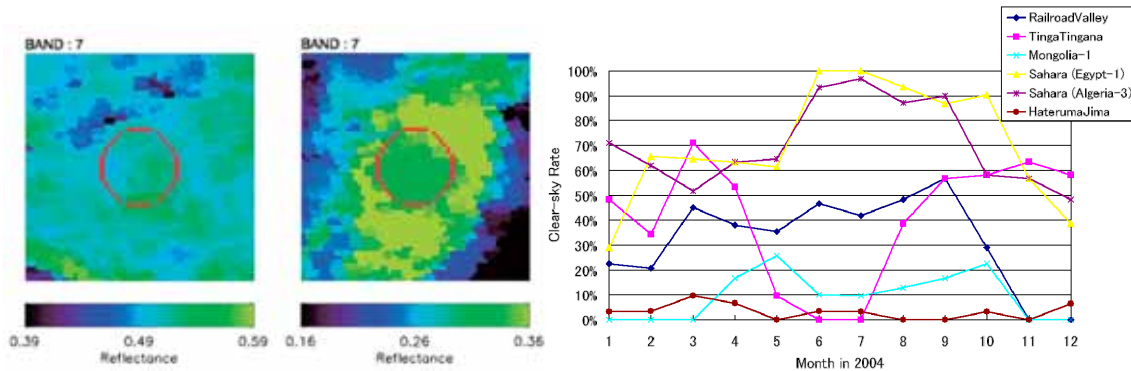


Fig. 2.1.5-6 Investigation of Calibration Sites Using Satellite Data: MODIS Radiance at Tinga Tingana (left), Railroad Valley (center), and Clear-sky Rates at Various Candidate Sites (right)

b. Calibration sites for cross-calibration with well-calibrated sensors on orbit

Selected calibration sites and analysis with available satellite sensor data, such as MODIS, are utilized for cross-calibration with other well-calibrated sensors. Data accumulation enables us to estimate the SNR and sensitivity on orbit.

AQUA/TERRA MODIS global reflectance of 16-day-average data are used as the surface-reflectance data. After we prepared one-year data, we found that 22 data sets are available in this study. The calculated indices are (1) Mean reflectance, (2) STDEV/Mean reflectance in a year, and (3) STDEV/Mean reflectance in 5 x 5 pixels (approximately a 25 km area). Index (2) indicates the time stability in a year; (3) indicates the spatial homogeneity in the large footprint of the TANSO-FTS IFOV. The sites at which indices (2) and (3) are low are appropriate and sufficiently stable and homogeneous for calibration. Figure 2.1.5-3 illustrates these three indices for the candidate calibration site the Sahara desert. The numbers in these index figures indicate priorities at the calibration sites, which are selected for their high homogeneity.

The desert has high reflectivity in the SWIR

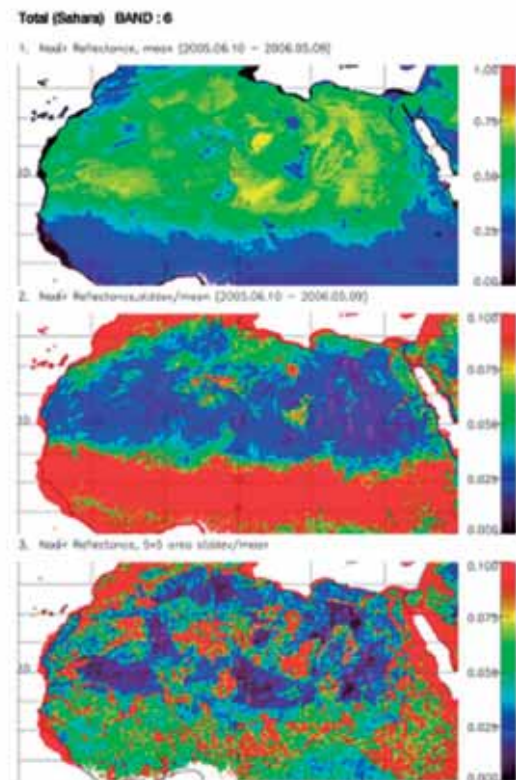


Fig. 2.1.5-7 Sahara Desert Calibration Site (Investigation for FTS and CAI SWIR with High Reflectivity Target)

bands. Several calibration sites were selected in the Sahara Desert (Fig. 2.1.5-3) and Rub Al Khali Desert using MODIS Band 6 (1.64  $\mu\text{m}$ ) data. Deserts have very stable reflectance throughout the year; hence, desert sites are utilized for accumulation of data sets. In-flight calibration of POLDER on ADEOS-I/-II was implemented using the Sahara Desert for performance characterization in orbit. The POLDER site is near the candidate site of this study. At the selected sites, the database of reflectance and BRDF will be prepared for the calibration system, especially for deserts, which are stable over time. Typical parameters are obtained through the current MODIS and multispectral sensor data. The database will work as climatology of surface parameters if we cannot obtain enough match-up data with other operating sensors.

#### c. Geometric correction of TANSO-CAI and -FTS

In this study, we use the 5-km resolution shoreline database GSHHS. The GCPs are selected from locations such as headlands after corner pattern detection along a shoreline. Figure 5 shows the GCPs around Japan that are useful for estimating CAI geometric accuracy.

For the FTS, however, the GCPs should be selected within the observation mesh points. The FTS has a large footprint of 10 km, and the observation points are distributed at a distance. The FTS carries the IFOV monitoring camera, which has 100 m spatial resolution and a 30 km VGA image area. The camera data will be obtained simultaneously with interferograms. The FTS geometric accuracy is estimated using camera data and GCPs selected using the 100-m resolution GSHHS.



Fig. 2.1.5-8 GCPs from 5-km resolution of GSHHS Database

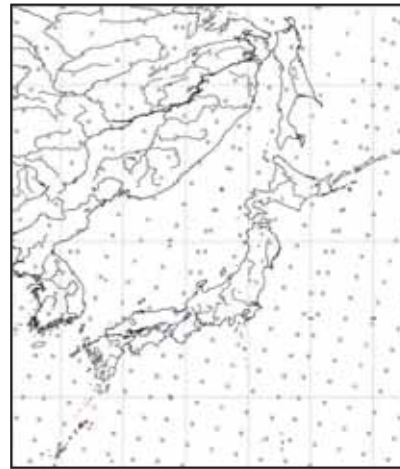


Fig. 2.1.5-9 TANSO-FTS Observation Mesh Points

#### d. Cross-calibration with the Orbiting Carbon Observatory (OCO)

Another calibration method is comparison with OCO data. Cross-calibration is scheduled both in Proto Flight Test (PFT) and after launching.

In the PFT, standard radiometers of GOSAT and OCO measure respective light sources (integrating spheres). The OCO and GOSAT ensure the accuracy of radiometric calibration in the PFT.

After launching, match-up data will be obtained at cross points of both orbits. We will compare spectral radiance,  $\text{CO}_2$  column density, and other physical parameters (surface reflectance, water

vapor, and aerosol) to ensure the product quality. Unfortunately, this method cannot proceed due to the failure of the OCO launch

#### 4) Algorithm development and data utilization

The primary objective of GOSAT is to observe column density of tropospheric CO<sub>2</sub> and CH<sub>4</sub> from SWIR bands implemented by the NIES. The algorithm for retrieving CO<sub>2</sub> and CH<sub>4</sub> density profiles from the TIR band is being developed by the Center for Climate System Research, University of Tokyo (CCSR), the University of Tokyo. These results from both SWIR and TIR bands will lead to estimating CO<sub>2</sub> sources and sinks using an inversion model prepared by the NIES. In addition, further research will be made from the TIR band for other trace gases.

EORC contributes to data utilization of the TIR band. The spectral coverage is 5.5 to 14.3 μm, which includes the 9.6 μm absorption band of O<sub>3</sub>, where tropospheric O<sub>3</sub> is an important greenhouse gas. Figure 2.1.5-6 presents the results of an O<sub>3</sub> retrieval test with TANSO-FTS specifications. The observed spectra are simulated with the addition of 30 percent O<sub>3</sub> to the US standard atmosphere with TANSO-FTS spectral resolution and sampling frequency. An *a priori* profile as a first guess is set to the US standard atmosphere. The figure illustrates the weighting functions of the O<sub>3</sub> emission band. The retrieved O<sub>3</sub> profile is estimated as a Maximum *A Posteriori* (MAP) solution using Rodgers' method. In the estimation of tropospheric O<sub>3</sub> below 12 km, the column density and density profile are in good agreement with true values.

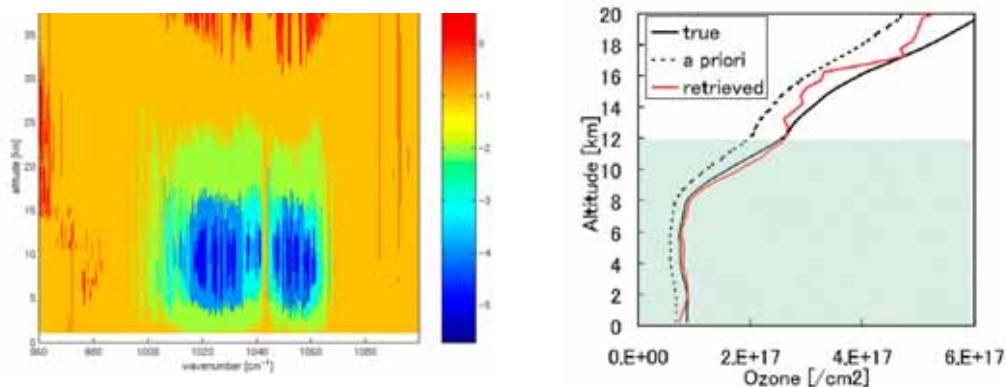


Fig. 2.1.5-10 O<sub>3</sub> Retrieval Test with TANSO-FTS Specifications: O<sub>3</sub> Weighting Function (left), and the Result of O<sub>3</sub> Retrieved Profile (right)

## 2.2 Cross-Cutting / interdisciplinary science

### 2.2.1 The Water Cycle Research Group

#### 1) Overview

The water cycle is essential for its direct relation to water hazards, as well as for preserving life. It is affected not only by climate variations, but also by human activities, such as accelerated food production, increase of water use, and land use changes associated with growing population and/or economic progress. As a result, variations in the water cycle affect society through increases/decreases of water stress, which indicates vulnerability of droughts or of risks of floods. From this perspective, it is understood that measurements of green house gases (which cause climate change) via satellite observation, variables related to food production (e.g., land surface, land use, and vegetation cover), water flow (e.g., precipitation, water vapor flux, latent heat flux, streamflow, etc.) and water reservoir variables (e.g., ice sheets, glaciers, snow, soil moisture, ground water, etc.) are also important to water cycles.

The major purpose of the “water cycle” research theme in the EORC is to develop a collaborative research plan to contribute to understanding the global water cycle system, through utilizing information of observation targets related to the water cycle obtained by multi-satellites and multi-sensors.

Cooperation with various research communities outside JAXA has also begun to demonstrate data utilization in the fields of flood forecasting, numerical models, and ecosystems. Those collaborative activities will accelerate utilization of transdisciplinary observation of JAXA’s satellite missions in broader fields.

#### 2) Objectives

Final goals of the water cycle research theme are to provide reliable water cycle information related to water resources, torrential rains, and the El Niño and La Niña phenomena, and to achieve integrated water resource management to reduce water issues and damages. To achieve those goals, research group targets to evaluate a global land data assimilation system, which will be established at the EORC, through experiments of land surface models using past observation data, and to contribute to real-time monitoring of global streamflow. The system will also contribute by providing input to monitoring and forecasting systems for water hazards, especially in the Asian region.

There are three main pillars in this research group:

1. Detection of long-term trends;
2. Real-time monitoring; and
3. Seasonal forecasts.

The first, detection of long-term trends in the water cycle, is scientifically important in connection with global warming issues. Data archiving over the long term and over a wide area and integration of data are essential for this purpose.

The second, real-time monitoring, is closely related to fields of disaster prevention. It is important to collect Earth observation data in real time, and data will contribute to the improvement of forecast accuracy of numerical models.

The last, seasonal forecasts, will effectively utilize the Earth’s surface observation information for which satellites have great advantages. Availability of near real-time data is needed, but its coverage should be balanced in instantaneousness and width.

3) Approach

To integrate various satellite mission products, the EORC started development of a global land data assimilation system, which simulates energy and water balances over the global domain in near real time using a Land Surface Model (LSM) driven by atmospheric forcing from satellite observations and assimilated data products. Currently, the system is just an offline simulation, using forecast data from the Japan Meteorological Agency (JMA) and satellite data as external forcing.

The EORC has been transporting the "Today's Earth" system from the Univ. of Tokyo to the EORC's computer system since 2008. The system will be improved at the EORC for combined use of satellite and Grid Point Value (GPV) data, which includes objective analysis and forecasts by JMA's operational Global-Scale Model. Figure 1 is a schematic flow chart of the original "Today's Earth" system and its improvement plan at the EORC. Figure 2 shows example results from the original "Today's Earth" system. An extended version of the MATSIRO (Minimal Advanced Treatments of Surface Interaction and Runoff) land surface model (LSM), called Iso-MATSIRO, developed by Yoshimura *et al.* (2006), and a 0.1-degree version of Total Runoff Integrating Pathways (TRIP) by Oki *et al.* (1999) were used. MATSIRO was originally developed by Takata *et al.* (2003) as a land surface model attached to an atmospheric general circulation model; it solves the vertical one-dimensional energy and water budgets in each grid cell explicitly (Yoshimura *et al.*, 2008).

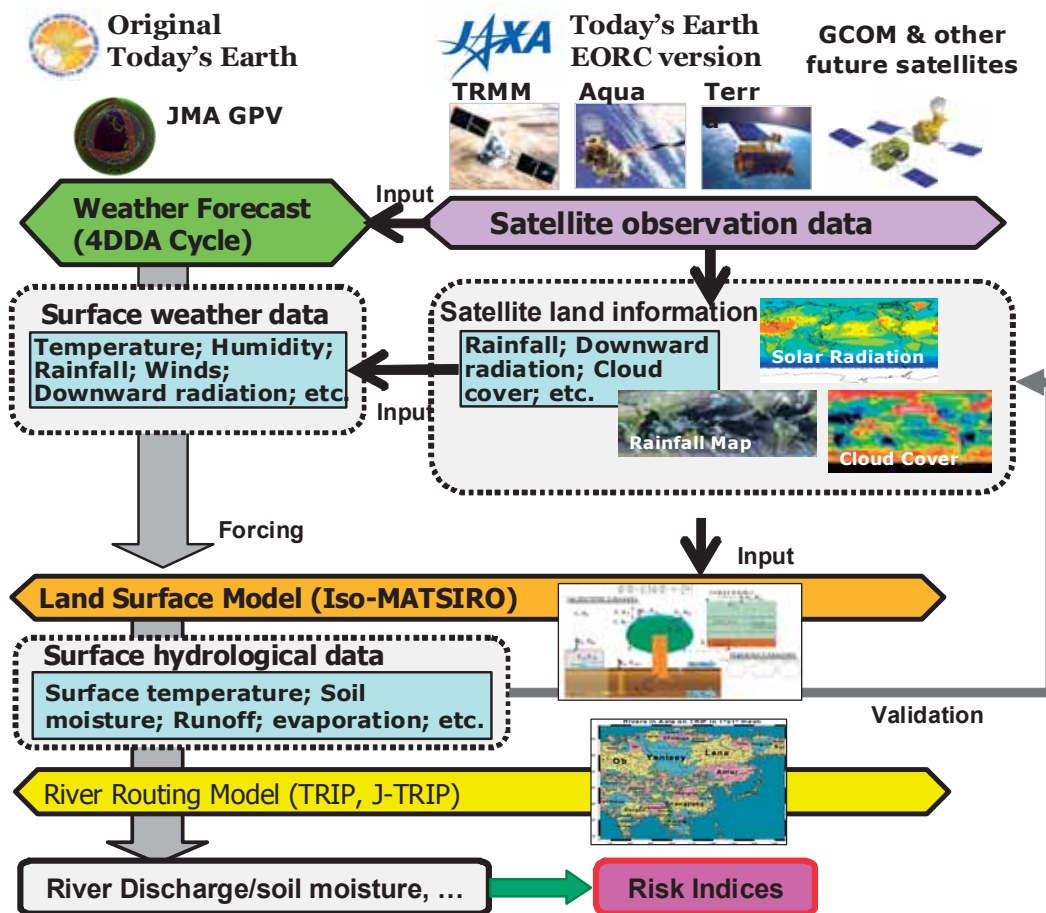


Fig. 2.2-1 Schematic flow chart of original "Today's Earth" system operating at the University of Tokyo (left column), and its improvement plan at the EORC (right column)

As shown in Figure 1, satellite data is mainly used to validate (compare to) LSM estimates in the initial stage, such as:

1. To validate soil moisture, snow cover, etc.;
2. To provide appropriate LSM parameters and initial conditions; and
3. To input as forcing data.

Although the current system is not capable of data assimilation, there are proposals to introduce the function in the system.

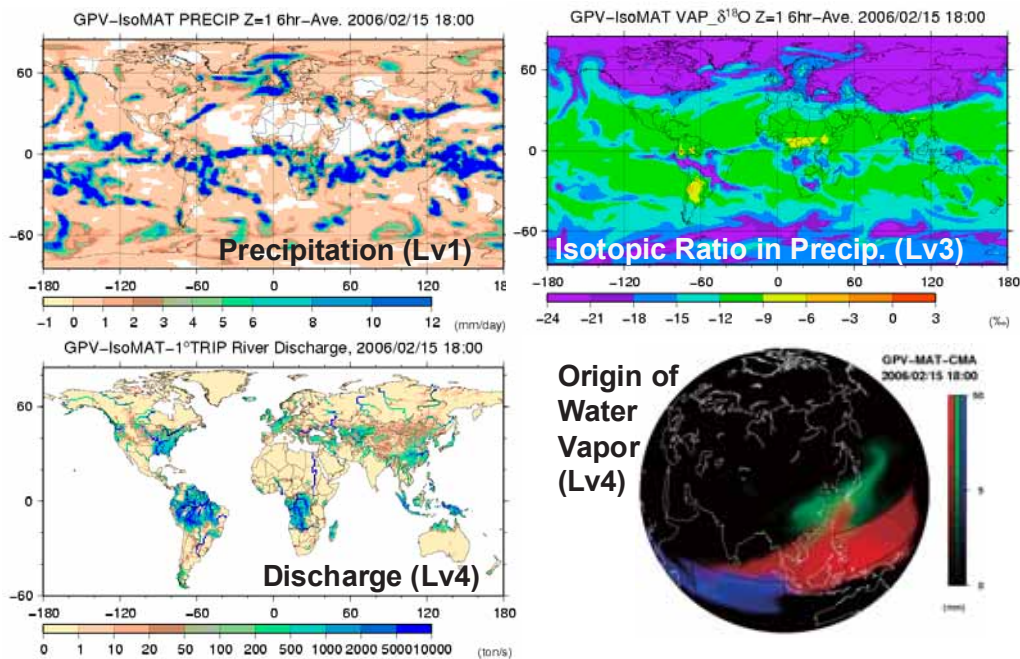


Fig. 2.2-2 Example of outputs from Today's Earth system at the University of Tokyo (<http://hydro.iis.u-tokyo.ac.jp/LIVE/>). (Upper left) Precipitation by GPV (Lv1: Resolution Converted). (Upper right) Isotopic ratio in precipitation calculated by Iso-MATSIRO (Lv3: Model Output). (Lower left) River discharge calculated by TRIP (Lv4: Value-Added Variables). (Lower right) Origin of water vapor calculated by water source model (Lv4: Value-Added Variables).

#### 4) Implementation Plan for JFY 2008

The 5-year Implementation Plan for the water cycle research group was developed in June 2008, and will be updated as the research progresses. The following are research plans for 5 years, from Japanese Fiscal Year (JFY) of 2008 to 2012.

The Implementation Plan for JFY 2008 mainly targets equipment servicing and installation of models.

1. Transportation of a land surface simulation system  
 "Today's Earth" system, which was originally developed and operated at the University of Tokyo, will be transported to the EORC.
2. Maintenance and improvement of the system  
 After the operation of transportation, modification and addition of codes and scripts will be performed to correspond to the EORC system and the new inputs.

### 3. Test processing using satellite data

As an initial test, simulation using multi-satellite merged rainfall data estimated by the Global Satellite Mapping of Precipitation (GSMaP) project will be performed.

### 5) Results of JFY 2008

In JFY 2008, a land surface water cycle simulation system, called “Today’s Earth,” was transported from IIS, the University of Tokyo, to the EORC. The “Today’s Earth” system was developed by and operated at IIS (Yoshimura *et al.*, 2006, 2008). It consists of a Land Surface Model (MATSIRO) and a River Routing Model (TRIP). Among inputs (forcing data) to MATSIRO, downward shortwave radiation (SWR) and downward longwave radiation at the Earth’s surface are not included in the GPV forecast parameters. Therefore, those parameters were estimated using the experimental method by Kondo and Miura (1983) using surface pressure, temperature, precipitation, and cloud cover forecasted by the GPV.

Modification and addition of codes and scripts were done at the EORC to correspond to the new computer environment. To distinguish the two systems, hereafter the system developed at the EORC will be called the “ETE system.” In addition, initial examination of possible utilization of satellite data to produce surface weather data was done for future improvement of the system. Figure 3 shows an example of results of the initial test at the EORC for the period of July 2008. Cloud cover (Lv1: Resolution converted from GPV) and 5-cm depth soil moisture (Lv3: Output of MATSIRO) were compared to satellite observation for the same period. Global distribution of cloud cover appears almost similar to that of Cloudiness by satellite observation.

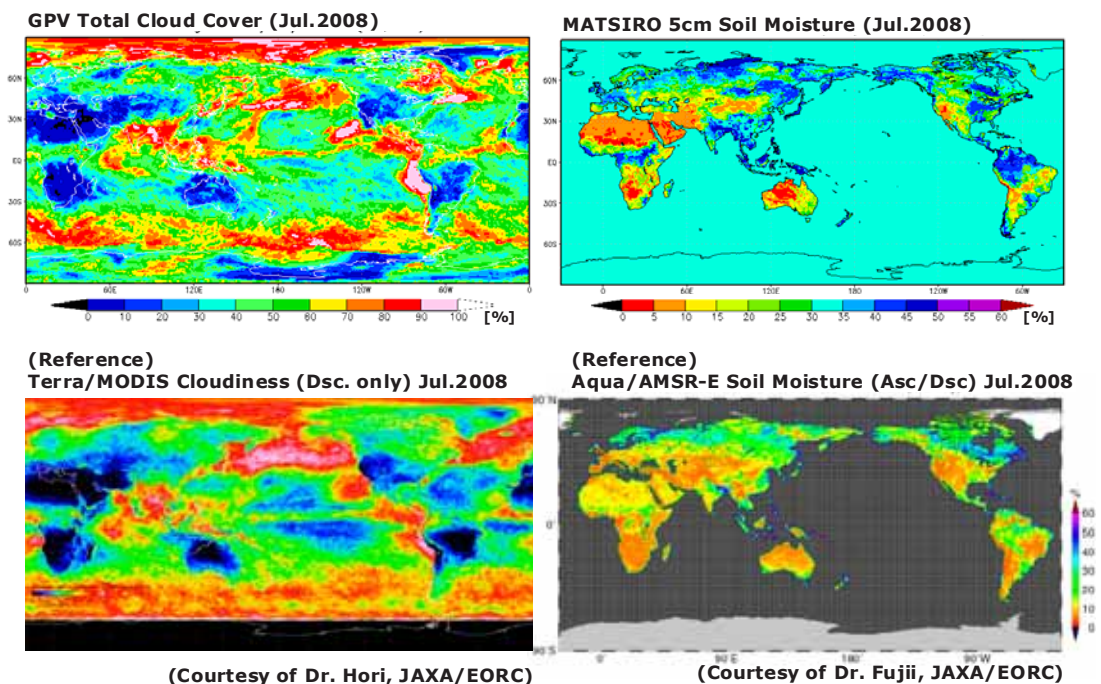


Fig. 2.2-3 Example of outputs from the ETE system (upper) and satellite data for comparison (lower). (Upper left) Monthly mean total cloud cover by the GPV for July 2008. (Lower right) Cloudiness by Terra/MODIS (descending orbit only) for the same period. (Upper right) Monthly mean 5-cm depth soil moisture by MATSIRO for July 2008. (Lower right) Soil moisture by Aqua/AMSR-E (ascending and descending orbits) for the same period.

To improve the system, possible utilization of satellite-based products and other data sources as forcing data (input to LSM) instead of GPV forecasts is examined in Table 1. The major advantage of utilization of GANAL (JMA Global Analysis) data as an alternative to GPV is to enable model calculation for a longer time period, since Total Cloud Cover in the GPV forecast parameter is only available after November 2007.

As the first step, satellite-based rainfall estimated by the GSMaP project was examined and system preparation has started. Six-hour accumulated precipitation is a forecast parameter in the GPV, and forcing data to the LSM. GSMaP rainfall is a production of a high precision and high-resolution global precipitation map using satellite-borne microwave radiometers (MWRs). An MWR algorithm (Aonashi *et al.*, 2009) was developed to be consistent with the Precipitation Radar (PR) on board the Tropical Rainfall Measuring Mission (TRMM) satellite and a precipitation physical model was developed using the PR. It also combines MWR retrievals with Geostationary Infrared (Geo-IR) instruments using the moving vector and Kalman filtering method to produce an hourly global rainfall map (Ushio *et al.*, 2009). Interface and time step of the ETE system was modified to treat GSMaP rainfall as inputs.

Table 2.2-1 Examination of Possible Utilization of Satellite-based Data in Forcing Data to LSM

Input Parameters (forcing data) to LSM	Calculation Method in Original Today's Earth System	Possible Alternative Data in ETE System
Surface Temperature, Surface Wind (U, V), Surface Pressure	GPV forecast parameters	GANAL objective analysis parameters
Surface Rainfall	GPV forecast parameter	GSMaP Rainfall and GPCP (Polar region)
Total Cloud Cover	GPV forecast parameter	Estimate from MODIS/SeaWiFS Shortwave Radiation
Surface Specific Humidity, Water Vapor Flux (U, V), Total Precipitable Water, Water Vapor Pressure	Calculate from GPV forecast parameters	Calculate GANAL objective analysis parameters
Downward Shortwave Radiation (Solar Radiation)	Estimate from GPV Surface Pressure, Total Precipitable Water, and Total Cloud Cover	MODIS/SeaWiFS Shortwave Radiation (daily mean)
Downward Longwave Radiation	Estimate from GPV Surface pressure, Water Vapor Pressure, Total Precipitable Water, Total Cloud Cover, and Surface Rainfall	Estimate from Total Cloud Cover estimated by MODIS/SeaWiFS Shortwave Radiation, GSMaP Rainfall, and others from GANAL objective analysis

Downward SWR at the surface estimated by MODIS on board Terra and Aqua satellites, and SeaWiFS data were examined to introduce to the LSM as forcing data. Currently, SWR and Photosynthetically Available Radiation (PAR) data estimated using MODIS and SeaWiFS data have been produced for more than 10 years on a daily basis and distributed at the EORC (<http://kuroshio.eorc.jaxa.jp/JASMES/index.html>). PAR was estimated from a visible unabsorbed channel, and translated to SWR using optical thickness of cloud and aerosols simultaneously estimated from satellite data, and water vapor content obtained by objective analysis. The data could be used as forcing data instead of an experimental estimated value by the GPV. Sensitivity tests, such as evaluating the impact of satellite-based direct and diffuse components of PAR for LSM

estimates, should be performed in future.

Figure 4 is the preliminary result of the monthly mean downward shortwave radiation at the surface calculated from GPV (upper) and MODIS (lower). Distribution of MODIS shortwave radiation is similar to that calculated from GPV, but underestimates over a global area.

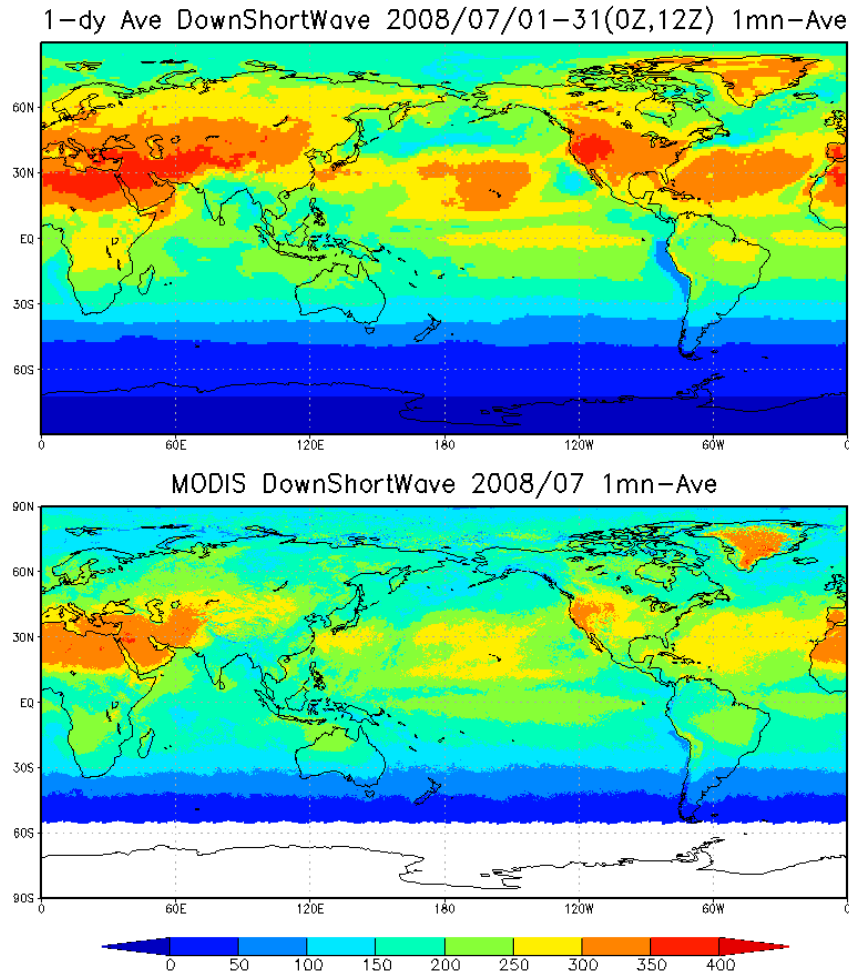


Fig. 2.2-4 Example of monthly mean downward shortwave radiation at the surface calculated from the GPV (upper) and MODIS (lower). Period of July 2008.

#### 6) Future

The following is the schedule of the “water cycle” research group:

##### JFY 2009

- Maintain and improve the land surface water cycle simulation system
- Implement test processing using objective analysis and satellite data as inputs
- Validation and evaluation

##### JFY 2010

- Develop and start test operation of the system
- Open the system to related researchers in Japan
- Adjustment and evaluation of parameters

##### JFY 2011

- Develop and start operational processing of the system

- Open the system to the public
- Investigate applicability of the system for regional use (Japan)

JFY 2012

- Investigate applicability to operational use (water hazard monitoring/warning system)

### 2.2.2 Ecology Research Group

The ecology research group worked on the following three activities:

- 1) Development of incoming solar radiation, particularly the photosynthetically active radiation (PAR), with satellite data
- 2) Development of a high-resolution land cover map with satellite data
- 3) Creating a community that collaborates with ecological study in JAXA

#### 1) Development of incoming solar radiation

Solar radiation is one of the most important components in the land surface process. It provides the energy that drives meteorological, hydrological, and ecological processes. A fraction of solar radiation, photosynthetically active radiation (PAR) is the wave band between 0.4  $\mu\text{m}$  and 0.7  $\mu\text{m}$ . Plants can use PAR to photosynthesize. Therefore, to estimate agricultural and forest productivity, accurate data about PAR is desired (Nasahara, 2009).

In this study, which is based on a radiative transfer study (Frouin and Murakami, 2007), we developed an algorithm for estimation of solar radiation with optical images taken by satellites, such as MODIS or SeaWiFS. The characteristic advantages of our approach are:

1. Capable of estimating PAR, shortwave, and ultraviolet (UV) radiation separately
2. Capable of estimating direct and diffuse radiation separately
3. High-spatial resolution (about 1 km)
4. High-temporal resolution (daily)

We started distributing this data via the FTP site of JAXA/EORC (JASMES). The following figures show examples of the product (Fig. 2.2-5, 2.2-6, and 2.2-7) and the validation result (Fig. 2.2-8).

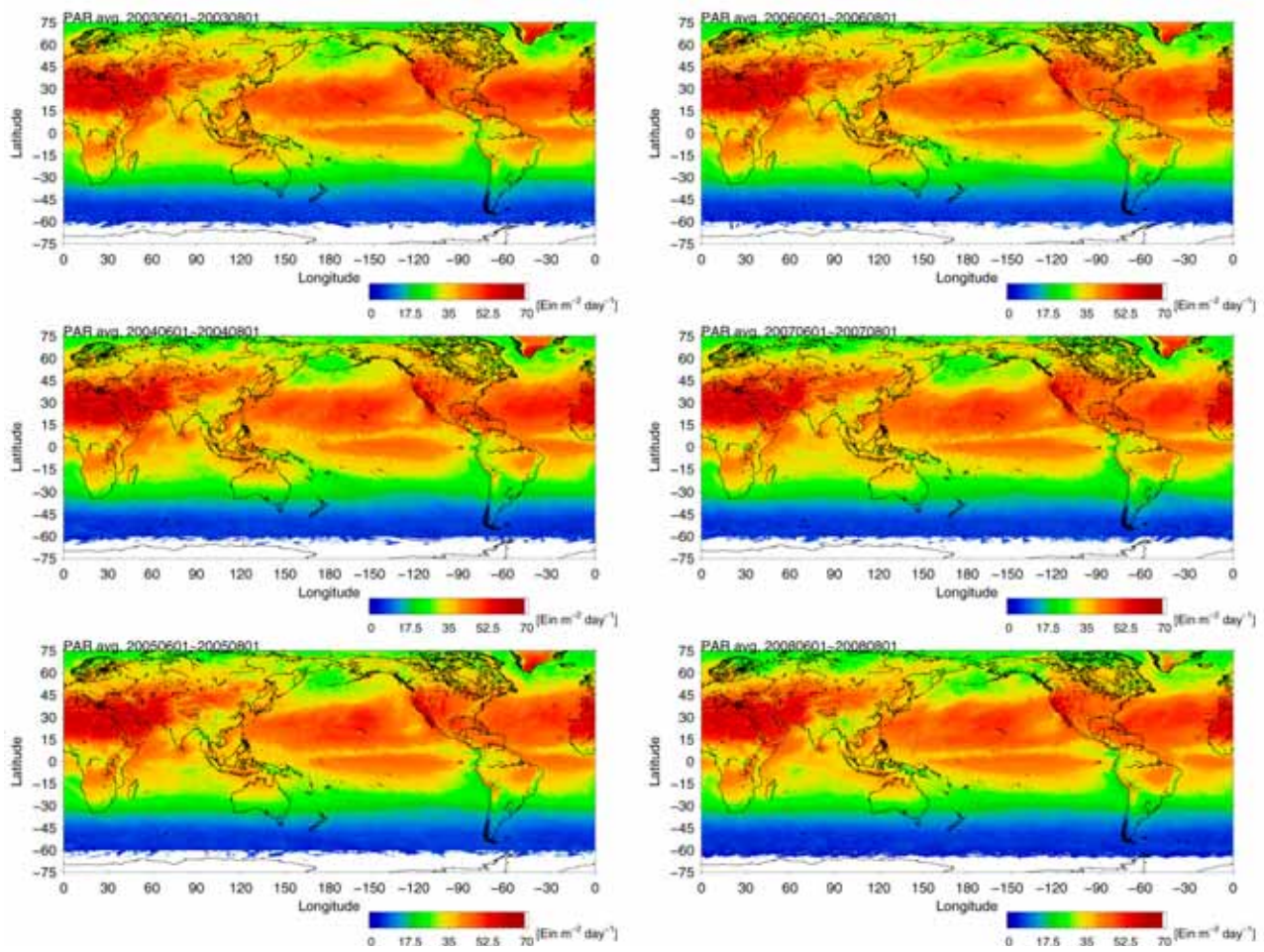


Fig. 2.2-5 Examples of global incoming PAR maps— 3-month average (June, July, and August) daily PAR for each year during 2003 and 2008

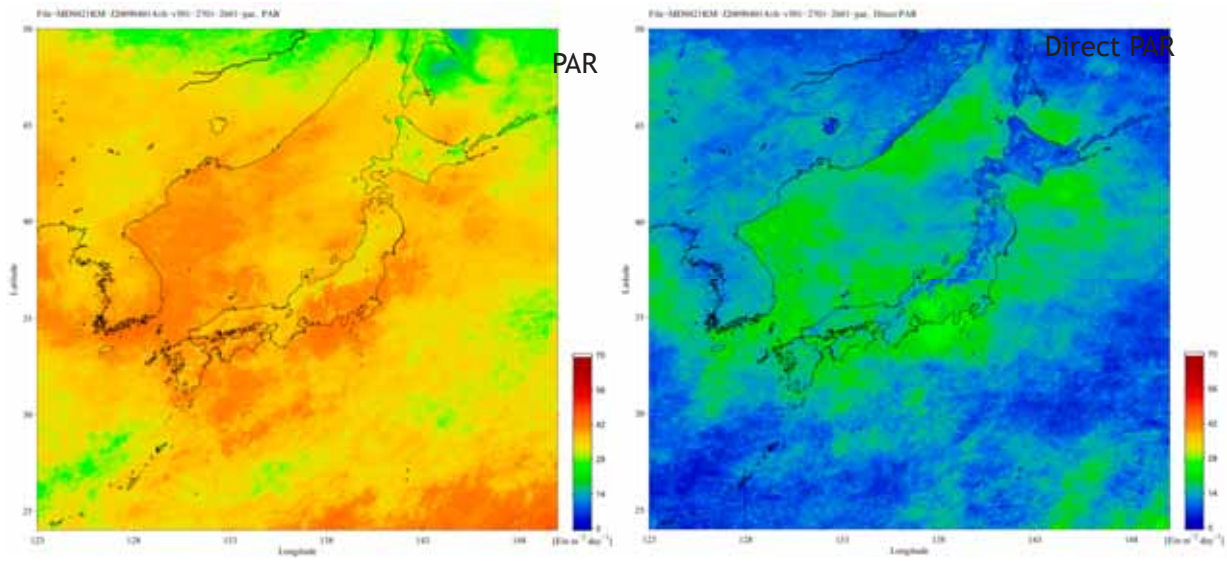


Fig. 2.2-6 An example of an incoming PAR map (left) and its direct component (right) around Japan

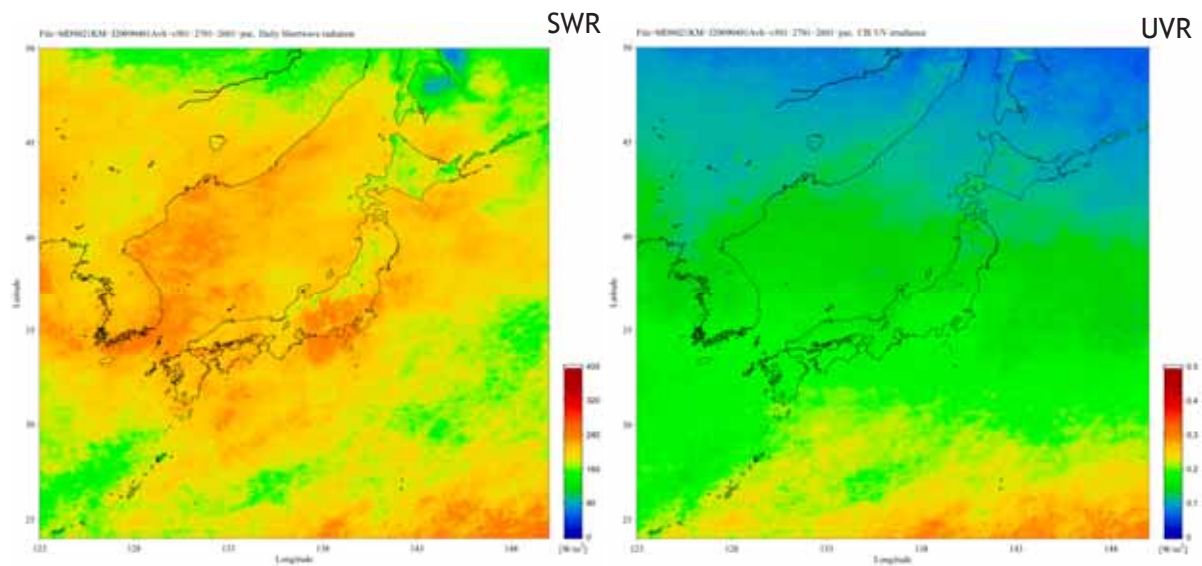


Fig. 2.2-7 An example of an incoming short-wave map (left) and ultraviolet map around Japan

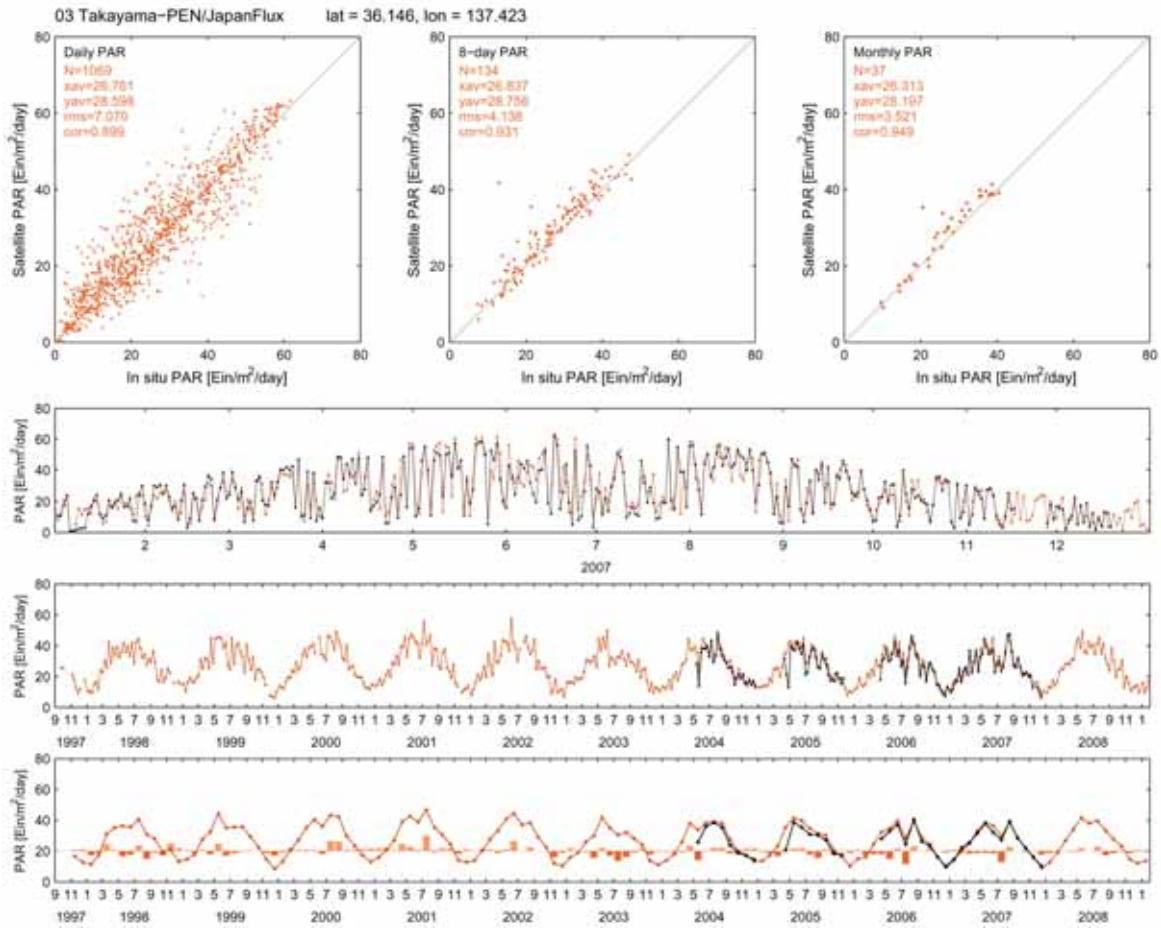


Fig. 2.2-8 Validation of estimated PAR against ground observation at the Takayama Flux Site (JapanFlux/JaLTER/PEN super-site)

## 2) Development of a high-resolution land cover map with satellite data

A land cover map, which reflects distribution of various ecosystems, is a critical source of information for environmental assessment. We are developing a land cover map with images taken by JAXA sensors. Particularly, in cooperation with an ALOS application study project, we are working on development of a land cover map with ALOS/AVNIR2 data. This year (FY 2008), we developed a prototype land cover map of Japan with the following characteristics:

Area: N30-N46, E128-E146

Resolution: 4 second (lat-lon projection; WGS84)

Categories: 6 (0: bare, 1: water, 2: urban, 3: paddy, 4: crop, 5: deciduous forest, 6: evergreen forest)

Data source: ALOS/AVNIR2, Terra/MODIS (MOD09 8-day composite), ALOS/PALSAR (K&C ortho-mosaic, 50-m resolution), topography (GSJ DEM, 50-m resolution)

Algorithm: Decision tree

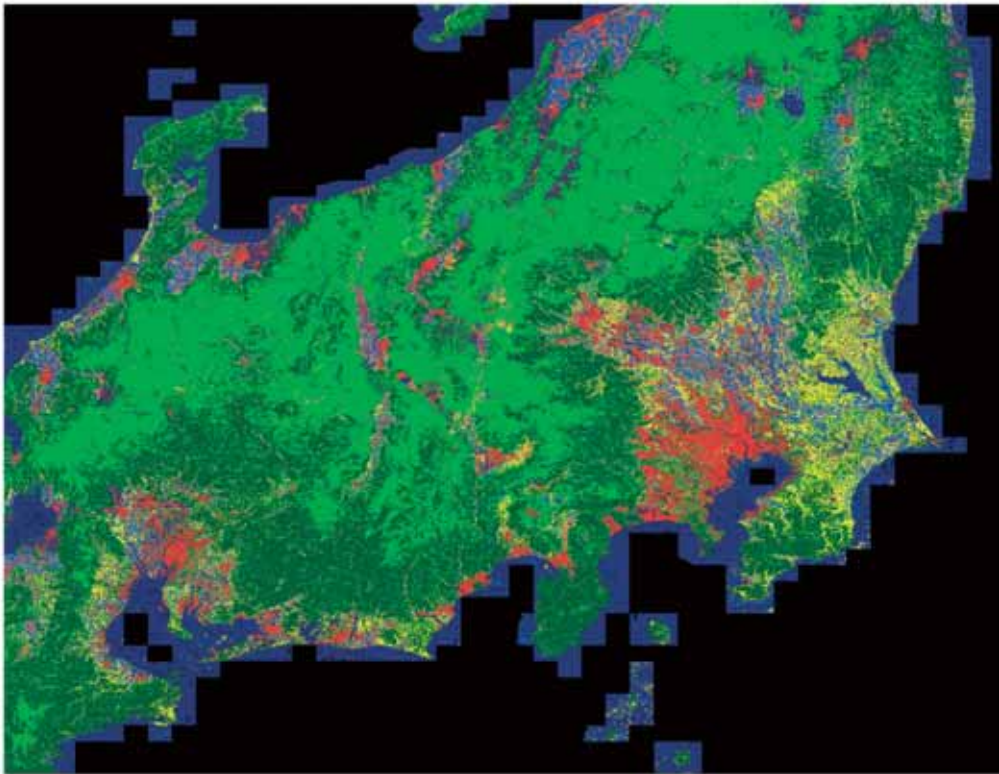


Fig. 2.2-9 Land cover map derived from AVNIR2, etc. Dark blue: water, red: urban area, light blue: paddy, yellow: crop, light green: deciduous forest, dark green: evergreen forest

### 3) Creating a community that collaborates with ecological study in JAXA

Monitoring and assessment of the ecosystem is critical in evaluating and mitigating the influence of climate change. We believe that satellite remote sensing plays a key role in the monitoring and assessment of the ecosystem, but we must rely on ground field studies for validation and interpretation of the satellite data. Therefore, we decided to construct collaborative relationships with field ecologists.

Recently, field ecologists are creating “networks” for their specific purposes. For example, JaLTER (Japan Long-Term Ecological Research Network), which is the Japanese subgroup of ILTER (International Long-Term Ecological Research Network), is a network for long-term ecological study. For another example, JapanFlux, which is the Japanese subgroup of AsiaFlux and the FluxNet network, is a network for the exchange of carbon, water, and energy between ecosystem and atmosphere.

We established a close connection with these two networks this year. On top of this, we have been closely working with JAMSTEC, which is an intensive research organization of global change study. We have integrated these relationships as the J-Community by joining JAXA, JaLTER, JapanFlux, and JAMSTEC through the following activities:

1. Kick-off Workshop for the J-Community was held on October 23, 2008 at JAXA’s Tsukuba Space Center. We had the following key-note speakers for the meeting: Hideaki Shibata (Hokkaido University, JaLTER), Masahiro Nakaoka (Hokkaido University, JaLTER), Keizo Hiura (Hokkaido University, JaLTER), Koji Hirano (Hokkaido University, JapanFlux), Nobuko Saigusa (NIES, JapanFlux), Akira Miyata (NIAES, JapanFlux), Hiroyuki Oguma (NIES, JaLTER), Kazuhito Ichii (Fukushima University, JapanFlux), Hiroyuki Muraoka (Gifu University, JapanFlux), and Hiroshi Murakami (JAXA).
2. We sponsored the AsiaFlux Workshop 2008 at Seoul (November 17-18, 2008).
3. We supported launching a project for GCOM-C RA by the J-Community for deriving integrated terrestrial ecology information.

### 2.2.3 Disaster Research Group

Change detection is a key issue in fully utilizing SAR data from ALOS-2 or later for disaster mitigation. Since the ALOS-2 research project ranks change detection as a highly weighted research theme, this disaster research theme in Yokogushi decided to conduct the following three activities. They are detection of change caused by flooding, massive landslides (including Dosekiryu), and minor landslides using the InSAR.

- 1) Flooding: Differentiation of the non-flooded and flooded ortho-rectified images provides information on the flooding region.
- 2) Massive landslides: Differentiation of accurately processed ortho-rectified SAR images using a fine resolution DEM provides the intensity difference related to the disaster. It still requires development of an accurate SAR processing engine to correct the radiometric and geometric property caused by the disaster.
- 3) Minor Landslides: Differential SAR interferometry provides information on a minor landslide.

Detection of a flooded area was demonstrated using the Pi-SAR-L over a simulation flooded area at a Tanegashima rice field. PALSAR data acquired for flooding in Aichi Prefecture in late summer 2008 was also used.

# ***3. RESEARCH AND DEVELOPMENT ON INSTRUMENTATION***

### 3. RESEARCH AND DEVELOPMENT ON INSTRUMENTATION

#### 3.1 Overview

The EORC sensor research group is conducting research on future Earth observation sensors. In FY 2008, we conducted research mainly on:

- (1) A lightweight large diameter mirror
- (2) The Geostationary Meteorology and Atmospheric Chemistry Mission
- (3) A compact infrared camera (CIRC) for Earth observation
- (4) Calibration of optical sensors
- (5) A next-generation Earth observation sensor

In the following sections, the detailed results of (1), (2), (3), and (4) are described.

#### 3.2 Large-diameter Mirror

It is expected that optical and/or infrared telescopes with larger diameter primary mirrors will be increasingly required in the near future in order to achieve higher spatial resolution images of the Earth's surface or celestial objects.

We have been studying lightweight large mirrors that are applicable to the next Japanese large infrared telescope, SPICA, and future large telescopes for Earth observations from a geosynchronous orbit. The SPICA telescope requires a  $\Phi=3.5$ -m primary mirror that can achieve diffraction-limited images at 5  $\mu\text{m}$ .

To realize such large spaceborne instruments, we have to achieve and establish integration and ground measurement techniques of large ( $\Phi\sim 1.5$ m or larger) optics as well as large mirror manufacturing technologies.

We have studied the applicability of silicon carbide mirrors for spaceborne telescopes in the past several years and manufactured a  $\Phi=800$ -mm lightweight mirror using a carbon fiber reinforced silicon carbide composite (C/SiC) material, HB-Cesic<sup>R</sup> developed by Mitsubishi Electric Corporation and ECM to verify the design and manufacturing technologies of a lightweight large silicon carbide mirror.

The final goals of our study are as follows: (a) verifying and confirming the manufacturing process of a lightweight large silicon carbide mirror, from designing of structure and mixing of raw material to final polishing; (b) developing methods to evaluate and guarantee ceramic mirror quality for space use; (c) achieving a matured design technique of a thermally stable mirror, an optical system, and evaluation of its thermal stability; and (d) achieving and establishing highly precise ground optical testing technology for large mirrors and large telescope systems.

This year, we have conducted (1) manufacturing components of all C/SiC optics models, (2) preparation for a large-scale optics test, (3) a low temperature test of the main mirror, and (4) stitching test method analysis. The results of these studies are described below.

### 3.2.1 Manufacturing Components of All C/SiC Optics Models

To master and establish a ground optical performance testing method and to relate expertise for large optical systems, an all C/SiC optics model was designed using an 800-mm mirror as the primary (Fig. 3.2-1) and its components were successfully manufactured (Fig. 3.2-2). The secondary mirror is a high order convex (Fig. 3.2-3). It is also silicon vapor deposited. Support of the secondary mirror will be a bipod structure that enables easier optical alignment during testing.

The optics model will be integrated next year after cryogenic measurement of the primary mirror. After integration, the model will be employed for ground testing simulations to develop optical measurement technologies.

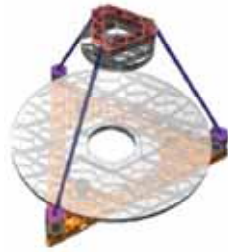


Fig. 3.2-1 FEM Model (left) and 1/1 Scale Plastic Model (right)



Fig. 3.2-2 Integrated Support Structure and Its 3D Measurement

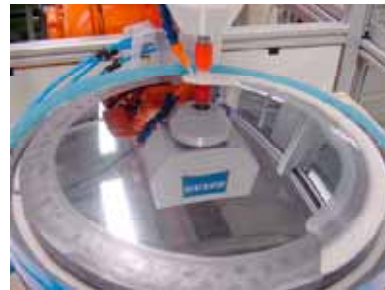


Fig. 3.2-3 Secondary Convex Mirror (being polished)

### 3.2.2 Preparation for Large-scale Optics Test

Spaceborne large optics will be required in future missions for astronomy and Earth observations. In order to realize large-optics missions, JAXA has started a study of ground measurement techniques of large optics. The 6-m diameter radiometer thermal vacuum chamber (6-m chamber) at Tsukuba Space Center will be used for tests of JAXA's future large-optics missions.

We are planning a test to establish a technique for a large-scale optics test.

Purposes of this test are:

- (1) to establish the algorithm for stitching interferometry (see "stitching test method"), and

(2) to establish a handling method of large-scale optics.

Fig. 3.2-4 shows a test configuration of the large-scale optics test. In this test, we simulate the subaperture stitching using a mask, which covers a part of the reference flat mirror. By comparing the measurement result of an auto-collimation method without the mask with that of the stitching method, we verify the feasibility of stitching interferometry.

In FY 2008, we prepared the tools necessary for the test. The tools are:

- (1) a rotation mask for the stitching simulation,
- (2) 5-axis precision stage, and
- (3) a pressure vessel for the interferometer.

These can be operated in a vacuum environment. Fig. 3.2-5 and Fig. 3.2-6 show pictures of these tools. In FY 2009, we are planning to evaluate the performance of these tools.

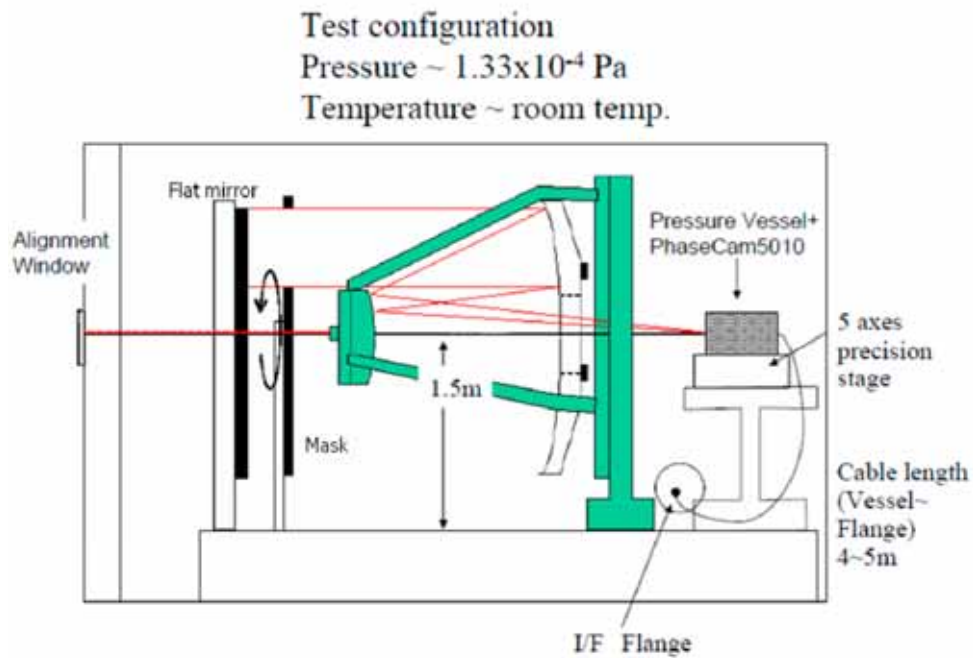


Fig. 3.2-4 Test Configuration of the Large-scale Optics Test



Fig. 3.2-5 Rotation Mask for Stitching Simulation (left) and 5-axis Precision Stage (right)



Fig. 3.2-6 Pressure Vessel for the Interferometer

### 3.2.3 Low Temperature Test for Main Mirror

C/SiC is now planned to be used for the next Japanese large infrared telescope, SPICA. Infrared telescopes are generally used in low temperature environments, so we conducted a low temperature test (at liquid nitrogen temperature) in order to examine the change of surface figure errors between those at room temperature and at low temperature. The result is shown in Fig. 3.2-7 and indicates that the change of surface figure errors is about  $0.253\lambda$ .

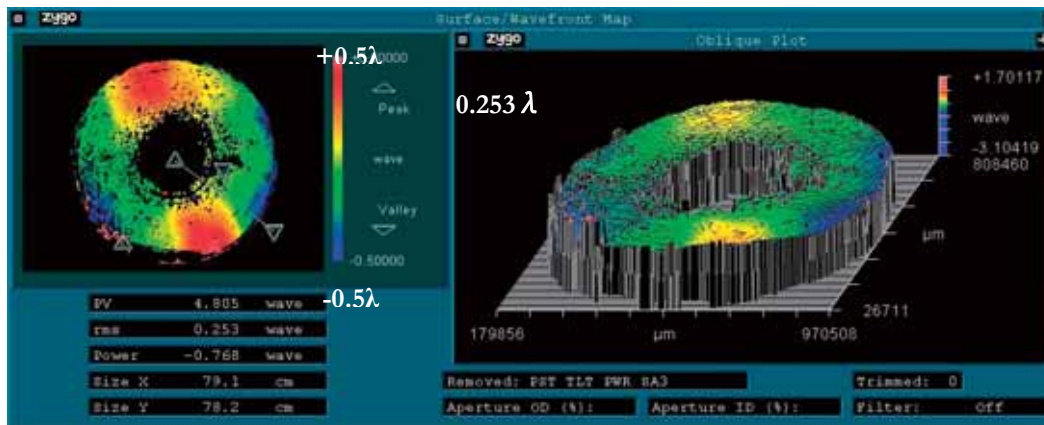


Fig. 3.2-7 Difference of Surface Figure Errors between at Room Temperature and at Liquid Nitrogen Temperature

### 3.2.4 Stitching Test Method

Stitching interferometry is a key technique for optical testing of future large telescopes. We have studied stitching algorithms by using numerical simulations. In the calculation, we have assumed realistic conditions such that the stitching of wave-front errors (WFEs) is applied to the full pupil of a 3.5-m telescope (e.g., SPICA: Swinyard et al. 2009) with a sub-pupil array consisting of two discrete flat reflectors of mirrors with diameters of 730 mm and 900 mm. The flat mirrors reflect those already existing or being fabricated. As shown in Fig. 3.2-8, a set of two flat mirrors is placed at the radial positions of 770 mm and 1400 mm from the center of the pupil and rotated together along the optical axis by a step angle of  $\lambda/8$  to cover the whole aperture of the telescope.

Fig. 3.2-9 shows the result of the stitching analysis performed based on the least-square method for the regions overlapped between the sub-pupils (Otsubo et al. 1994). Here, for the total WFEs of the telescope, we have utilized the data measured for the AKARI telescope (Kaneda et al. 2005), and assumed the surface figure errors of the flat mirrors to be  $0.1\lambda_{\text{rms}}$  ( $\lambda = 633 \text{ nm}$ ; the specifications of the 900-mm flat mirror under fabrication). The result shows that an error due to the stitching analysis (i.e., difference between the WFEs before and after stitching) is about  $0.13\lambda_{\text{rms}}$ , which is slightly worse than our required accuracy of  $0.1\lambda_{\text{rms}}$ . However, we have found that stitching accuracy can be improved to meet the requirement by reducing the step angle of  $\lambda/8$  down to  $\lambda/10$ .

In FY 21, we are planning to conduct real optical measurements of a telescope to verify the feasibility of the stitching interferometry with the numerical tool/algorithms developed in FY20.

Reference:

- Otsubo, M., K. Okada, and J. Tsujiuchi. *Optical Engineering*, 33, (1994): 608  
 Swinyard, B., et al. *Experimental Astronomy*, 23, (2009): 193  
 Kaneda, H., et al. *Applied Optics*, 44, (2005): 6823

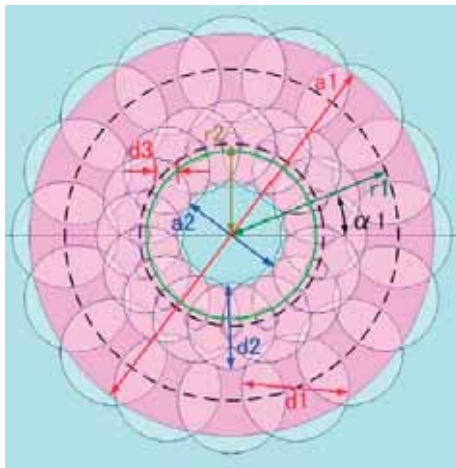


Fig. 3.2-8 Configuration for Stitching of Sub-pupils

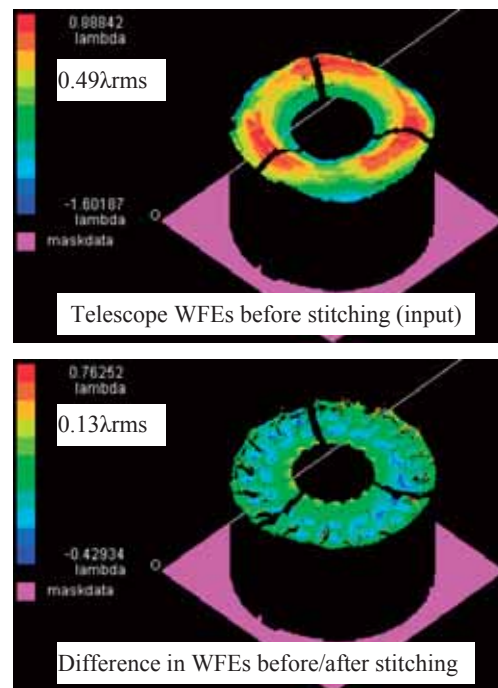


Fig. 3.2-9 Result of Stitching Interferometry Simulation

### 3.3 Geostationary Meteorology and Atmospheric Chemistry Mission

#### 3.3.1 Mission

##### (1) Contribution to numerical weather prediction

The improvement of numerical weather prediction needs frequent sounding of temperature, water vapor, and wind profiles. These measurements also enable forecasting where and when thunder and storms will form before they can be seen on radar or satellite imager. The meteorological sounder aboard the geostationary satellite has the great advantage of frequent measurements, which also enables it to derive the atmospheric motion vectors (AMV). These vectors of wind direction and velocity are derived by tracking water vapor distribution patterns. AMV is a significant meteorological data used for numerical weather prediction.

##### (2) Atmospheric pollution in Asia, such as trans-boundary pollution

Atmospheric ozone affects human health, damages forests, and reduces agricultural production. A photochemical smog alert is issued when ozone concentrations exceed 120 ppb. Ozone is produced through the photochemical reaction of nitrogen oxides (NO<sub>x</sub>) and other precursor gases.

In recent years, atmospheric ozone concentrations are increasing throughout Japan. In particular, photochemical smog alerts have been issued in several prefectures that had never experienced such events in the past. Long-range trans-boundary atmospheric pollution has been suggested as one of the causes of this rise in atmospheric pollution. However, the true nature of this increase has yet to be determined.

The geostationary sounder can provide data sets of continuous distribution of ozone and its precursors over a wide area and 24-hour continuous diurnal variation, which help the understanding and prediction of atmospheric pollutants. Fig. 3.3-1 shows an example of such data, which is the tropospheric nitrogen dioxide (NO<sub>2</sub>) column density over Asia obtained by the Ozone Monitoring Instrument (OMI) aboard the EOS Aura satellite.

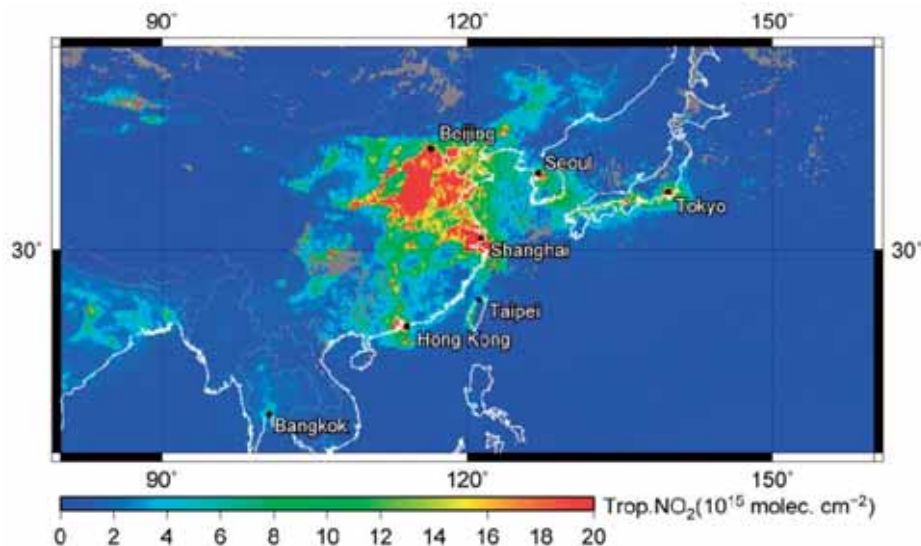


Fig. 3.3-1 Distribution of Tropospheric NO<sub>2</sub> Column Density over East Asia  
Obtained by OMI in December 2007 (data provided by NASA)

### 3.3.2 Target of Measurement

#### (1) Meteorology Mission

The targets of measurement are temperature and water vapor profiles and atmospheric motion vectors (AMV). The target precision of measurement is shown in Table 3.3-1.

Table 3.3-1 Target Measurement Precision

	Precision	Vertical Resolution
Temperature	1 K	2 – 3 km
Water Vapor	10 %	2 – 3 km
AMV	TBD	TBD

#### (2) Atmospheric Chemistry Mission

The targets of measurement are tropospheric ozone (O<sub>3</sub>) and its precursor gases, such as nitrogen dioxide (NO<sub>2</sub>), carbon monoxide (CO), formaldehyde (HCHO), nitric acid (HNO<sub>3</sub>), and aerosol optical depth (AOD). Vertical resolution is needed to distinguish between the tropospheric column and the stratospheric column. The target precision of the tropospheric column is shown in Table 3.3-2 considering the urban pollution level.

Table 3.3-2 Target Measurement Precision of Tropospheric Column

	Ave in East Asia [molecules/cm <sup>2</sup> ]	Urban Pollution [molecules/cm <sup>2</sup> ]	Target Precision
O <sub>3</sub>	1.1 x 10 <sup>18</sup>	1.9 x 10 <sup>18</sup>	10%
NO <sub>2</sub>	7.3 x 10 <sup>14</sup>	6.0 x 10 <sup>16</sup>	10%
CO	2.5 x 10 <sup>18</sup>	5.3 x 10 <sup>18</sup>	10%
HCHO	3.2 x 10 <sup>15</sup>	1.2 x 10 <sup>16</sup>	25%
HNO <sub>3</sub>	3.3 x 10 <sup>15</sup>	1.4 x 10 <sup>16</sup>	25%

### 3.3.3 Sensor Specification

This mission consists of two optical sensors: a UV/VIS sensor and an IR sensor. The sensor specifications are summarized in Table 3.3-3. The IR sensor continuously measures temperature, water vapor profiles, and the tropospheric column of ozone and carbon monoxide over 24 hours. The UV/VIS sensor measures precise total column of ozone and nitrogen dioxide. UV/VIS sensors use an established technology and have a long record of success in the observation of atmospheric pollution. However, UV/VIS sensors have the disadvantage of daytime only observation and difficulty in producing vertical concentration profiles. Both sensors have their advantages and disadvantages, so it is ideal to use a combination of these sensors.

The IR sensor shall cover the spectral range of 650–1200 and 1600–2250 cm<sup>-1</sup>. High vertical resolution of temperature and water vapor sounding requires the spectral resolution of 0.6 cm<sup>-1</sup>. The IR sensor must provide Full Disk Coverage with a repeat cycle of 0.5–1 hour.

Table 3.3-3 Sensor Specifications

	UV/VIS	IR
Spectral Range	280-600 nm	650-1200, 1600-2250 $\text{cm}^{-1}$
Spectral Resolution	0.6 nm (0.1 nm sampling)	0.6 $\text{cm}^{-1}$
SNR	500	
NEdT		0.5 K (700-800 $\text{cm}^{-1}$ , 280K) 0.2 K (1600-2000 $\text{cm}^{-1}$ , 280K) 0.25 K (1030 $\text{cm}^{-1}$ , 260K) 0.85 K (2160 $\text{cm}^{-1}$ , 280K)
IFOV	< 10 km	< 10 km
Observation Area	(1) Meteorology Mission: Full Disk (2) Atmospheric Chemistry Mission: ① (Japan region) 20-50N, 105-150E (4000 km square) ② (Asia region) 15S-60N, 60-160E	
Observation Interval	(1) Meteorology Mission : 0.5–1 hour (2) Atmospheric Chemistry Mission: 1–2 hour	

### 3.3.4 IR Sensor Overview

The baseline concept of the IR sensor system is an imaging Fourier Transform Spectrometer (FTS). The imaging FTS acquires image and spectrum simultaneously using an array detector at the focal plane of the FTS. The schematic diagram of the IR sensor system is shown in Fig. 3.3-2. The IR sensor consists of following components:

- 2-axis gimballed scanner
- Telescope:  $\Phi 30$  cm, afocal magnification of 5
- Interferometer (MOPD 1.6 cm) (Double Corner Cube, Flexible Blade Type)
- 2 Bands (650-1200, 1600-2250  $\text{cm}^{-1}$ )
- PV-HgCdTe array detector
- Pixel Size IFOV 10 km  $\rightarrow$  150  $\mu\text{m}$   $\rightarrow$   $5 \times 5$  subpixels of 30  $\mu\text{m}$   
IFOV 4 km  $\rightarrow$  60  $\mu\text{m}$   $\rightarrow$   $2 \times 2$  subpixels of 30  $\mu\text{m}$
- Array Size IFOV 10 km  $\rightarrow$   $20 \times 20$  (TBD)  
IFOV 4 km  $\rightarrow$   $128 \times 128$  (TBD)
- 14 bit ADC
- Detector is operated at 50 K.
- FTS and Aft-Optics are cooled to 150 K by a radiation cooler.

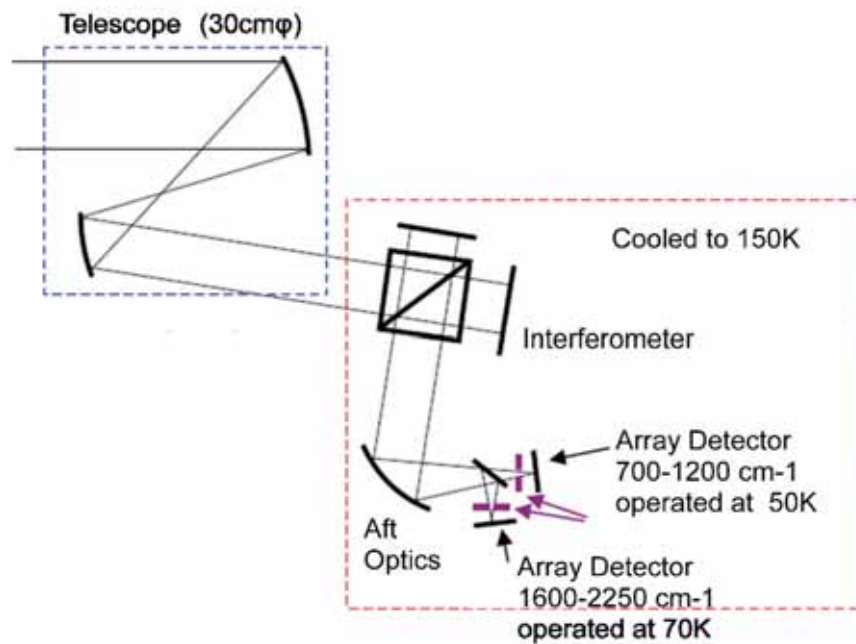


Fig. 3.3-2 Schematic diagram of IR Sensor System

### 3.4 Compact Infrared Camera (CIRC) for Earth Observation

#### 3.4.1 The Compact Infrared Camera (CIRC)

The compact infrared camera (CIRC) is a technology demonstration payload of the Small Demonstration-Satellite type-2 (SDS-2). The CIRC is an infrared camera equipped with an uncooled infrared array detector (microbolometer). The main mission of the CIRC is the technology demonstration of wildfire detection using the microbolometer.

Microbolometers are widely used in commercial and military applications, such as for night vision. Microbolometers have an advantage of not requiring cooling mechanisms, such as a mechanical cooler. Eliminating the detector cooling system can reduce the size, cost, and electrical power of the sensor. Although the sensitivity of microbolometers is lower than that of HgCdTe-based photonic infrared detectors, the advantage of not needing a cooling mechanism is suitable for small satellites or resource-limited sensor systems.

JAXA/EORC has started research on application of microbolometers to Earth observation since 2000. The Wide-Angle Multi-band Sensor-Thermal Infrared (WAMS-TIR)<sup>1)</sup>, aboard the station-keeping test airship (SPF-II) for the stratospheric platform project, is a thermal infrared multi-band radiometer using a microbolometer FPA.

In order to demonstrate the potential of microbolometers to thermal infrared imaging from space, the compact infrared camera (CIRC) was chosen as a technology demonstration payload of the Small Demonstration Satellite (SDS). The SDS program is a JAXA activity to demonstrate a variety of new technologies and missions.

The main mission of the CIRC is the technology demonstration of wildfire detection using the microbolometer. Wildfires are one of the major and chronic disasters affecting many countries in the

Asia-Pacific region, and some suggestions are that this will get worse with global warming and climate change. In the Sentinel Asia project to share disaster information in near real-time across the Asia-Pacific region, wildfire detection has been chosen as an important activity.

A baseline specification of the CIRC is shown in Table 3.4-1. We set the baseline specification to meet requirements for wildfire detection. The detector is a large format (640 x 480) to obtain a wide field of view. The spatial resolution is an important factor for wildfire detection. The baseline specification of the spatial resolution is 200 m from the altitude of 600 km. Fig. 3.4-1 shows a system block diagram of the CIRC. In order to reduce the size, weight, and cost, we minimized the functions of the CIRC. The optics unit of the CIRC is f/1-f/1.5. We are discussing employment of athermal optics to maintain optical performance in a wide range of temperatures. This will be an advantage of the CIRC for small satellites, because we will not need an active thermal control for the optics.

Table 3.4-1 Baseline Specifications of the CIRC

Item	Characteristics
Size	< 150 mm x 150 mm x 300 mm
Mass	< 5 kg
Detector	Uncooled infrared detector
Wavelength	8-12 $\mu\text{m}$
Number of Pixels	640 x 480
Spatial Resolution	< 200 m observed from 600 km (< 0.33 mrad)
Field of View	12° x 9°
Frame Rate	30 Hz
Dynamic Range	180 K-450 K
NE $\delta$ T	0.2 K@300 K

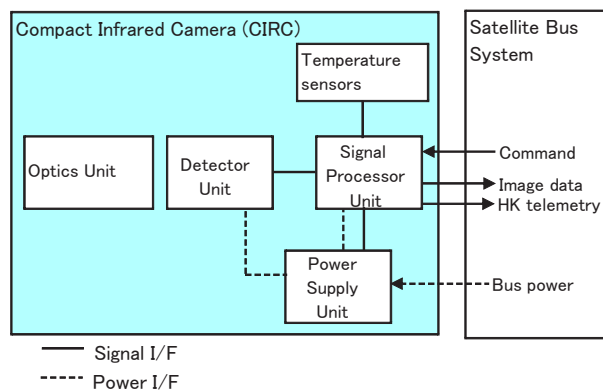


Fig. 3.4-1 System Block Diagram of the CIRC

### 3.4.2 Feasibility Study of Wildfire Detection

In order to investigate the difference of wildfire detectability depending on spatial resolution, we made simulated images of which spatial resolutions are 180 m and 270 m from the original

ASTER/TIR image.

Fig. 3.4-2 shows simulated images of the forest fire in California and the peat fire in Indonesia. We searched the image for regions of anomalously high brightness to detect wildfires. In general, wildfire detection using satellite data uses short or medium infrared images. However, by optimizing a threshold level, we can detect a wildfire only from the thermal infrared image.

Hotspots are detected by a contextual threshold method. A pixel is defined as a hotspot if the anomaly in  $11\mu\text{m}$  brightness is higher than  $3\sigma$ , where  $\sigma$  is a standard deviation of brightness in pixels within a 1-km radius. Details of this algorithm will be published in 2).

To check detectability, we used the Moderate-resolution Imaging Spectroradiometer (MODIS) Thermal Anomalies/Fire products (MOD14v4). The MOD14 algorithm detects fire locations using  $4\mu\text{m}$  and  $11\mu\text{m}$  brightness temperatures with a spatial resolution of 1 km.

From this simulation, we find that the detectability of forest fire or tundra fire using thermal infrared images of which spatial resolution of 180 m is comparable to that of the MOD14 algorithm. On the other hand, detection of peat fire requires higher spatial resolution because the burning temperature of peat fires is lower than that of other wildfires.

Although further improvements of the detection algorithm are needed, especially for peat fires, we find that 200-m spatial resolution is almost appropriate for wildfire detection. The detectability of wildfires should have a dependency to the burning area. In addition, there is a possibility of detecting a “false alarm” wildfire in a city due to various heat sources like power plants. Thus, we are planning to apply this algorithm to other various data sets and check detectability.

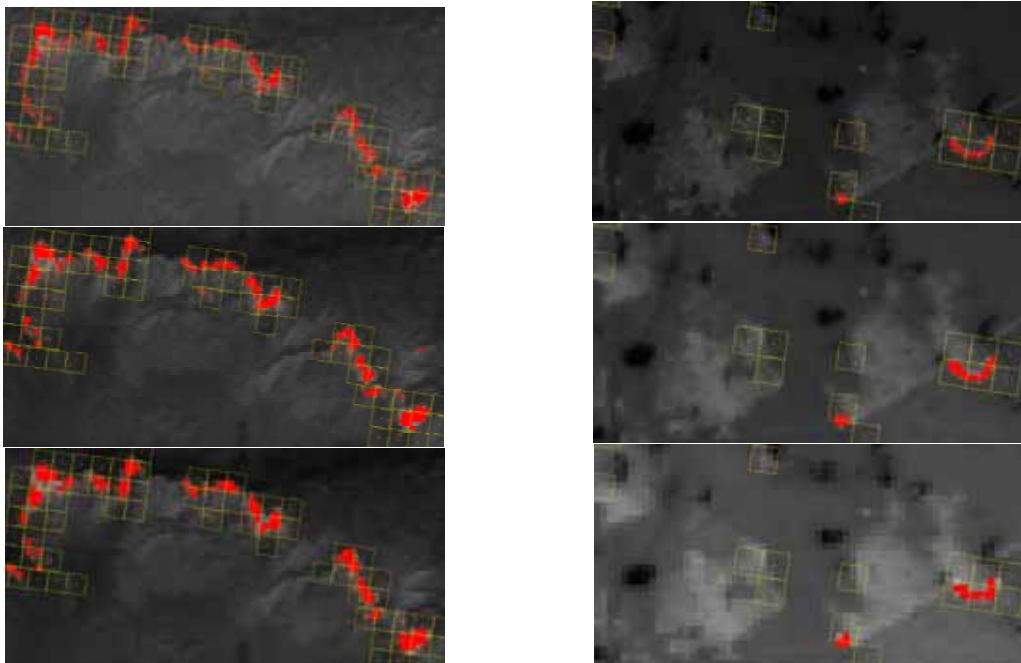


Fig. 3.4-2 ASTER/TIR images of a forest fire in California on October 26, 2003 (right) and a peat fire in Indonesia on October 12, 2006. The spatial resolutions are 90 m (top), 180 m (middle), and 270 m (bottom). Red filled squares are the results of wildfire detection using thermal infrared data only. Yellow open squares are results using MOD14.

## References

- 1) Okamura, Y., et al. "Development of the WAMS-TIR Instrument for SPF-II." *Proc. SPIE*, **5659** (2005): 105-114.
- 2) Nakau, K., et al. In preparation

## 3.5 Calibration of Optical Sensors

### 3.5.1 Introduction

Optical sensors are usually radiance-calibrated against a halogen lamp integrating sphere, the spectral radiance of which is calibrated traceable to fixed-point black bodies. In the visible and near infrared (VNIR, 380 to 1000 nm) range, the uncertainty of radiance calibration has been evaluated in detail. However, in the shortwave infrared (SWIR, 1000 to 2500 nm) range, the uncertainty of radiance calibration has not been evaluated. Furthermore, there are large uncertainty factors in properties of the integrating sphere. The target of this study is to achieve the same accuracy in the SWIR range as that in the VNIR range, and to develop a calibration light source for the SWIR range.

In addition, the wavelength calibration system using wavelength-tunable lasers was investigated to calibrate spectral responsivities of an optical sensor with a large aperture, which were previously impossible to measure.

### 3.5.2 Calibration System

The overview of the radiance calibration system is shown in Fig. 3.5-1. It consists of fixed-point black bodies (FPBB) as the primary standards and integrating spheres (IS) as the working standards. The spectral radiance of the IS was calibrated against the FPBB by a standard radiometer. The optical sensors were radiance-calibrated against the IS.

FPBBs of the aluminum point (933.47 K) and zinc point (692.68 K) were used in the SWIR range. These were traceable to the national standard. The aperture diameter of the IS was set to cover the aperture of the optical sensor. The spectral radiance level of the IS was set close to that of the Earth's surface by adjusting the number of lamps and the lamp voltage. The standard radiometer measured the ratio of the spectral radiance between the FPBB and IS in 20-nm steps from 1000 to 2500 nm. The spectral radiance of the IS was calculated from this ratio and the spectral radiance of the FPBB, which was calculated from Planck's law. This calibration was cross-checked using an independent radiometer.

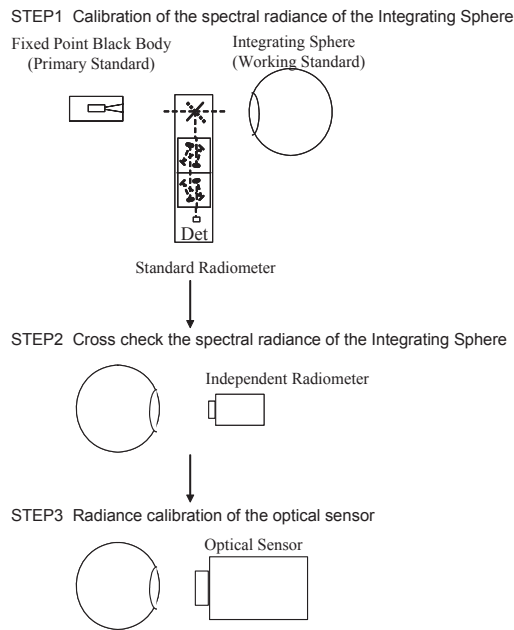


Fig. 3.5-1 Schematic Diagram of the Radiance Calibration System

The schematic diagram of the wavelength calibration system is shown in Fig. 3.5-2. The system consists of a monochromatic light source and a standard detector. Spectral responsivities of an optical sensor were calibrated against the standard detector by changing the wavelength of the light source. The light source consists of wavelength-tunable lasers and an integrating sphere. A continuous-wave (CW) dye laser and a CW titanium sapphire laser were used as the monochromatic light sources. The laser output was directed into the integrating sphere, which made the light source large, spatially uniform, and depolarized at the aperture. A Michelson interferometer determined the laser wavelength. An EO modulator stabilized the laser intensity. The standard detector was calibrated traceable to the cryogenic radiometer of the national standard, and was located at the integrating sphere wall or at the sensor position by a substitution method.

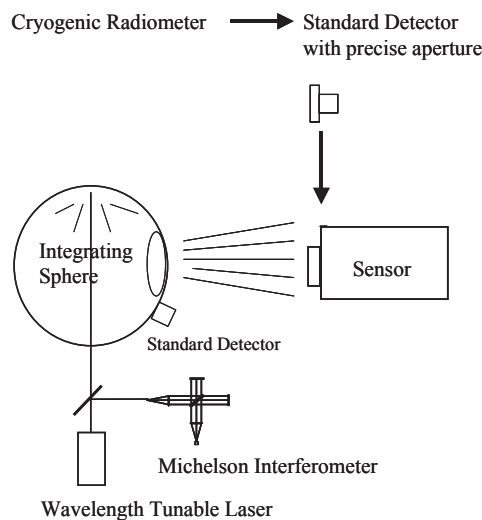


Fig. 3.5-2 Schematic Diagram of the Wavelength Calibration System

### 3.5.3 Gold-coated Integrating Sphere

Barium sulfate is generally used as the inner wall of an IS. Barium sulfate is an ideal material in the VNIR range due to its high reflectance (98%) and Lambertian behavior, which produces a uniform light source at the aperture. However, in the SWIR range, a barium sulfate IS is unsuitable for the working standard, i.e., the calibration light source, because of the hydrophilic nature of barium sulfate. The spectral radiance spectrum of the barium sulfate IS is not smooth and has many bumps caused by water absorption in the SWIR range, although the spectrum is smooth with no bumps in the VNIR range. These bumps degrade the calibration accuracy of the spectral radiance, which is usually measured in 20-nm steps, and it is difficult to evaluate the uncertainty. Furthermore, the radiance stability near water absorption bands greatly depends on the temperature and moisture in the room, which also degrades the calibration accuracy.

Therefore, integrating spheres made from materials that are not hydrophilic, such as gold and polytetrafluoroethylene, were studied as the working standard instead of barium sulfate. Gold has a flat reflectance spectrum of 95% between 1 and 20  $\mu\text{m}$  and is not hydrophilic. Therefore, gold is an ideal material for the sphere's inner wall in the SWIR range. In this study, a gold-coated IS was developed by the following manufacturing process: The sphere's inner wall was sandblasted to ensure diffuseness, which is necessary to achieve radiance uniformity at the aperture. After sandblasting, the inner wall was gilded with gold 0.1  $\mu\text{m}$  thick. Fig. 3.5-3 shows a photograph of the gold-coated IS. The inner diameter of the gold-coated IS was 150 mm and the aperture diameter was 50 mm.

The spectral radiance of the gold-coated IS is shown in Fig. 3.5-4. The gold-coated IS had a smooth spectral radiance spectrum, although there was a water absorption spectrum. A smooth spectral radiance spectrum is ideal as a calibration light source. This is because the reflectance of gold is flat in the SWIR range and has no spectral structure. The reason for the water absorption spectrum is under investigation, which existed under the purging environment with nitrogen gas. The radiance uniformity of the gold-coated IS at the aperture of 50 mm  $\phi$  was measured in each 5-mm grid at 763, 1640 and 2210 nm. The radiance uniformity at 1640 nm is shown in Fig. 3.5-5. The radiance uniformity of the aperture was within 1%, which is the typical performance of a barium sulfate IS.

In this study, the gold-coated IS was confirmed to have sufficient properties for the working standard and to be superior to the barium sulfate IS in the SWIR range. The remaining problem is the development of a large IS with a 1000-mm inner diameter, which is necessary to calibrate an optical sensor with a large aperture, such as the 177-mm-diameter aperture of the Global Imager (GLI) on the ADEOS-II satellite.



Fig. 3.5-3 Gold-coated Integrating Sphere

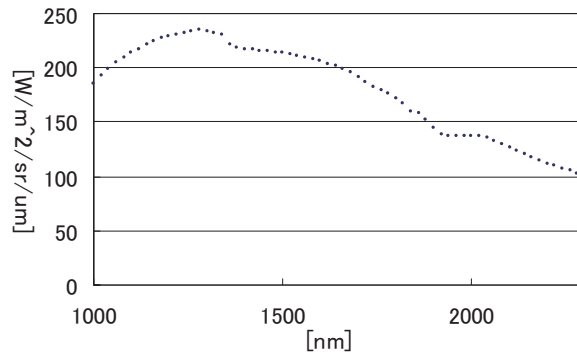


Fig. 3.5-4 Spectral Radiance of the Gold-coated Integrating Sphere

	2.0cm	1.5cm	1.0cm	0.5cm	中心	0.5cm	1.0cm	1.5cm	2.0cm
2.0cm			0.64%	0.30%	0.25%	0.16%	0.06%		
1.5cm		0.84%	0.43%	0.05%	-0.07%	0.10%	0.15%	0.43%	
1.0cm	0.64%	0.50%	0.22%	-0.12%	-0.24%	0.04%	0.36%	0.52%	0.81%
0.5cm	0.24%	0.14%	-0.01%	-0.07%	-0.11%	0.06%	0.26%	0.52%	0.75%
中心	0.10%	-0.10%	-0.14%	-0.10%	0.00%	0.12%	0.22%	0.47%	0.77%
0.5cm	0.23%	-0.05%	-0.24%	-0.25%	-0.12%	0.01%	0.08%	0.42%	0.83%
1.0cm	0.42%	0.03%	-0.30%	-0.33%	-0.39%	-0.28%	0.06%	0.60%	0.95%
1.5cm		0.22%	-0.05%	-0.21%	-0.32%	-0.18%	0.34%	0.82%	
2.0cm			0.41%	0.14%	0.04%	0.23%	0.55%		

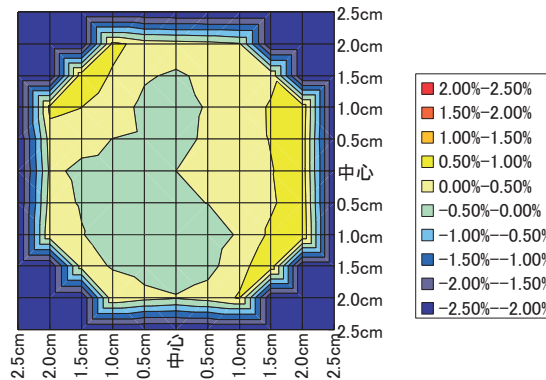


Fig. 3.5-5 Radiance Uniformity of the Gold-coated Integrating Sphere

A large IS with a 1000-mm-inner diameter and 300-mm-aperture diameter is under development. The radiance uniformity of the IS greatly depends on the reflectance uniformity and diffuseness of the backside inner wall, which is the opposite side of the IS aperture. Therefore, the manufacturing processes of a large and uniform diffuser plate for the backside inner wall were studied, such as sandblasting, washing, the preparation process, gold gilding, gold vapor deposition, and so on. In this study, the gold gilding approach and gold vapor deposition approach were investigated. Both approaches have different advantages and difficulties. The results of both approaches will be compared and an approach will be selected. This year, the manufacturing processes of the gold gilding approach were investigated.

It is difficult to evaluate optical properties of large samples; therefore, the following method was adopted to evaluate reflectance uniformity. Firstly, a diffuser plate with a 350-mm diameter was manufactured, after that, 34 witness samples with 40-mm diameters were made by laser cutting, all

from the 50-mm grid position. The reflectance of the witness samples were measured. Fig. 3.5-6 shows a witness sample and the original diffuser plate. Fig. 3.5-7 shows the reflectance distribution corresponding to the position on the original diffuser plate. The reflectance was uniform within 0.5%. In this study, the gold gilding approach was confirmed to be a reliable approach for the large and uniform diffuser plate. Next year, the manufacturing process of the gold vapor deposition approach will be investigated.



Fig. 3.5-6 Witness Sample Made by the Gold Gilding Approach

	15.0 cm	10.0 cm	5.0 cm	0.0 cm	5.0 cm	10.0 cm	15.0 cm
15.0 cm			-0.33%	-0.38%	0.00%		
10.0 cm		-0.23%	-0.35%	-0.20%	-0.10%	0.30%	
5.0 cm	-0.38%	-0.23%	-0.18%	-0.20%	0.10%	0.28%	0.18%
0.0 cm	-0.08%	-0.35%	-0.20%	0.00%	0.15%	0.30%	0.28%
5.0 cm	0.00%	0.10%	-0.03%	0.13%	0.05%	0.13%	0.45%
10.0 cm		0.20%	0.15%	0.15%	0.20%	0.30%	
15.0 cm			0.18%	0.08%	0.40%		

Fig. 3.5-7 Reflectance Distribution of Witness Samples Corresponding to the Position on the Original Diffuser Plate



## ***4. DEVELOPMENT ON GROUND SYSTEMS***

## 4. DEVELOPMENT ON GROUND SYSTEMS

### 4.1 Overview

The EORC Ground System Development Group has been working on future Earth observation satellite projects, GPM, GCOM, and EarthCARE. System development for GOSAT and the studies on GPM, GCOM, EarthCARE, and the initial operation of GOSAT in FY 2008 and future data utilization are summarized below.

### 4.2 GPM Mission Operation System

#### 1) Overview

Global Precipitation Measurement (GPM) is composed of one core satellite and about eight constellation satellites. The GPM core satellite is the TRMM follow-on mission conducted in cooperation with NASA. It carries a dual-frequency precipitation radar (DPR) and a GPM microwave imager (GMI). It is scheduled to be launched in 2013. The GPM mission concept is to observe precipitation more frequently and globally compared to the TRMM by employing the TRMM design, but with a high-inclination core satellite and a fleet of constellation satellites. The GPM program will be conducted in cooperation with NOAA, CNES, ISRO, EUMETSAT, China, etc. The partner countries and organizations are responsible for development of the constellation satellites. Multiple numbers of constellation satellites will enable global measurement of precipitation about every 3 hours.

#### 2) Status of mission operation system

The operational concept for GPM/DPR was defined and the GPM/DPR ground segment completed its system definition review (GS-SDR) in March 2009. A conceptual idea for all GPM/DPR ground systems and functions has been studied.

#### 3) GPM data flow

GPM core satellite data are received at White Sands via the Tracking and Data Relay Satellite (TDRS). The received data are transmitted to NASA's GSFC and processed into APID sorted data. NASA's Precipitation Processing System (PPS) transfers the DPR APID sorted data and GMI products to the EORC via the Internet. The EORC processes the DPR products, such as precipitation rate, and distributes the products to operational users and public users via the Internet.

Most constellation satellite data are gathered at NASA's PPS. The PPS also transmits the constellation's microwave sensors data to the EORC. The EORC processes the precipitation map frequently and provides it to the operational agencies in near real-time.

Figure 4.2-1 shows the overview and system interfaces of the EORC GPM/DPR mission operation system.

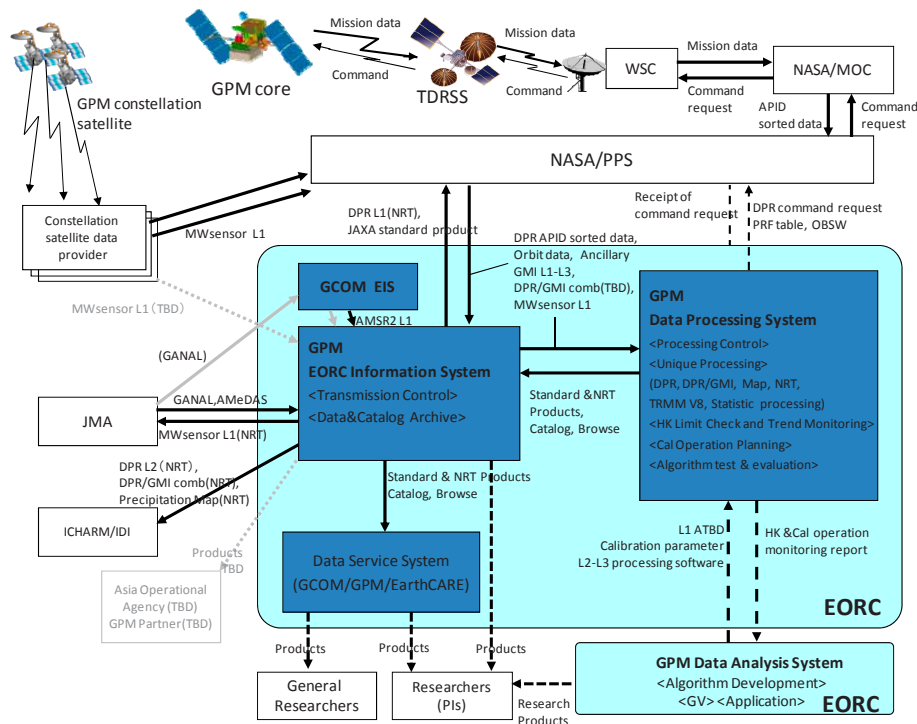


Fig. 4.2-1 Overview of GPM/DPR Mission Operation System

4) GPM Data Working Group (GDaWG)

GPM products are composed of many satellites' data and ancillary data, whose origins are different. It is important to discuss effective utilization of data and data systems. The GPM Data Working Group (GDaWG) had been established to discuss the data system development plan for data exchange among data partners. The GDaWG website, which targets information sharing, was released in August 2008.

4.3 GCOM Mission Operation System

The Global Climate Observation Mission (GCOM) is an ADEOS-II follow-on mission that focuses on continuing and improving Earth observation related to global change phenomena. GCOM consists of two series of satellites, GCOM-W and GCOM-C, each of which consists of three sequentially launched satellites covering 10 to 15 years starting in 2011 (GCOM-W) and 2013 (GCOM-C). JAXA and NOAA have started discussion on GCOM (-W and C) and NPOESS collaboration (data receiving/exchange and science activities).

4.3.1 Status of the GCOM-W1 Mission Operation System

1) Overview

GCOM-W will carry the AMSR/AMSR-E follow-on sensor, AMSR2, to contribute to the study of the water cycle.

## 2) Status of mission operation system

The operational scenario for GCOM-W1 was established and the GCOM-W1 ground segment completed its Preliminary Design Review (PDR) in March 2009, advancing it to the critical design phase.

## 3) GCOM-W1 data flow

GCOM-W1 science global data are received at a high-latitude ground station, i.e. Svalbard, every orbit via X-band. Other backup stations are under consideration. Real-time data, in the area of Japan, are received mainly at JAXA's KTCS (Katsuura Tracking and Communication Station), and TKSC (Tsukuba Space Center) is the backup system via X-band. The received data are processed into APID sorted data at each station and transferred to the EORC via the Internet. Level 1 and higher processing will be done at the EORC, and the products will be distributed to operational users and public users from the EORC information system via the Internet.

S-band uplink and downlink for TT&C will be done via JAXA's ground network, and the Svalbard station is the backup.

Figure 4.3-1 shows the overview of the GCOM-W1 operation system.

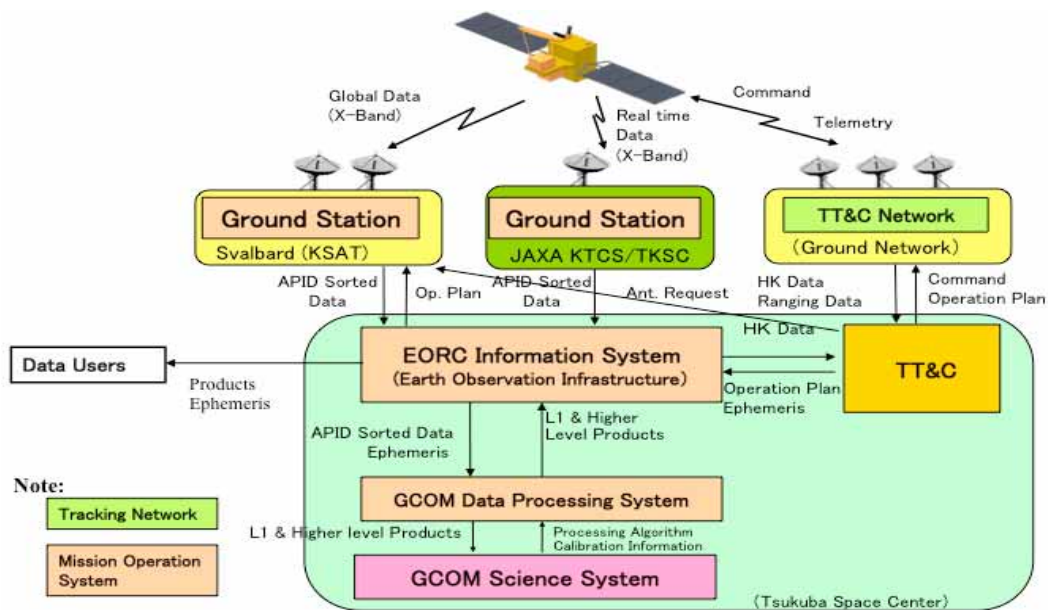


Fig. 4.3-1 Overview of the GCOM-W1 Operation System

### 4.3.2 Status of the GCOM-C1 Mission Operation System

GCOM-C will carry the GLI follow-on sensor, SGLI, to observe the Earth's atmosphere and surface to contribute to the understanding of the carbon cycle, radiation budget, and to enhance the investigation of climate change.

The operational scenario for GCOM-C1 will be established by the end of 2009.

#### 4.4 EarthCARE Mission Operation System

##### 1) Overview

Earth Clouds, Aerosols and Radiation Explorer (EarthCARE) is a mission for climate change observation conducted in cooperation with ESA. EarthCARE will carry four sensors to measure the vertical distribution of cloud particles and aerosols and to measure the speed of ascending and descending cloud particles. Japan is responsible for developing the Cloud-Profiling Radar (CPR) and its data processing. EarthCARE is scheduled to be launched in 2013.

##### 2) Status of mission operation system

The JAXA EarthCARE project was initiated in September 2008. Through a satellite system requirement review (SRR), the requirements for ground segments were agreed upon by ESA and JAXA.

ESA and JAXA ground segments are in the conceptual design phase to allocate requirements to the system functions in preparation of the ESA ground segment requirement review (GS-RR) and JAXA ground segment system definition review (GS-SDR) in FY 2009.

#### 4.5 GOSAT Mission Operation System

##### 4.5.1 System Overview

The Greenhouse Gases Observing Satellite (GOSAT) is a mission for greenhouse gases observation conducted in cooperation with the Ministry of the Environment (MoE) and the National Institute of Environmental Studies (NIES) to observe greenhouse gases, including carbon dioxide (CO<sub>2</sub>) and methane (CH<sub>4</sub>). GOSAT will carry a Michelson Fourier transform spectrometer (TANSO-FTS) to measure the amount of greenhouse gases and a cloud and aerosol imager (TANSO-CAI). GOSAT was launched successfully on January 23, 2009.

JAXA's GOSAT Mission Operation System (MOS) is responsible for sensor operation and X-band downlink stations planning, accumulation of downlink data to TKSC, Level 0 processing of mission data and housekeeping (HK) data, Level 1 processing of TANSO-FTS/CAI data, archiving TANSO data, and delivering data to data users, including the National Institute of Environment Studies (NIES) during routine operation. Level 1 processing gives radiometric and geometric correction to the TANSO data obtained with onboard sensors. The NIES is responsible for Level 2 and higher-level processing, which includes the retrieval of column densities of greenhouse gases, global mapping of greenhouse gases, and identification of their source and sink region.

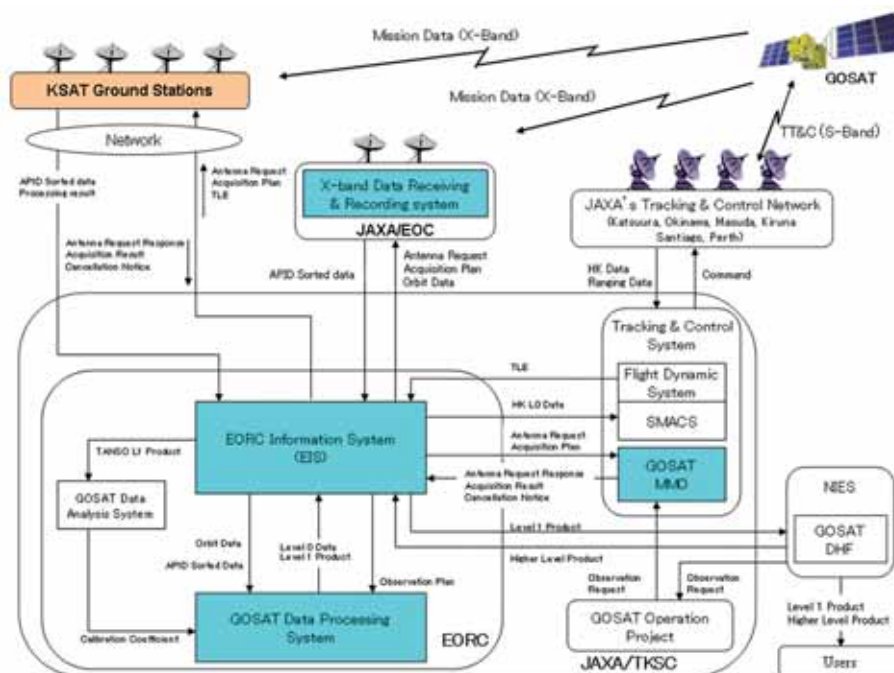


Fig. 4.5 Overview of the GOSAT MOS (Light blue and light brown segments)

The GOSAT MOS consists of the Data Receiving and Recording Systems in the EOC, overseas ground stations, i.e., SvalSat stations of Kongsberg Satellite Services (KSAT), the EORC information System (EIS), the Data Processing System (DPS), and the Mission Management Organization system (MMO) in TKSC. Figure 4.1 shows the overview of the GOSAT MOS.

The EOC Data Receiving System tracks GOSAT to receive and demodulate GOSAT mission data downlinked via X-band. The MOS antenna is assigned as the main domestic antenna for GOSAT and the ADEOS antenna is the domestic backup. The Data Recording System records demodulated data sent from an X-band receiving system JAXA as raw data. Simultaneously, it divides the demodulated data according to their APID (Application Process ID) and records them as APID sorted data files.

After completion of data acquisition in the domestic station, APID sorted data are delivered to the EIS in the EORC at TKSC. Operations of these systems are done by the same operator simultaneously. These systems are also applicable to any other satellites using the CCSDS format.

SvalSat is an X-band receiving station located at 78 degrees north latitude and run by KSAT.

SvalSat has visibility for every GOSAT orbit, fourteen to fifteen per day. Five to seven GOSAT downlinks to SvalSat per day are being performed to enable a downlink every two orbits in conjunction with EOC downlinks. SvalSat sends APID sorted data to the EORC at TKSC. Data transmission uses academic networks and its performance is near 40 Mbps using a WAN accelerator.

MMO receives observation requests for GOSAT mission sensors and make plans for sensor operation and data downlinks. MMO is also responsible for downlink antenna assignments. MMO is located at the TT&C operation room for GOSAT and the same operator controls it along with the Satellite Management and Control System (SMACS).

The EIS is constructed as a common infrastructure for the EORC at TKSC. For GOSAT, it takes care of data interface control, data archiving, and user services. The EIS is the data gateway between the GOSAT MOS in TKSC and the other systems, such as KSAT, the EOC, the NIES, JAXA's TT&C, and so on. The EIS also has the capability to archive GOSAT data and products for the long

term. The NIES is generally responsible for user services, while JAXA's EIS takes care of distributing of GOSAT products to specified organization users like the NIES under certain agreements. Delivery of GOSAT products from the EIS to ESA is under discussion. NASA/JPL and ECMWF are also candidates of organization users.

The GOSAT DPS consists of the Processing Control System (PCS) and the GOSAT Specific Data Processing System (GSDPS). The PCS controls the GSDPS as an outer function. The PCS takes care of planning for data processing, definition of product scene extraction, data interface control, results management, etc. The PCS was developed to be applicable to other global observation satellites' data processing with relatively simple revision. The GSDPS performs Level 0 processing for all GOSAT APID sorted data extracted at X-band downlink stations. Level 0 HK data are sent to the SMACS of the TT&C via the EIS for limit checks to monitor the health status of the satellite and the onboard sensors. Level 0 GPS data are also delivered via the EIS to the flight dynamics system in JAXA to determine the satellite's orbit. The GSDPS performs Level 1 processing for TANSO-FTS and CAI to produce FTS Level 1A/1B products and CAI Level 1 products. These products are sent to the EIS, archived, and delivered to the NIES from the EIS.

#### **4.5.2 MOS Preparation for GOSAT Launch**

In FY 2008, the GOSAT MOS carried out mission simulation tests of GOSAT ground segments involving external ground systems, i.e., KSAT, the NIES, and JAXA-related systems (TT&C, FDS, and so on), which were initiated in FY 2007. An end-to-end test involving GOSAT and onboard sensors was also carried out under the conduction of JAXA's GOSAT project. Through these tests, the GOSAT MOS was confirmed to be ready for launch. The results from these tests were reported in Completion Review of GOSAT Development on November 6, 2008, and its delta Review on December 28, 2008. The largest hurdles in launch preparation were delays in TANSO Level 1 algorithm development and in the deciding of the nominal mission sensors operation in detail. To handle the delay of Level 1 processing algorithm development, the MOS GSDPS prepared a pre-launch version of processing software for the end-to-end test and a launch version for initial operation after the launch. MMO could not complete the implementation of all new operation requirements before the launch, but since operation using the MMO begins in the routine operation phase (3 months after the launch), all remaining implementation of MMO software is scheduled to be completed during routine operation of GOSAT.

In the course of launch preparation, the GOSAT MOS scheduled and carried out training for GOSAT initial operation and evaluation of the MOS during the initial operation phase. In addition, the MOS participated in two mission rehearsals of GOSAT launch and critical phase operation.

#### **4.5.3 GOSAT Initial Checkout Operation and the MOS Evaluation in Initial Operation**

GOSAT was successfully launched on January 23, 2009. There were a couple of X-band downlink failures at both stations in the EOC and KSAT during the early orbits when the ephemeris information was not sufficiently accurate, but the operational efforts enabled recovery from the unstable situations. GOSAT obtained first light data for TANSO-FTS in the short wave infrared (SWIR) band and CAI on February 7, 2009, as well as that for TANSO-FTS in the thermal infrared (TIR) band on March 3, 2009. The MOS produced FTS and CAI Level 1 data for these first light observations to support the publication of the first light results by the GOSAT project and

calibration/analysis group. The GOSAT MOS has been evaluating system performance according to the prefixed ground mission evaluation plan (GMEP) and the evaluation will be completed in FY 2009 after GOSAT enters the routine operation phase.

#### **4.5.4 Products Release plan**

JAXA plans to release JAXA TANSO-FTS/CAI Level 1 products to users in the following schedule:

1) Uncollected Products:

To be released to calibration PIs and science teams 3 months after launch with an authorization in the GOSAT Readiness Review for Routine Operation (calibration/validation operation) Phase.

2) Initially Calibrated Products

To be released to research announcement (RA) users and to the Uncollected Products users 6 months after launch with an authorization in the GOSAT Review for Completion of Calibration/Validation Operation Phase.

3) Confirmed Products

To be released to public users 9 months after launch with an authorization in the GOSAT Review for Completion of TANSO Level 1 calibration.

Level 1B and 1B+ products of TANSO-CAI are produced by the NIES according to agreements between the NIES and JAXA, which also follows the same release schedule as that of JAXA TANSO L1 products.

As for Level 2/3 products processed by the NIES, Uncollected Products, Initially Calibrated Products, and Confirmed Products are planned to be released on the timeframe of 6, 9, and 12 months after launch, respectively.

#### **4.6 Research and Development for Data Utilization**

Technology for data utilization, such as data access, data distribution, and data searching, changes very rapidly. In order to track new and effective technology, the EORC continues to participate in Committee on Earth Observation Satellite/Working Group on Information and Service System (CEOS/WGISS) meetings, the Group on Earth Observations (GEO) Architecture Implementation Pilot (AIP), and other related activities. In 2008, prototype servers for the Web Map Service (WMS) and a catalog service using “de facto” standards were set up. These two services work in connection with each other and can be used via the GEO portal, a GEO Common Infrastructure (GCI).

## ***5. GROUND SYSTEM OF OPERATIONS***

## 5. GROUND SYSTEM OF OPERATIONS

### 5.1 The EOC (Earth Observation Center)

The Earth Observation Center (EOC), located about 50 km northwest of Tokyo, was founded in October 1978 to establish and develop satellite remote-sensing technologies. The EOC has facilities for mission management and operations, and a public information service for Earth observation satellite data. Its activity covers JAXA-owned Earth observation satellites and other satellites operated by foreign agencies.

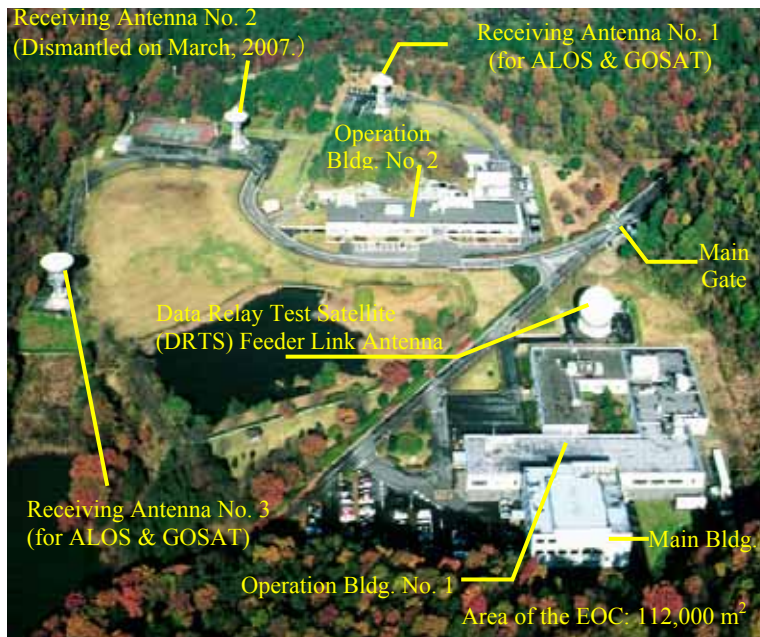


Fig. 5.1-1 Bird's-eye View of the EOC.

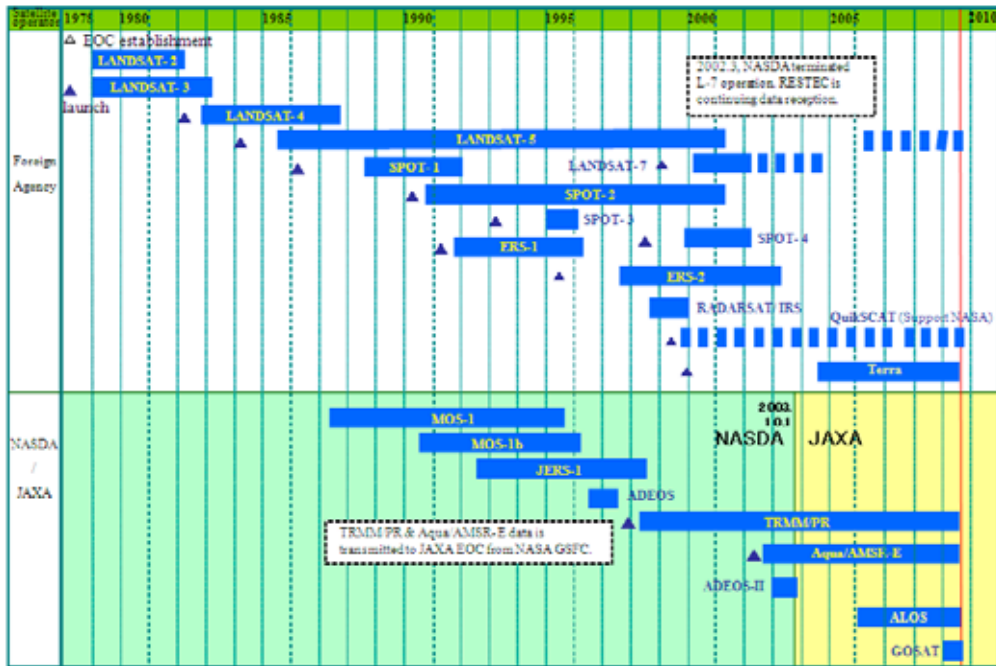
#### 5.1.1 History and Current Operations

The first program at the EOC started in 1978 using NASA's Earth observation satellites Landsat-2 and -3, and afterward using Japanese satellites, including the Marine Observation Satellite (MOS-1a and -1b), the Japanese Earth Resources Satellite-1 (JERS-1), the Advanced Earth Observation Satellite (ADEOS), and the Precipitation Radar carried on NASA's Tropical Rainfall Measurement Mission satellite (TRMM/PR).

Foreign satellite programs with the French Satellite Pour l'Observation de la Terre (SPOT), the European Remote-Sensing Satellite (ERS), the Canadian Radar Satellite (RADARSAT), and the Indian Remote-Sensing Satellite (IRS) has been added to EOC activities.

The Greenhouse gases Observing Satellite (GOSAT), launched in 2009, and the Advanced Land-Observing Satellite (ALOS), launched in 2006, joined the ongoing operations, Aqua/AMSR-E and TRMM/PR. In the collaboration for worldwide user services, the EOC has been archiving data for 30 years.

Table 5.1.1-1 Operation History of the EOC.



5.1.1.1 TRMM Mission Operation

1) TRMM/PR overview

The EOC has been processing Tropical Rainfall Measurement Mission (TRMM)/precipitation radar (PR) data and delivering it to the science community and users since its launch in November 1997.

2) TRMM/PR data flow

Telemetry and science observation data are transmitted to the ground via NASA's Tracking and Data Relay Satellite (TDRS), which is operated by NASA's GSFC. All acquired data are transmitted to the GSFC Sensor Data Processing Facility (SDPF) online and processed to Level 0 data within 48 hours of observation. The processed data are distributed to sensor providers to generate standard products. The EOC then processes the PR data with its own TRMM/PR data processing system.

The TRMM/PR data processing system consists of three subsystems. Two subsystems are set up in the EOC for processing and PR operations planning. One subsystem, the Active Radar Calibrator (ARC), is operated in the Kansai branch of the National Institute of Information and Communications Technology (NICT).

3) PR science data management

The PR science products presented in Table 5.1.1.1-1 are distributed to users such as worldwide scientists in a variety of fields, including meteorology and hydrology. The EOC distributes the processed data to the EORC and NICT via an online network. The EOC receives the near real-time data of PR 2A25-R1, PR 2A25-R2, and TMI 1B11 from the Precipitation Processing System (PPS) of NASA's GSFC online and forwards them to the Japan Meteorological Agency (JMA).

## 4) Version 6 PR data

The EOC processes and provides the PR data based on a version 6 algorithm.

Table 5.1.1.1-1 TRMM Data Products Available from the EOC (as a “full scene”).

Sensor	PR	TMI	VIRS	COMB
Level	1B21, 1C21 <sup>*1</sup> , 2A21, 2A23, 2A25 <sup>*1</sup> , 3A25, 3A26	1B11, 2A12, 3A11	1B01	2B31, 3B31, 3B42, 3B43

<sup>\*1</sup>: Fixed subscene distribution is also available.

### 5.1.1.2 AMSR-E Mission Operation

#### 1) AMSR-E overview

The Advanced Microwave Scanning Radiometer for EOS (AMSR-E) aboard NASA’s EOS-Aqua satellite has been making observations since its launch in May 2002. AMSR-E flies on an afternoon ascending orbit at approximately 1330.

The AMSR-E is a twelve-channel passive microwave radiometer operating at 6.925, 10.65, 18.7, 23.8, 36.5, and 89.0 GHz with vertical and horizontal polarization.

#### 2) Aqua/AMSR-E data flow

The AMSR-E data recorded on the Solid State Recorder (SSR) are received at the NASA ground station in Alaska or Svalbard once per orbit in accordance with the operation flow. The received data are transferred to NASA’s GSFC and processed into rate-buffered data (RBD). The GSFC transfers the AMSR-E Science RBD and ground-based attitude determination (GBAD) RBD to the EOC via the Internet. The National Snow and Ice Data Center (NSIDC) also provides the EOC with a production data set (PDS) as a backup of RBD via compact disc (CD) for orders of more than ten files, and via FTP for orders of ten or fewer files. The AMSR-E data processing system at the EOC generates near real-time products and standard products.

#### 3) AMSR-E science data management

##### a. Product specifications

The AMSR-E products are in Hierarchical Data Format (HDF). Each AMSR-E Level 1A product contains a “scene” of data acquired during half of a satellite orbit. A scene contains data between the northernmost and southernmost observed points at the center of a scan.

##### b. Product release

The EOC distributes all updated versions of AMSR-E Level 1 and higher-level products to the public. The current version is Version 2 for Level 1 products and Version 6 for the higher levels.

#### 4) Operation summary

AMSR-E is currently in the routine operation phase. AMSR-E data processing, product distribution, and system maintenance are being carried out normally. The number of scenes of Level 1 processed data for distribution was 71,560 at the end of March 2009.

Table 5.1.1.2-1 AMSR-E Science Products.

Level	Science Products
1A	Engineering values corresponding to the digital number (DN) converted from the instrument output voltage. Other necessary information for higher-level processing, such as satellite attitudes and instrument conditions are included. Data are not map-projected, but stored in the swath format.
1B	Fundamental physical values corresponding to brightness temperature. Data location and quality information are included. Data are not map-projected, but stored in the swath format.
2	Geophysical parameters calculated using retrieval algorithms. Sea surface temperature, sea surface wind speed, water vapor, precipitation, sea ice concentration, snow water equivalent, cloud liquid water, and soil moisture Data location and quality information are included. Data are not map-projected, but stored in the swath format.
3	Temporally and spatially averaged values at global grid points for brightness temperature and geophysical parameters. Daily and monthly averaged global mapping are available.

### 5.1.1.3 ADEOS-II Mission Operation

#### 1) ADEOS-II overview

The major purposes of the ADEOS-II mission were to advance Earth observation technologies and to provide global observation data as a follow-on to the ADEOS mission. ADEOS-II carried five Earth observing instruments (see Table 5.1.1.3-1). ADEOS-II also carried the Data Collection System (DCS), which is compatible with the ARGOS system being operated with NOAA meteorological satellites.

Table 5.1.1.3-1 Instruments aboard ADEOS-II and Their Providers

Instrument/System name	Acronym	Provider
Global Imager	GLI	JAXA
Advanced Microwave Scanning Radiometer	AMSR	JAXA
Improved Limb Atmospheric Spectrometer-II	ILAS-II	NIES
SeaWinds	SeaWinds	NASA JPL
Polarization and Directionality of the Earth's Reflectances	POLDER	CNES
Data Collection System	DCS	JAXA/CNES

NIES: National Institute of Environmental Studies (Japan) [<http://www.nies.go.jp/>]

JPL: NASA Jet Propulsion Laboratory [<http://www.jpl.nasa.gov/>]

CNES: Centre National d'Etudes Spatiales (France) [<http://www.cnes.fr/>]

Operation of ADEOS-II was cut short at 9 months (January-October 2002) because the satellite power system failed. The data obtained by two JAXA instruments, GLI and AMSR, were processed and archived at the EOC.

## 2) ADEOS-II science data management

ADEOS-II science data were managed separately by sensor providers, with independent data management, i.e., data processing, archiving, and distribution service for users. The interface with data users was based on global Internet connections providing the functions of catalog information search, data ordering, and online and/or offline data delivery, together with the associated observation information.

### a. GLI science product

GLI is an optical imager that observes reflected solar radiation from the Earth's surface, including the land, oceans, and clouds, and/or infrared radiation with a multi-channel system for measuring biological parameters, such as chlorophyll, organic substances, and the vegetation index, as well as temperature, snow and ice, and cloud properties. More than 100,000 scenes with 1-km and 250-m resolution (scene size: 1,600 km [W] x 1,600 km [L]) were acquired and archived.

The Version 2 algorithm for GLI data processing was released in November 2004, and all data have been reprocessed to yield Version 2 products.

### b. AMSR science product

AMSR is a radiometer with eight frequency bands from 6.9 GHz to 89 GHz. Six frequency bands have vertical and horizontal polarization capabilities. The 50.3 GHz and 52.8 GHz bands have only vertical polarization. AMSR acquires radiance data by scanning the Earth's surface conically or mechanically rotating its antenna along the satellite flight path. The aperture of AMSR's antenna is 2 m in diameter, and its instantaneous field of view is about 5 km (89GHz band). It scans the Earth's surface conically with a nominal incident angle of 55 deg to be constant, minimizes the effect of sea surface wind on observation data, and achieves a swath width of about 1600 km.

AMSR can retrieve various geophysical parameters of the Earth's surface and atmosphere, such as water vapor content, precipitation, sea surface temperature, sea surface wind, and sea ice both day and night regardless of cloud cover. An updated version of the higher-level (Version 6) products was released on March 25, 2008. GLI and AMSR science products are summarized in Table 5.1.1.3-2.

Table 5.1.1.3-2 GLI/AMSR Science Products

Sensor	Level	Science Products
AMSR	Level 1B	Brightness temperature
	Level 2	Sea surface temperature, sea surface wind, water vapor, precipitation, ice concentration, snow water equivalent, cloud liquid water, and soil moisture
	Level 3	Brightness temperature, sea surface temperature, sea surface wind, water vapor, precipitation, ice concentration, snow water equivalent, cloud liquid water, and soil moisture
GLI-1 km	Level 1B	Radiance
	Level 2/2A Level 3 binned Level 3 STA map	Atmosphere: Cloud flags, aerosol parameters (angstrom exponent, optical thickness), cloud parameters (optical thickness, effective radius, top height, top temperature, liquid/ice water path, fraction of 10 cloud types), precipitable water Ocean: Water-leaving radiance, chlorophyll-a, absorption of colored dissolved organic matter, attenuation coefficient at 490 nm, suspended solid weight, bulk sea surface temperature Land: Atmospheric corrected radiance, precise geometric corrected map projection parameter, vegetation index Cryosphere: Snow grain size, snow impurities, snow/cloud flag, Snow surface temperature, snow grain size 1.64 $\mu\text{m}$
GLI-250 m	Level 1B	Radiance

Table 5.1.1.3-3 ADEOS-II Observed Data Amounts

Sensor	Data Amount	Remarks
AMSR	6,648 scenes	Scene size: 1,600 km (W) x 20,000 km (L)
GLI 1 km	93,338 scenes	Scene size: 1,600 km (W) x 1,600 km (L)
GLI 250 m	10,601 scenes	Scene size: 1,600 km (W) x 1,600 km (L)
ILAS-II	3,450 downlink segments	1 downlink segment is roughly equal to 1 path
SeaWinds	3,728 downlink segments	1 downlink segment is roughly equal to 1 path
POLDER	3,287 downlink segments	1 downlink segment is roughly equal to 1 path

#### 5.1.1.4 ALOS Mission Operation

##### 1) ALOS overview

The Advanced Land-Observing Satellite (ALOS) was successfully launched on January 24, 2006 by an H-IIA launch vehicle from Tanegashima Space Center and was renamed "Daichi," which means "Terra" in Japanese.

##### a. Mission objective

The major objectives of the ALOS mission are to serve as a follow-on to the JERS-1 and ADEOS missions and to enhance land-observing technology further. ALOS data are being used for

cartography, regional observation, disaster monitoring, and resource surveying. ALOS carries three instruments developed by JAXA: PRISM, AVNIR-2, and PALSAR. PRISM has three optical systems for forward, nadir, and backward viewing with 2.5-m spatial resolution to obtain terrain images and develop elevation maps. AVNIR-2 has better spatial resolution than ADEOS/AVNIR to provide land cover and land use classification maps for monitoring the regional environment. PALSAR is an active microwave instrument for cloud-independent, all day land observation and provides higher performance than JERS-1 SAR.

Table 5.1.1.4-1 ALOS Instruments and Their Providers

Instrument	Acronym
Panchromatic Remote-sensing Instrument for Stereo Mapping	PRISM
Advanced Visible and Near Infrared Radiometer type 2	AVNIR-2
Phased Array type L-band Synthetic Aperture Radar*	PALSAR

\* Joint development with the Ministry of Economy, Trade and Industry.

## 2) Mission operations

### a. ALOS data acquisition baseline

The primary links to transmit ALOS data are the Ka-band receiving station (via DRTS-W) and the EOC X-band station, both at Hatoyama. The Ka-band receiving station at TKSC (via DRTS-W) serves as a backup. Apart from these operations, X-band foreign stations operated by “ALOS Data Nodes” (see item “d.”) receive ALOS data.

### b. ALOS instrument operation guidelines

The following basic operations for the mission instruments are planned:

- Land and daytime: Observation by one to three sensors of PRISM, AVNIR-2, and PALSAR
- Land and nighttime: Observation by PALSAR, calibration of PRISM and AVNIR-2 (as needed)
- Ocean, etc.: Reproduction of High-rate mission data Solid State Recorder (HSSR)

Nominal operations will be conducted according to the basic observation scenario.

### c. ALOS data products

The ALOS mission data are shown in Table 5.1.1.4-2.

Table 5.1.1.4-2 ALOS Mission Data (Level 0, 1 data)

Processing Level	Definition	
Level 0 (only for ERSDAC, GSI, EORC, Data Nodes)	AVNIR-2 Level 0 data for distribution (including TT&C, AOCS, PCD telemetry)	
	PRISM Level 0 data for distribution (including TT&C, AOCS, PRISM mission telemetry)	
	PALSAR Level 0 data for distribution (including TT&C, AOCS, PALSAR mission telemetry)	
Level 1 (Processed data)	AVNIR-2, PRISM	
	1A	Uncorrected image, scene unit
	1B1	Radiometrically calibrated image
	1B2	Geometrically corrected image
	PALSAR	
	1.0	Uncorrected image, scene unit
	1.1	Single look complex data on slant range
1.5	Multi-look processed image	

d. ALOS data node framework

A new data delivery framework is being discussed with the data nodes to promote worldwide distributed processing. As illustrated in Fig. 5.1.1.4-1, each node is responsible for distributing the data to the users within its assigned area. JAXA will provide Level 0 data to the nodes.

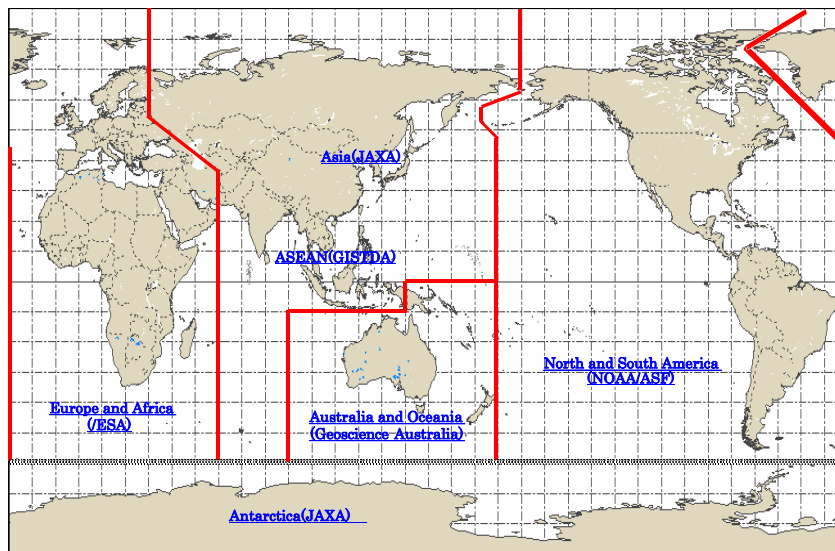
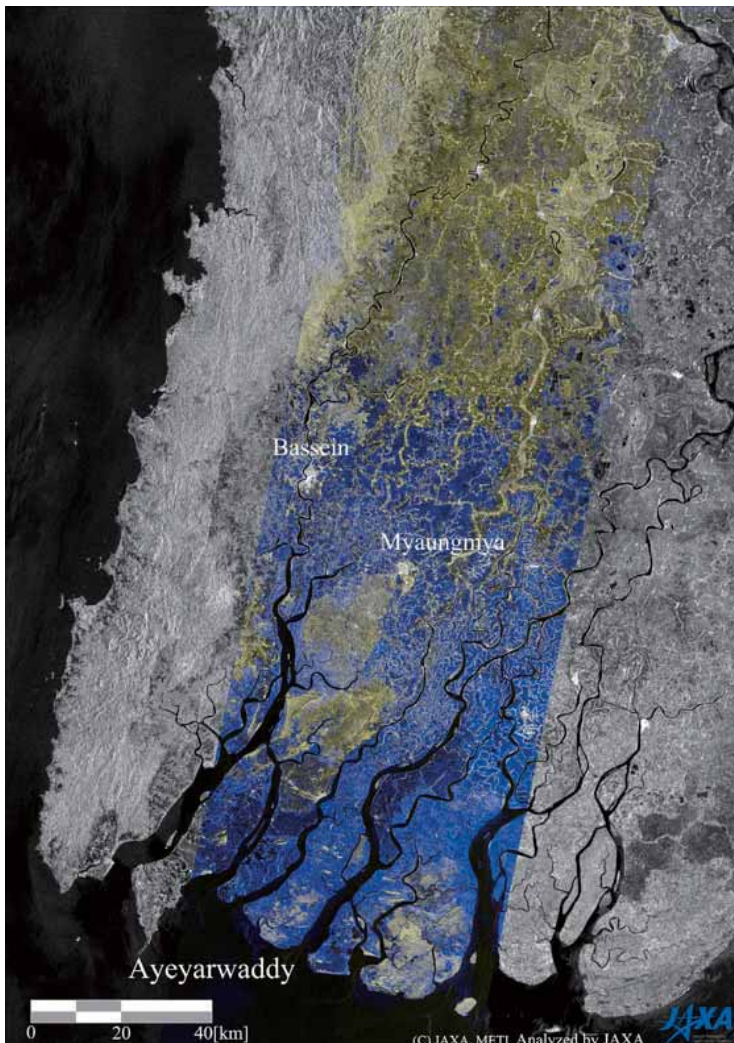


Fig. 5.1.1.4-1 Areas of Responsibility for Data Nodes.

3) Emergency observation

Emergency observation for disaster monitoring is an important role of ALOS. Since its launch, more than 120 emergency observations have been conducted, and the data were provided to the relevant domestic and international agencies, including the International Charter “Space and Major Disasters.”

Example: Myanmar flood water observation by PALSAR



Myanmar was heavily flooded from May 2 to May 3, 2008, due to Cyclone Nargis. JAXA decided to activate ALOS/PALSAR to observe the area quickly, and succeeded in imaging the area on May 6, 2008. The data were provided to the "Disaster Charter" and "Sentinel Asia".

A color composite of these images (Fig. 5.1.1.4-2) shows the land surface change in color, RED and GREEN for after the flood of May 6 and BLUE for before April 24. The BLUE in the figure shows the flooding in dominance and it spread out widely in the image.

Fig. 5.1.1.4-2 A color composite of the pre- and post-disaster images, RED and GREEN for after the flood of May 6 and BLUE for before April 24.

#### 4) Future plan

JAXA and NASA started a new cooperation in 2008 to implement data transmission via NASA's TDRS F-10 satellite. System development is now ongoing and the initial operation will start in JFY 2009.

5.1.1.5 User Service

5.1.1.5.1 ALOS

ALOS data service categories and their contents are listed in the table below.

Table 5.1.1.5.1-1 ALOS Data Service Categories and Contents

Type	Definition	User
Urgent	Mainly for disaster monitoring - First priority (from observation to delivery) - Request file accepted up to 72 hours before the observation - Urgent request less than 4.5 hours before the observation (operator call) - Level 1 data ready for distribution within 3 hours after data reception - Image catalog updated within 1 hour (3 hours for PALSAR) - Data provided either by CD-ROM or online	Japanese Government User (Cabinet office, MEXT office, ERSDAC, GSI, ADRC) International Charter, JAXA internal user, Data distributor
Near Real-Time	Sea ice monitoring - Request must be submitted as a standing request. - Near real-time Level 1 via online data delivery within 3 hours of the observation	Japanese Government User (JCG)
Normal	- Request submitted at least 1 week before the observation - Three request methods: Standing request, On-demand file request, and On-demand WWW request	Japanese Government User, JAXA internal user, General user, Data distributor

Level 0 data will be delivered on media (SONY DTF-2) to dedicated users. Level 1 data will be delivered on media (DVD) and online to all users. The Level 1 data format is CEOS superstructure and CEOS SAR. Catalog data and data sets will be delivered online to all users. However, users will be categorized according to the ALOS data policy. Higher-level products will be generated by the Data Utilization System at the EORC and other data utilization organizations. Figure 5.1.1.5.1-1 depicts the ALOS User Interface Gateway (AUIG), the web-user interface. Anyone can search ALOS data through the AUIG, but only ALOS PIs can order the data.



Fig. 5.1.1.5.1-1 AUIG

#### 5.1.1.5.2 Direct Data Receiving from EOS

The EORC began receiving data from EOS satellites (Terra and Aqua operated by NASA) directly in July 2004, and can now provide substitute data for the lost ADEOS-II mission data (GLI and AMSR).

By using the receiving antenna installed at the EOC, the EORC acquires and processes data from MODIS instruments aboard Terra and Aqua and data from AMSR-E aboard Aqua at the EOC and EORC. The processed data are provided on a near real-time basis (within 3 to 5 hours of observation) to institutional users, such as the Japan Meteorological Agency (JMA), the Japan Fisheries Information Service Center (JAFIC), and the Japan Coast Guard (JCG), who use the data for operational applications of weather forecasts and fishery and Tokyo Bay monitoring. General users can also use these data through the Internet by contracting with the data distributor. MODIS data service has been available since September 2004, and AMSR-E data service since April 2005.

#### 5.1.1.5.3 Other Satellites

##### 1) Catalog information service

Data from MOS-1, JERS-1, ADEOS, ADEOS-II, Aqua/AMSR-E, TRMM, ERS, LANDSAT, SPOT, RADARSAT, and IRS are archived and have reached about 230 TB in 30 years. The data can be identified, previewed, and ordered as products. Catalog information is accessible via the Internet by using the Information Service System (ISS). Public users can use the ISS WWW gateway at <https://www.eoc.jaxa.jp/iss/jsp/indexEn.html>. User accounts will be provided from the EORC order desk.

##### 2) Offline data distribution service

Earth observation data are available on digital recording media, by ordering products chosen scene-by-scene using the EOIS WWW service interface or order sheets. CD-ROMs (650 MB) and DVD-Rs (4.5 GB) are available.

##### 3) Online data distribution service

The EOC provides standard products of higher-level processed data via the Internet. All users can download small products of a higher order from the EOC data server via WWW. In January 2006, the EOC started online data distribution free of charge to Japanese general researchers who have service equivalent to PIs after online registration. In April 2007, the same distribution service became available to foreign general researchers.

The EOC provides download service for AMSR-E, ADEOS-II, and TRMM data. User registration is necessary to access the server, but accounts are issued immediately via online sign up.

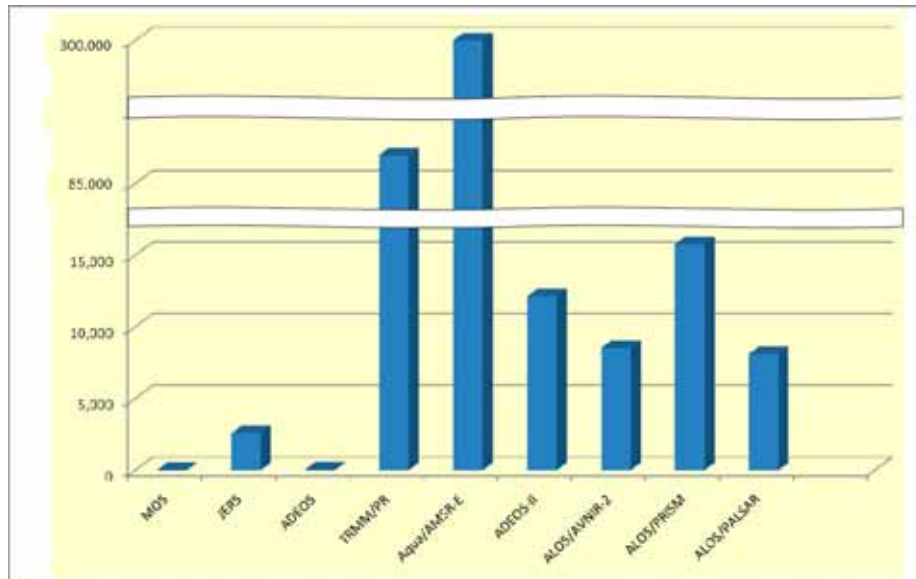


Fig. 5.1.1.5-1 Number of Downloads of Online Data Distribution Service in FY 2008

### 5.1.2 System Overview

#### 5.1.2.1 ALOS Mission Operation System

The ALOS Mission Operation System is the ground system installed at the EOC for managing ALOS mission operations and for receiving, recording, archiving, processing, and distributing ALOS data to various users. The ground segment related to the ALOS mission operations is shown in Fig. 5.1.2.1-1. The ALOS Data Acquisition and Processing System and the ALOS Information System are the two main components of the ALOS Mission Operation System.

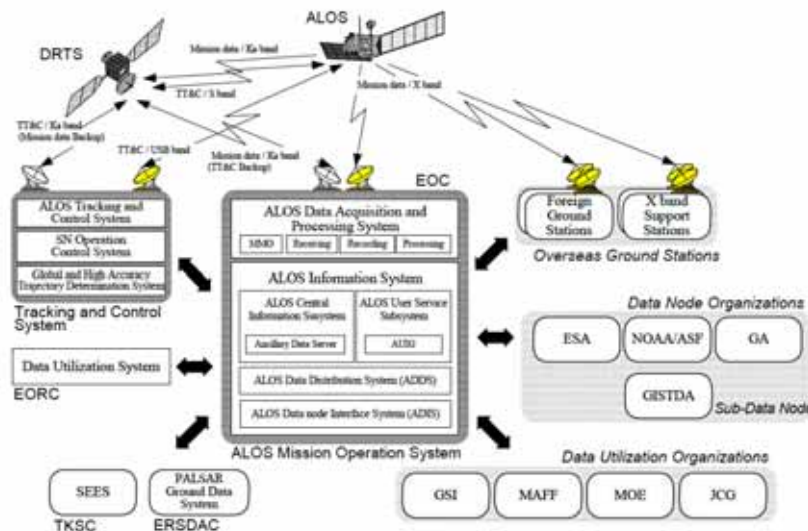


Fig. 5.1.2.1-1 ALOS Mission Operation and Related System Overview

5.1.2.2 Other System

Figure 5.1.2.1-2 presents a flow chart of the EOC system (excluding ALOS).

The data from Earth observation satellites or transmitted via networks are archived and processed for a variety of applications and research. The data are delivered primarily in the form of CD-ROM, DVD-ROM, and online. The Earth Observation Information System (EOIS) and Data Distribution and Management System (DDMS) archive a master data set, generate media for delivery, and control the network and service users.

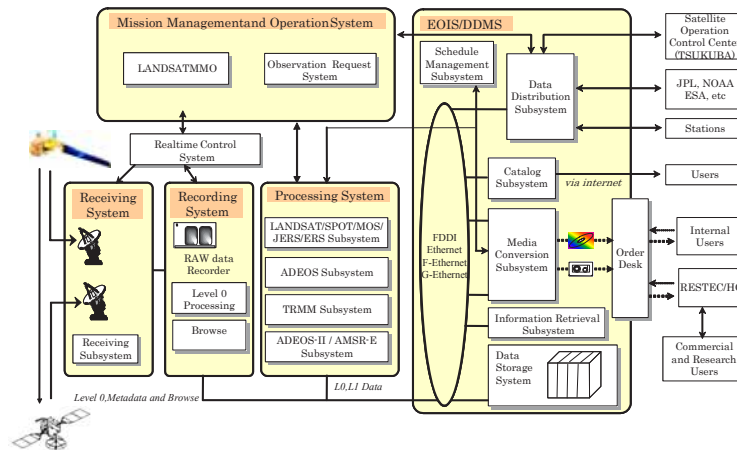


Fig. 5.1.2.2-1 Flow Chart of the EOC System.

## 5.2 Data Analysis System

The Data Analysis System (DAS) is a computer and network infrastructure that supports research and promotion activities at the EORC.

### 5.2.1 History and Current Operations

DAS was developed for ADEOS data analysis as a part of the EOC's Earth Observation Information System (EOIS) in 1995, at the time of the EORC establishment, and supported the EORC's WWW and FTP servers. Due to relocation of the EORC office from Roppongi to Harumi, DAS was switched over in July 2001 to a new computer system, and further office relocation from Harumi to Tsukuba in October 2006 resulted in another new computer system.

Power conditions of DAS worsened. DAS at Tsukuba was not supported by emergency power. In August 2008, a thunderstorm caused commercial power loss to DAS; however, shutting down all systems sequentially prevented any damage.

#### 1) Mission data flow

The EORC has been using DAS to provide data handling and distribution, user support, and homepage operation. After GOSAT launch in January 2009, the EIS (EOC Information System) within DAS has delivered data from/to the National Institute for Environmental Studies (NIES) and from Kongsberg Satellite Services (KSAT) in Norway. Additional distribution plans to ESA/Tromso and NASA/JPL are being developed and new FTP servers for other researchers are also being developed for GOSAT.

The 200-Mbps communication line between the EOC and the EORC has been used for daily data transfer of TRMM, AMSR-E, and ADEOS-II/AMSR standard products; AMSR-E and MODIS near real-time data; ALOS Level 0 data and ALOS Mission Operation Interface Files (MOIF); and others.

These data transfers were implemented using the Network Control System (NCS). The On-demand Data Server (ODS) is mainly used for researchers within the EORC to retrieve and acquire necessary data archived at the EOC online or to order data processing.

The Internet (Asia Pacific Advanced Network (APAN) with TsukubaWAN and/or the Science Network (SINET)) is being used for data transfer. Both SINET and APAN have a 1-Gbps bandwidth.

#### 2) Data management

The EORC has been acquiring the following data online (through NCS and ODS) or by DVD media and storing them in the LTO mass storage data archive. GOSAT Level 0 data as master data has also been stored since GOSAT launch.

- MODIS data received and processed at TSIC-TRIC and JAXA's EOC (since July 2004)
- ADEOS-II/GLI standard products processed at JAXA's EOC
- ADEOS-II/AMSR standard products processed at JAXA's EOC
- TRMM standard products processed at JAXA's EOC
- TRMM standard products processed at NASA's GSFC (via JAXA's EOC)
- AMSR-E standard products processed at JAXA's EOC
- AMSR-E near real-time data processed at JAXA's EOC

- ADEOS-II orbit data
- TRMM orbit data produced at NASA (via JAXA's EOC)
- Meteorological data acquired from the JMA (via JAXA's EOC)
- Meteorological Information Comprehensive Online Service (MICOS) data from the JWA
- GOSAT Level 0 data product at Tsukuba (since February 2008)

The EORC bought the SSM/I data aboard DMSP satellites and ECMWF data. All these data are used for EORC research activities, such as calibration and validation, and algorithm improvement.

### 3) The EORC Homepage and FTP server

JAXA Earth Observation Satellite sample images archived at the EORC are open to the public worldwide through the EORC homepage and on media such as CD-ROM and DVD-ROM free of charge for the purpose of research and public benefit. The EORC has continued to offer the FTP services of MODIS data to organizations with a cooperative agreement or those holding a contract with RESTEC since July 2004. Organizations directly connected to JAXA include the Japan Coast Guard and the Japan Meteorological Agency, and those connected through RESTEC were Chiba University, VisionTech Inc., Prefectural Fisheries Experimental Stations, and Tohoku University.

The EORC regularly updates "Seen from Space," which is mainly composed of ALOS (AVNIR-2, PRISM and PALSAR) and Aqua/AMSR-E images with brief explanations on the EORC top homepage every two weeks, for a total of 35 times during FY 2008. We also update the following major areas included in the EORC homepage:

- Global Rainfall Map (since November 2007)
- ALOS Latest Image (since February 2006)
- TRMM Typhoon Database page by the TRMM research project (since October 2002)
- EORC Kids page (since February 2003)
- TRMM Typhoon Quick Report page by the TRMM research project (since September 2003)
- AMSR-E Typhoon Quick Report page by the ADEOS-II research project (since May 2004)
- "Kuroshio Monitoring" page by the ADEOS-II research project (since June 2004)
- "El Nino Watch" page by the ADEOS-II research project (since December 2004)
- AMSR/AMSR-E Tropical Cyclone Database page by the ADEOS-II research project (since December 2004)
- "Sea Ice Concentration in the Sea of Okhotsk" by AMSR-E and MODIS in the ADEOS-II research project (since February 2003; added MODIS data in December 2003 and updated during the winter season)
- Today's Image from AMSR-E and MODIS provided by the ADEOS-II research project (since November 2003; originally started by AMSR and GLI in April 2003)

The EORC changed the portal system from the EORC's own portal system to JAXA's new portal system to reduce costs in December 2008.

### 5.2.2 System Overview

DAS is composed of the internal Data Analysis System (iDAS) and three networks: the Internet-Connected Segment, the External-Interface Segment, and the EORC Internal LAN. The Internet-Connected Segment of DAS is connected to the Internet through JAXAnet. The External-Interface Segment of DAS has been connected to the EOC with the Data Distribution and Management System (DDMS) at 200 Mbps through JAXAnet since the end of September 2007, and is connected to Kongsberg Satellite Services (KSAT) in Norway and the National Institute for Environmental Studies (NIES).

The following table and figure outline the present DAS:

Table 5.2.2-1 Data Analysis System Outline

Operation	Since the end of October 2006
Security Measures	Firewall, virus pattern compulsive distribution system, Secure Socket Layer/Virtual Private Network (SSL-VPN)
Internet-Connected Segment	De-Militarized Zone (DMZ)
External-Interface Segment	External-Interface Segment with EOC, NIES, and KSAT
Composition of EORC Internal LAN	<ul style="list-style-type: none"> <li>▪ Eight subnetwork segments</li> <li>▪ Four subnetworks by project</li> <li>▪ GOSAT ground system subsegment</li> <li>▪ EORC Information System (EIS) subsegment</li> <li>▪ Common subsegment</li> <li>▪ System operation sub-segment</li> </ul>
Computers (WS & PC)	About 400 machines, including all computers in the server and operation room
Mass-storage Tape Archive	600 TB with 100 TB disk cache
Large-capacity Shared Disk Equipment	37 TB
Network	10 Gbit Ether, 1 Gigabit Ether, 100 Mbps Fast Ether
Power-supply Capability	450 KVA (C-4:300 KVA, E-2:150 KVA)
Floor Space of Server Room and Power Supply Room	915 m <sup>2</sup> in Tsukuba Space Center Bldg. C-4

The Internet-Connected Segment and External-Interface Segment are in the De-Militarized Zone (DMZ: including public WWW and FTP servers).

The External-Interface Segment includes the Network-Control System (NCS), the On-demand Data Server (ODS) for data transfer from the EOC to the EORC, and the EORC Information System (EIS) for data transfer.

The EORC Internal LAN consists of eight subsegments corresponding to the four research projects (i.e., TRMM, GCOM, JERS-1/ALOS, and GOSAT), the GOSAT ground-system subsegment, the EORC Information-System subsegment, the common subsegment, and the system-operation subsegment.

The common subsegment includes the main routers for DAS, the Mass Storage Tape Archive, large-capacity shared-disk equipment, common printers, and photograph quality printers. The Mass Storage Tape Archive consists of an LTO tape library (600 TB) with a disk cache (100 TB).

The system-operation subsegment includes computers to manage all DAS machines and the entire network, and to monitor machines for the common segment, media conversion system, etc.

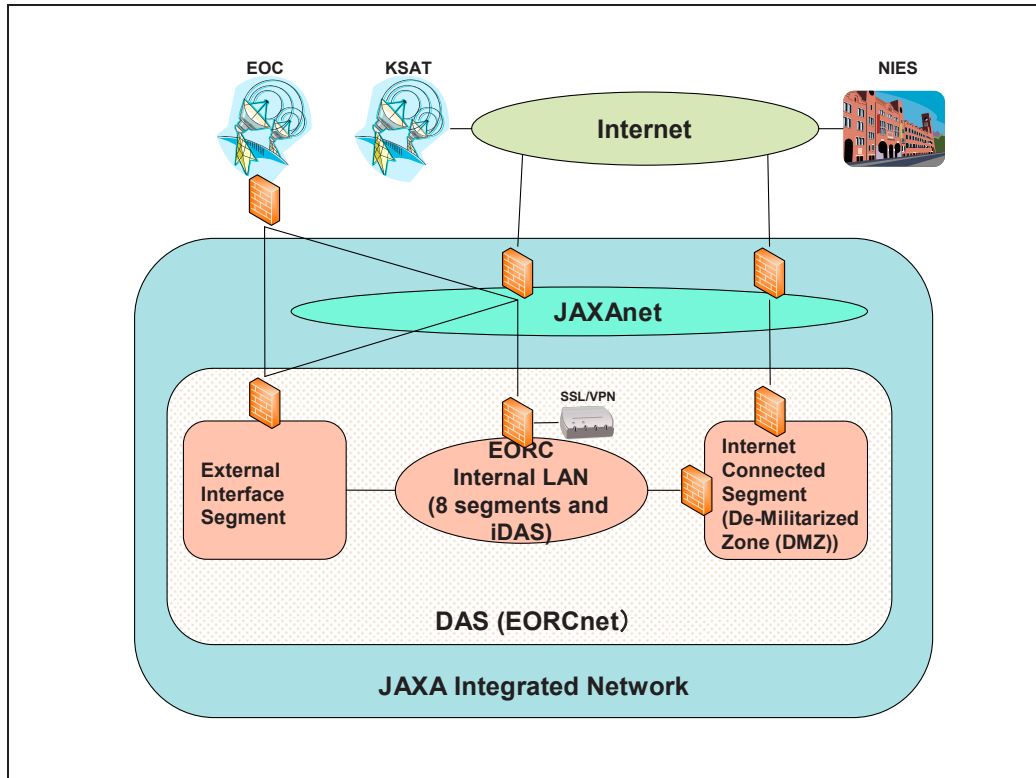


Fig. 5.2.2-1 Flow Chart of DAS

## ***6. DATA OF EORC ACTIVITIES***

## 6. DATA OF EORC ACTIVITIES

### 6.1 Publicity

#### Access statistics of the EORC homepage and its operation

Access to the EORC homepage was approximately 1,900,000 pages per month in September 2005 when a major typhoon struck Japan. Figure 6.1-1 indicates the trend of access to the EORC homepage from April 2003 to March 2008.

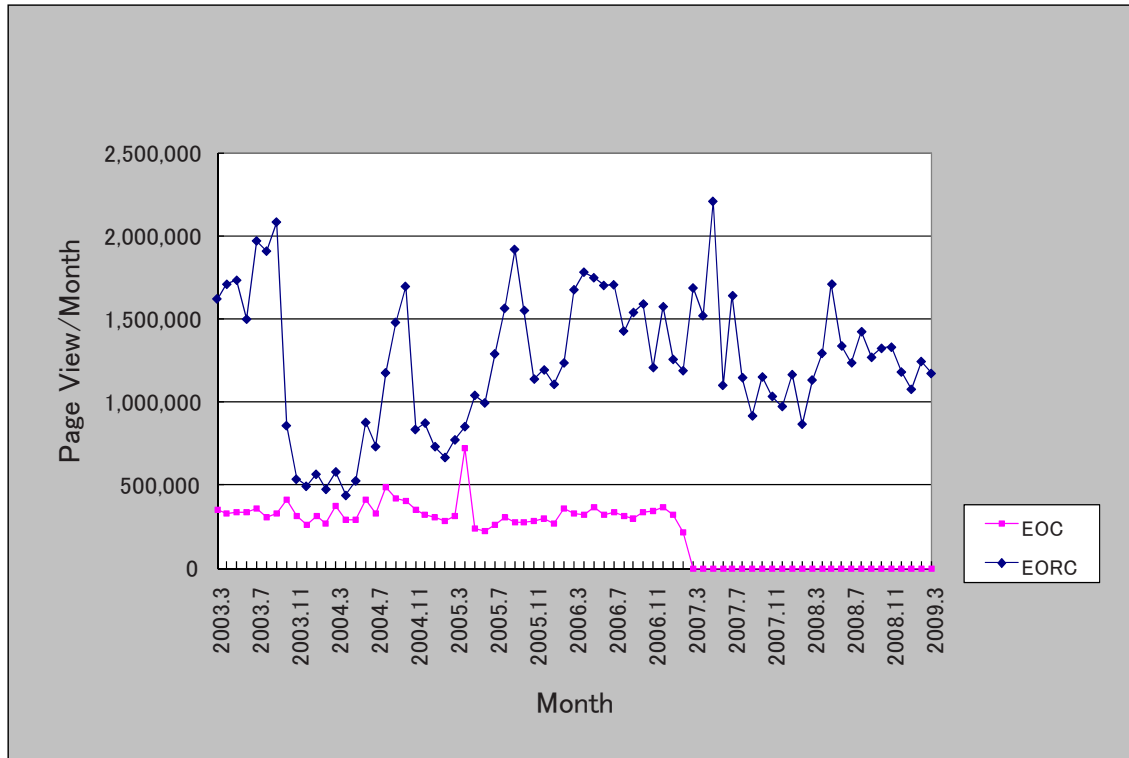


Fig. 6-1 Trend of Access to EORC and EOC Homepages

During FY 2007, we continuously updated “Seen from Space,” which is mainly composed of ALOS/(AVNIR-2, PRISM and PALSAR) and Aqua/AMSR-E images with brief explanations on the EORC top homepage once a week or more for a total of 54 times during FY 2007. We also updated the following major areas included on the EORC homepage:

- Global Rainfall Map (since November 2007)
- ALOS Latest Image (since February 2006)
- TRMM typhoon database page by the TRMM research project (since October 2002)
- EORC kids page (since February 2003)
- TRMM typhoon quick report page by the TRMM research project (since September 2003)
- AMSR-E typhoon quick report page by the ADEOS-II research project (since May 2004)
- “Kuroshio Monitoring” page by the ADEOS-II research project (since June 2004)
- “El Nino Watch” page by the ADEOS-II research project (since December 2004)

- AMSR/AMSR-E tropical cyclone database page by the ADEOS-II research project (since December 2004)
- “Sea Ice Concentration in the Sea of Okhotsk” by AMSR-E and MODIS in the ADEOS-II research project (since February 2003; MODIS data was added in December 2003 and updated during the winter season)
- Today's Image from AMSR-E and MODIS provided by the ADEOS-II research project (since November 2003; originally started by AMSR and GLI in April 2003)

## 6.2 Data Delivery Statistics

Table 6-1 Statistical Summary of EORC Data Deliveries

	Satellite	FY 2004	FY 2005	FY 2006	FY 2007	FY 2008	
		Total	Total	Total	Total	Distributed by JAXA	Distributed by Private Distributors
Distribution Results per Satellite	MOS	42	39	179	15	15	8
	JERS-1	8,575	4,504	5,284	2,889	1,594	980
	ADEOS	193	6	43	8	7	49
	TRMM (1)	182,445	139,235	107,800	39,770	87,379	0
	Aqua (2)	252,678	211,536	289,806	461,386	672,925	1,288
	ADEOS-II	98,540	37,108	107,660	7,396	12,135	0
	ADEOS-II (Substitute)	17,742	36,054	39,294	84,590	1,514	49,825
	ALOS	-	-	10,287	27,443	9,698	31,077
	ALOS L0 (3)	-	-	58,005	189,679	193,670	-
Total		560,215	428,482	618,358	813,176	978,937	83,227
						1,062,164	

1. PR only
2. AMSR-E only
3. ALOS/PALSAR Level 0 data delivery to the Geographical Survey Institute of Japan

N.B.

- Only satellites or sensors developed by JAXA are included in this table, except ADEOS-II substitutes, i.e., data received directly from EOS. Data users outside of JAXA are considered here; JAXA's internal users are not included. Data are counted by scene, and the number comes from the sum of scene orders and standing orders.
- ALOS data delivery started in Oct. 2006.

### 6.3 International Collaboration

#### 6.3.1 International Meetings

International meetings organized by EORC in FY 2005 are listed in Section 8.

#### 6.3.2 International Collaboration Research

The EORC accommodates foreign researchers as PIs for TRMM, ADEOS-II, and ALOS science projects through Research Announcements (RA). Some of these researchers develop, calibrate, and validate algorithms for higher level products and engage in scientific research.

#### 6.3.3 Foreign Guest Researchers

The EORC was established as a field center that unites experts of Earth science and remote-sensing applications. Since its establishment, it has conducted cooperative research in fields relating to satellite Earth observation data and Earth science, together with application fields with close collaboration among Earth science specialists inside and outside of Japan. The EORC receives foreign guest researchers not only to promote cooperative activities but also for individual research by various systems and purposes.

Number of Foreign Guest Researchers in EORC

	No. of Persons
JAXA Invited Researchers	3
Post-doctorates	0

Numbers at the beginning of FY 2008

#### 6.3.4 International Arctic Research Center (IARC)

IARC was established to promote international cooperation and coordination for arctic climate change research at the University of Alaska Fairbanks. JAXA (formerly NASDA) commissioned Hokkaido University and the University of Alaska to conduct Arctic research on global change using the IARC-JAXA Information System (IJIS) and satellite data. The joint science team includes U.S. and Japanese researchers from various science fields. The team is divided into two categories: Terrestrial and Ocean. JFY 2008 is the first year of the third research plan (JFY 2008-2010).

##### 6.3.4.1 Terrestrial research

JAXA and IARC conduct terrestrial research for two purposes: one is to understand the relationship between the lifecycle of forests and wild fire and the other is to contribute to improvement of climate models. To evaluate the comprehensive impact of wild fire, we need to look into five phases as shown in the figure below. These five phases include damaged forest prior to fire, pre-fire climate condition, under combustion, posterior fire recovery phases, and undisturbed forest.

We set up five themes corresponding to phases we defined above to achieve comprehensive research on the relationship between wild fire and the life cycle of arctic vegetation.

P1	Risk assessment of wildfire before ignition
P2	Estimation of pre-fire condition
P3	Impact estimation of wildfire in combustion process
P4	Impact assessment in vegetation recovery process
P5	Estimation of GH gas budget in healthy forest and tundra

#### 6.3.4.2 Ocean Research

We would like to propose an integrative approach (Ship Survey - Satellite Remote Sensing - Ice-ocean-ecosystem Modeling) to elucidate the linkage of ice/ocean/ecosystem in the Arctic Ocean and subarctic seas, especially ice melting/formation dynamics and its impact on primary production. Our main target area is the Bering/Chukchi Seas where we can conduct ship surveys and where rapid changes are ongoing. We are also targeting other subarctic seas such as Okhotsk Sea and Barents Sea for comparative studies to clarify key processes controlling phytoplankton dynamics.

We focus on the following issues and elucidate the role of sea ice cover change on the marine ecosystem using multi-sensor remote sensing:

- The mechanisms whereby seasonal **sea ice cover** affects the amount, timing, and fate of primary production and other biota in the ice and the adjacent waters
- How the **thickness**, timing of retreat, and temporal and spatial extent of the **sea ice cover** influences ecosystem processes at a variety of latitudes from the low latitudes found in the Bering Sea to the high latitudes characteristic of the Chukchi Sea
- Land-Ocean interaction through Yukon/Mackenzie river plume dynamics

To clarify those scientific questions, this project consists of five sub-groups as follows:

SG1	Development of ice thickness algorithm for the Arctic Ocean
SG2-1	Evaluation/Development/Improvement of ocean color algorithms
SG2-2	Investigation of the linkage between ice-ocean dynamics and phytoplankton dynamics
SG2-3	Investigation of ocean circulation and sea ice dynamics in the Arctic Ocean
SG2-4	Investigation of the freshwater, sediment, and nutrient fluxes from the Yukon/Mackenzie river basins and their dispersal in the ocean

#### 6.3.5 Space Applications For Environment (SAFE)

SAFE (Space Applications For Environment) is a voluntary-based initiative in Asia Pacific, born from the Asia Pacific Regional Space Agency Forum (APRSAF). It aims to encourage

environmental monitoring on a long-term scale to grasp environmental change and to mitigate global warming hazards using space applications, especially remote sensing technology. It also aims to detect changing environmental parameters early, such as water resources, river water level, land cover, deforestation, agricultural production, ecosystem, and so on. These environmental changes could be identified through government public services as a part of SAFE prototyping. Figure 6-2 shows the entire structure of SAFE activity

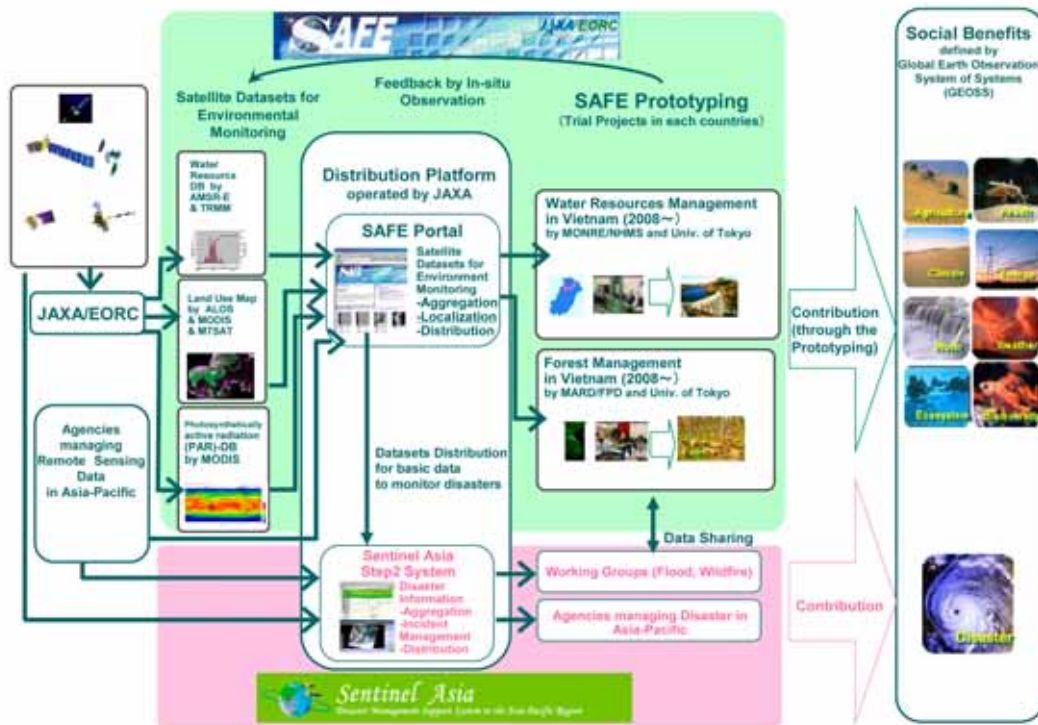


Fig. 6-2 Overview of SAFE

The participants of SAFE are categorized into three groups: “Prototyping Executor,” “Technical Supporter,” and “Data & Application Creator.” All SAFE activities are designed to be carried out through collaboration among these groups. Because SAFE is a voluntary-based initiative, each group should respect the other group’s regulations and motivation. SAFE will provide opportunities to encourage the collaboration among the three groups. Figure 6-3 shows the relationship among the three groups.

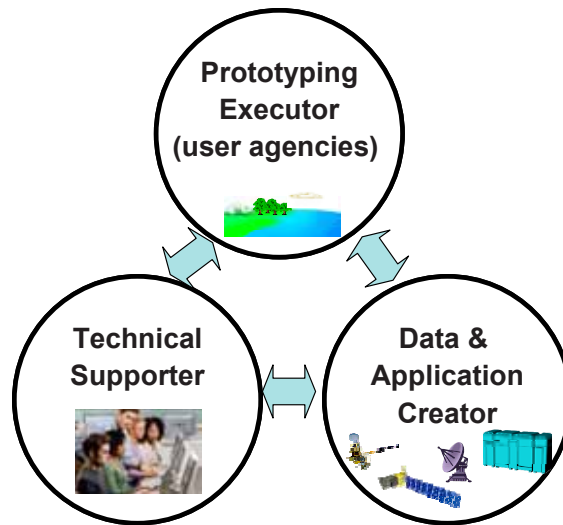


Fig. 6-3 The Relationship among SAFE Participants

JFY 2008 was the start-up year of SAFE. As a trial, JAXA started prototyping activities from June 2008 in cooperation with the University of Tokyo, the Asian Institute of Technology, the Vietnam Academy of Science and Technology (VAST), the Vietnam Ministry of Agriculture and Rural Department (MARD), and the Vietnam Ministry of Natural Resources and Environment (MONRE) on two issues: forest monitoring and water resources management.

Confirming the earlier achievements of these two prototyping activities, the annual APSARF Meeting held at Hanoi (APRSAF-15) officially endorsed SAFE as the official initiative related to APRSAF.

#### 6.4 Affiliated Graduate School

The EORC is affiliated with graduate schools of two universities in the field of Earth observation. A contract with Chiba University concerning cooperation between the EORC and their graduate schools was made on March 31, 1998, with Tokai University on February 18, 2004, and with Hokkaido University on April 1, 2008. As a part of this cooperation, the EORC provided lectures in Tokai University and Hokkaido University by dispatching personnel as affiliate professors in FY 2008.

## 6.5 List of Scientific Contributions (January-December 2008)

### 6.5.1 Journal Articles

- Nakagawa, H., Bzowski, M., Yamazaki, A., Fukunishi, H., Watanabe, S., Takahashi, Y., Taguchi, M., Yoshikawa, I., Shiomi, K., Nakamura, M., UV optical measurements of the Nozomi spacecraft interpreted with a two-component LIC-flow model, *Astronomy and Astrophysics*, Vol.491 No. 1, 29-41.
- Shimada, M., Ozawa, T., Fukushlma, Y., Furuya, M., Rosenqvist, A., Japanese l-band radar improves surface deformation monitoring, *Eos Transactions American Geophysical Union*, Vol.89 No. 31, 277-278.
- Maeda, T., Takano, T., Discrimination of local and faint changes from satellite-borne microwave-radiometer data, *IEEE Transactions on Geoscience and Remote Sensing*, Vol.46 No. 9, 2684-2691.
- Hirose, M., Oki, R., Shimizu, S., Kachi, M., Higashiawatoko, T., Finescale diurnal rainfall statistics refined from eight years of TRMM PR data, *Journal of Applied Meteorology and Climatology*, Vol.47 No. 2, 544-561.
- Oyama, K.-I., Kakinami, Y., Liu, J.-Y., Kamogawa, M., Kodama, T., Reduction of electron temperature in low-latitude ionosphere at 600 km before and after large earthquakes, *Journal of Geophysical Research A: Space Physics*, Vol.113 No. 11.
- Shimada, T., Isoguchi, O., Kawamura, H., Numerical simulations of wind wave growth under a coastal wind jet through the Kanmon Strait, *Weather and Forecasting*, Vol.23 No. 6, 1162-1175.

### 6.5.2 Conference Proceedings

- Takaku, J., Tadono, T., Shimada, M., High resolution DSM generation from ALOS prism - calibration updates, *International Geoscience and Remote Sensing Symposium (IGARSS)*, Vol.1 No. 1, I181-I184
- Shimada, M., Isoguchi, O., Rosenqvist, A., Palsar calval and generation of the continent scale mosaic products for kyoto and carbon projects, *International Geoscience and Remote Sensing Symposium (IGARSS)*, Vol.1 No. 1, I17-I20.
- Murakami, H., Tadono, T., Imai, H., Shimada, M., Improvement of AVNIR-2 radiometric calibration by toa directionalreflectance cross-calibration and on-board calibration data, *International Geoscience and Remote Sensing Symposium (IGARSS)*, Vol.1 No. 1, I189-I192.
- Isoguchi, O., Shimada, M., Polarization dependence of l-band measurements over the ocean on surface wind at 23-25 incidence angles, *International Geoscience and Remote Sensing Symposium (IGARSS)*, Vol.1 No. 1, I25-I28.
- Tadono, T., Shimada, M., Murakami, H., Takaku, J., Kawamoto, S., Updated results of calibration and validation of alos optical sensors, *International Geoscience and Remote Sensing Symposium (IGARSS)*, Vol.1 No. 1, I177-I180
- Longépé, N., Allain, S., Portier, E., Toward an operational method for refined snow characterization using dual-polarization C-band SAR data, *International Geoscience and Remote Sensing Symposium (IGARSS)*, Vol.2 No. 1, II57-II60.

- Shimada, M., Muraki, Y., Otsuka, Y., Discovery of anomalous stripes over the Amazon by the PALSAR onboard ALOS satellite, International Geoscience and Remote Sensing Symposium (IGARSS), Vol.2 No. 1, II387-II390.
- Shimizu, S., Iguchi, T., Oki, R., Hirose, M., Tagawa, T., Evaluation of the effect of the orbit boost of the TRMM satellite on the rain estimates, International Geoscience and Remote Sensing Symposium (IGARSS), Vol.4 No. 1, IV133-IV136.
- Tagawa, T., Shimizu, S., Oki, R., Derivation of sub-footprint scale  $\sigma^0$  observed by TRMM precipitation radar, International Geoscience and Remote Sensing Symposium (IGARSS), Vol.4 No. 1, IV137-IV140
- Shimada, M., PALSAR scansar interferometry, International Geoscience and Remote Sensing Symposium (IGARSS), Vol.4 No. 1, IV93-IV96
- Longépé, N., Shimada, M., Allain, S., Pottier, E., Capabilities of full-polarimetric PALSAR/ALOS for snow extent mapping, International Geoscience and Remote Sensing Symposium (IGARSS), Vol.4 No. 1, IV1026-IV1029
- Nakajima, H., Matsuura, D., Anabuki, N., Miyata, E., Tsunemi, H., Doty, J.P., Ikeda, H., Katayama, H., Development of X-ray CCD camera system with high readout rate using ASIC, Proceedings of SPIE - The International Society for Optical Engineering, Vol.7011
- Matsuura, D., Nakajima, H., Anabuki, N., Tsunemi, H., Doty, J.P., Ikeda, H., Katayama, H., Development of an ASIC for multi-readout X-ray CCDs, Proceedings of SPIE - The International Society for Optical Engineering, Vol.7021
- Shimoda, H., Overview of Japanese Earth Observation programs, Proceedings of SPIE - The International Society for Optical Engineering, Vol.7106
- Shimada, M., Isoguchi, O., Rosenqvist, A., Tadono, T., PALSAR calibration and generation of the continent scale mosaic products for Kyoto and Carbon Project, Proceedings of SPIE - The International Society for Optical Engineering, Vol.7106
- Tadono, T., Shimada, M., Takaku, J., Kawamoto, S., Updated results of calibration and validation of ALOS optical instruments, Proceedings of SPIE - The International Society for Optical Engineering, Vol.7106
- Shiomi, K., Kawakami, S., Kina, Y., Mitomi, Y., Yoshida, M., Sekio, N., Kataoka, F., Higuchi, R., GOSAT level 1 processing and in-orbit calibration plan, Proceedings of SPIE - The International Society for Optical Engineering, Vol.7106
- Misako Kachi; Keiji Imaoka; Hideyuki Fujii; Akira Shibata; Marehito Kasahara; Yukie Iida; Norimasa Ito; Keizo Nakagawa; Haruhisa Shimoda, Status of GCOM-W1/AMSR2 development and science activities, Proceedings of SPIE - The International Society for Optical Engineering, Vol.7106
- Misako Kachi; Shuji Shimizu; Naofumi Yoshida; Takuji Kubota; Riko Oki; Toshio Iguchi, Development of the DPR algorithms and products for GPM, Proceedings of SPIE - The International Society for Optical Engineering, Vol.7106
- Yoshihiko Okamura; Kazuhiro Tanaka; T. Amano; M. Hiramatsu; K. Shiratama, Breadboarding activities of the Second-generation Global Imager (SGLI) on GCOM-C, Proceedings of SPIE - The International Society for Optical Engineering, Vol.7106
- Murakami, H., Frouin, R., Correction of sea surface reflection in the coastal area, Proceedings of SPIE - The International Society for Optical Engineering, Vol.7150

- Miyamoto Yukihiro , Yamawaki Masakatsu , Tsuchiya Mitsuhiro , Nakanishi Isao, ALOS Mission Operation Status and Ground Data Processing, Technical report of IEICE. SANE 電子情報通信学会技術研究報告. SANE, 宇宙・航行エレクトロニクス 108(318) pp.75-77, 2008 The Institute of Electronics, Information and Communication Engineers
- Shimoda, H., Global Change Observation Mission (GCOM), Proceedings of SPIE - The International Society for Optical Engineering, Vol.7151
- Shimada, M., PALSAR SCANSAR SCANSAR Interferometry, Proceedings of ALOS PI 2008 SYMPOSIUM, ESA SP-664 (European Space Agency, Special Publication)
- Takaku, J., Tadono, T., Prism geometric cal/val and DSM performance, Proceedings of ALOS PI 2008 SYMPOSIUM, ESA SP-664 (European Space Agency, Special Publication)
- Tadono, T., Shimada, M., Iwata, T., Takaku, J., Kawamoto, S., Accuracy Assessment of ALOS Optical Instruments: PRISM and AVNIR-2, Proceedings of ISCO 2008, International Conference on Space Optics, Toulouse, France, 14-17 October, 2008
- Tadono, T., Shimada, M., Fujii, H., Kaihotsu, I., Estimation and Validation of Soil Moisture Using PALSAR Onboard ALOS over Mongolian Plateau, PIERS Proceedings, 253 - 256, July 2-6, Cambridge, USA, 2008

### 6.5.3 Oral Presentations

#### 6.5.3.1 Open Conferences

- Kachi, M. , Kubota, T. , Oki, R., Ushio, T. , Okamoto, K. , Near-real-time global precipitation map using multi-satellite data, European Geosciences Union General Assembly 2008 Vienna, Austria, 13-18 April 2008
- Maeda, T., Takano, T., Detection of the earthquake-origin microwave emission in the passive sensor data of a remotesensing satellite, European Geosciences Union General Assembly 2008 Vienna, Austria, 13-18 April 2008
- Shiomi, K., Kawakami, S., Kina, T., Mitomi, Y., Yoshida, M., Sekio, N., Kataoka, F., Higuchi, R., Calibration processing of GOSAT TANSO, European Geosciences Union General Assembly 2008 Vienna, Austria, 13-18 April 2008
- Tsuchiya, M., Fujisawa, T., Miura, S., ALOS Mission Operation 2008 in JAXA, SpaceOps 2008 Conference, Heidelberg, Germany, 12-16 May 2008
- Shige, S., Yamamoto, T., Kida, S., Tsukiyama, T., Kubota, T., Okamoto, K., On the use of microwave sounder data for high-temporal rainfall maps based on microwave radiometers, 2008 Microwave Radiometry and Remote Sensing of the Environment - 10th Specialist Meeting, 11-14 March 2008
- Okada, K., Kojima, M., Iida, Y., Kimura, T., Horie, H., Kankaku, Y., Kumagai, H., Sato, K., Okumura, M., Development of a W-band Antenna for Space-borne 94GHz Doppler Radar, 26th International Symposium on Space Technology and Science (ISTS), Hamamatsu, Japan, 1-6 June 2008
- Katayama, H., Okamura, Y., Tange, Y., Nakau, K., Design and Concept of The Compact Infrared Camera (CIRC) with Uncooled Infrared Detector, 26th International Symposium on Space Technology and Science (ISTS), Hamamatsu, Japan, 1-6 June 2008

- Shiomi, K., Suto, H., Kawakami, S., Kuze, A., Nakajima, M., TANSO On-Orbit and Vicarious Calibration Plan, 26th International Symposium on Space Technology and Science (ISTS), Hamamatsu, Japan, 1-6 June 2008
- Tadono, T., Shimada, M., ALOS satellite imagery utilization for Global Mapping project, Global Mapping Forum 2008, Tokyo, Japan, 5-7 June 2008
- Kachi, M., Imaoka, K., Future plans of JAXA for GHRSSST-PP, The 9th meeting of the GODAE High Resolution Sea Surface Temperature Pilot Project, Perros-Guirec, France, 9-13 June 2008
- Shiomi, K., Kawakami, S., Onboard and vicarious calibration of GOSAT, 5<sup>th</sup> International Workshop on Greenhouse Gas Measurements from Space (IWGGMS-5), Pasadena, California, USA, 24-26 June 2008
- Kubota, T., Kachi, M., Shimizu, S., Oki, R., Aonashi, K., Precipitation monitoring of Cyclone Nargis using TRMM Precipitation Radar data and near-real-time satellite-based rainfall estimates (GSMaP) by Japan Aerospace Exploration Agency, International Geoscience and Remote Sensing Symposium (IGARSS), Boston, Massachusetts, USA, 7-11 July 2008
- Maeda, T., Takano, T., ANALYSIS TECHNIQUE FOR EXTRACTION OF LOCAL AND FAINT CHANGES FROM A SATELLITE-BORNE MICROWAVE RADIOMETER DATA, International Geoscience and Remote Sensing Symposium (IGARSS), Boston, Massachusetts, USA, 7-11 July 2008
- Okamura, Y., Tanaka, K., Amano, T., Hiramatsu, M., Shiratama, K., Breadboarding activities of the Second-generation Global Imager (SGLI) on GCOM-C, SPIE Europe Remote Sensing 2008, Cardiff, Wales, United Kingdom, 15-18 September 2008
- Kubota, T., Ushio, T., Shige, S., Kida, S., Kachi, M., Okamoto, K., GSMaP validation activities of high resolution satellite-based precipitation products around Japan, 4th IPWG Workshop on Precipitation Measurements, Beijing, China, 13-17 October, 2008
- Miyagi, Y., Shimada, M., Tadono, T., Isoguchi, O., Ohki, M., ALOS emergency observations by JAXA for monitoring earthquakes and volcanic eruptions in 2008, Use of Remote Sensing Techniques for Monitoring Volcanoes and Seismogenic Areas, 2008. USEReST 2008. Second Workshop on, 11-14 Nov. 2008
- Dim, J. R., Murakami, H., Hori, M., Use of ADEOS-II/GLI Radiometric and Geometric Characteristics for the Simulation of Moisture Variations in the Upper Troposphere, AGU Fall Meeting 2008, San Francisco, California, USA, 15-19 December 2008
- Shiomi, K., Kawakami, S., Kina, T., Sakaizawa, D., Mukai, M., GOSAT On-orbit and Vicarious Calibration Plan, AGU Fall Meeting 2008, San Francisco, California, USA, 15-19 December 2008
- Maeda, T., Takano, T., Detection of Land-surface Deformations Associated with Earthquakes from a Satellite-borne Microwave Radiometer Data, AGU Fall Meeting 2008, San Francisco, California, USA, 15-19 December 2008

### 6.5.3.2 EORC International Workshops

- Oki, R., TRMM and GPM research activities in Japan, The Third NASA/JAXA International TRMM Science Conference, Las Vegas, Nevada, February 4-8, 2008

- Kachi, M., Near-real-time System of Global Precipitation Map from Satellite Data, The Third NASA/JAXA International TRMM Science Conference, Las Vegas, Nevada, February 4-8, 2008
- Shimizu, S., JAXA Ground Validation Plan in Asia, The Second Global Precipitation Measurement (GPM) Asia Workshop, Hamamatsu, Japan, 2 June 2008
- Tadono, T., Updated results of calibration and validation of PRISM and AVNIR-2, ALOS PI Symposium 2008, Rhodes, Greece, 3-7 November 2008
- Tadono, T., Process Study for Developing Algorithms to Quantitatively Estimate Hydrological Parameters Based on ALOS Data, ALOS PI Symposium 2008, Rhodes, Greece, 3-7 November 2008
- Shimada, M., PALSAR SCANSAR-SCANSAR Interferometry, ALOS PI Symposium 2008, Rhodes, Greece, 3-7 November 2008
- Tamotsu Igarashi, GCOM Mission and Challenges for Applications Research, GCOM Symposium, Yokohama, Japan, 13 January 2009

## 6.6 Budget and Personnel

### 6.6.1 Budget

1995	3,145
1996	4,557
1997	4,438
1998	3,304
1999	3,629
2000	4,974
2001	11,789
2002	12,106
2003	10,363
2004	9,762
2005	10,273
2006	8,143
2007	8,432
2008	7,646

For fiscal years 1995 to 2008, units in million yen

### 6.6.2 Number of Personnel

	FY 1995	FY 1996	FY 1997	FY 1998	FY 1999	FY 2000	FY 2001
NASDA Workers	16	27	24	26	29	31	77
Invited Scientists	5	11	22	29	36	39	71
Post-doctorates	0	2	1	3	3	9	10
STA Fellows	0	1	1	2	2	2	2
Contract Workers	5	10	12	17	16	18	18
Total	26	51	60	77	86	99	178

	FY 2002	FY 2003	FY 2004	FY 2005	FY 2006	FY 2007	FY 2008
NASDA/JAXA Workers	57	80	78	81	82	55	73
Invited Scientists	72	14	15	15	11	20	23
Post-doctorates	11	8	7	4	5	5	4
STA Fellows	0	0	0	0	0	0	0
JSPS Postdoctoral Fellowship	0	0	0	0	0	0	1
Contract Workers	25	19	21	23	19	9	10
Total	165	121	121	123	117	89	101

Numbers at the beginning of FY

## 6.7 History of EORC

### 1995

- April 1 Earth Observation Research and Application Center (EORC) established.
- June 6 Global Observation Information Network (GOIN) conference held jointly with NASA and USA. Ms. Makiko Tanaka, Minister of the Science and Technology Agency, was invited.

### 1996

- March 5-9 First EORC Symposium
- August 14 First Earth Observation Research Committee meeting
- August 17 Advanced Earth Observation Satellite (ADEOS) was launched from Tanegashima Island.
- September 1 First image from ADEOS released.
- September 25-27 Remote Sensing Technology Fair held in Makuhari Messe.

### 1997

- January 2 Observation of spilled oil from Russian tanker that sank in the Japan Sea
- March 10-14 Second ADEOS Workshop held in Yokohama.
- June 30 ADEOS ceased functioning.
- July 3 Observation of spilled oil from Liberian tanker in Tokyo Bay
- August 21 Third Earth Observation Research Committee meeting
- October 1 Earth Frontier Research System established.
- November 28 TRMM was launched from Tanegashima Island.
- December 17 First image from TRMM released.

### 1998

- January 26-30 Third ADEOS Symposium held in Sendai.
- April 1 Dr. Toshihiro Ogawa appointed Executive Director of EORC.
- April 15-June 15 and August 31-September 15 GEWEX/GAME-Tropics Campaign in Thailand
- May 13 Joint TRMM Science Team (JSTS)
- May 14-September 30 GEWEX/GAME-Tibet Campaign
- May 20-June 1 TRMM Validation Project IMCET
- June 2 Global Rainfall Forest Mapping Project Workshop
- June 26 Fourth TRMM Science Team Meeting
- July 6 Press release on TRMM/TMI observing El Nino/La Nina sea-surface temperature
- July 6-9 Earth Observation Subcommittee organized to evaluate NASDA's Earth Observation field.
- July 10 Press release on TRMM/PR 3-D Rainfall Image of Typhoon No. 1
- September 1 TRMM data release
- September 1-2 Earth Observation Fair 1998 in Tokyo

September 9-11	Second GLI Workshop
September 21-October 10	BIBLE experiment in Darwin and Indonesia
October 12	ADEOS Research Report Symposium JERS-1 ceased to function.
November 4-6	ADEOS Research Report Workshop
November 9-12	Second AMSR Workshop
November 16-17	ADEOS PI meeting for ESCAP countries
November 16-20	JERS-1 PI/GRFM/GBFM Workshop
November 24	SeaWiFS data release
December 9-10	PALSAR, AIR SAR & INSAR Workshop
December 14-16	Symposium on the Precipitation Observation from Non-Sun Synchronous Orbit held in Nagoya.

**1999**

January 13-14	International Workshop on Earth Science Study in Asia-Pacific Region
March	International PR Team Meeting
April 2	ADEOS-II Program Meeting
May 15-June 7	TRMM Ishigaki/Miyako Islands Campaign
May 17-18	JERS-1 Symposium
June 21-23	TRMM Kyoto Symposium
July 6-8	BIBLE Workshop
September 14-15	Earth Observation Fair 1999 in Yokohama
October 4-5	Remote Sensing Training Seminar in Marine Application
October 12-14	Airborne SAR observation experiments conducted in Tsukuba, Mt. Fuji, and Tomakomai.
November 2-12	Applications of Marine Remote Sensing Training Course held in Bangkok in cooperation with IOCCG, NASA, JRC/EC, and AIT.
November 4-5	PALSAR Workshop
December 6-10	ADEOS/ADEOS-II Symposium/Workshop held in Kyoto.

**2000**

February 14-15	CEOS Disaster Management WG meeting
February 18	Earth Observation Lecturing Tour #1 held at Ino Junior High School in Kochi Prefecture.
March 11	Earth Observation Lecturing Tour #2 held at Misato Observatory in Wakayama Prefecture.
April 3	Press release on Mt. Usu's volcanic activities using Earth Observation satellite data
May 16	Press release on Mt. Usu's volcanic activities using Earth Observation satellite data
May 22-24	Sponsored ASSFTS meeting in Kyoto
June 26	Ad-hoc committee decided major specifications for next EORC Data Analysis System.
June 16-17	Fifth GAME International Science Panel meeting

June 28	GLI science leaders meeting decided policy for ocean channels saturation issue.
July 3-8	Sponsored International Ozone Symposium in Sapporo
July 9-13	Sponsored IGARSS 2000 in Hawaii
July 10	TRMM 3 <sup>rd</sup> Research Announcement issued.
July 13	ADEOS-II Joint Program Meeting
July 19	ALOS 1 <sup>st</sup> Research Announcement PIs selected.
August 2-3	Earth Observation Fair
September 14	Progress Meeting for joint Research with Fisheries Agency on Ocean Biology and Fishery Application
October 9-12	Sponsored SPIE Meeting in Sendai
October 30-November 1	AMSR/AMSR-E Workshop
November 7-10	GLI Workshop
November 13-14	NOAA-NASDA Earth Observation Joint Working Group
November 27	ATMOS-A1/GPM Meeting
November 28	Symposium Commemorating the Third Anniversary of the Launch of the TRMM Satellite
November 29-30	Joint TRMM Science Team Meeting
November 28-December 14	BIBLE Experiment in Darwin
December 1	International Symposium on Earth Observation from Space
December 13-14	Symposium on ADEOS-II data utilization in Asia and Pacific, co-organized by UN/ESCAP and NASDA EORC

## 2001

January 22	Meeting for Joint Research with Fisheries Agency on Ocean Biology and Fishery Application
January 26	TRMM 3 <sup>rd</sup> Research Announcement selected
January 29-February 2	WCRP/GEWEX Science Steering Group meeting
January 30-February 1	Participation in EOS Workshop
February 19-20	ALOS Data Node Technical Interface Meeting #1
March 27-30	ALOS Symposium/1 <sup>st</sup> PI Workshop
April 1	Merging of EORC, involving former EOSD and EOC functions
April 2-4	Host of CEOS SAR CAL/VAL meeting
June 1	First TRMM (3 <sup>rd</sup> RA) PI Meeting
June 7	ALOS Ground System Design Review
June 13	TRMM/SDPF Operation Readiness Review
July 30	Opening of new office in Harumi; moved from Roppongi
August 1	Special Lecture by Nobel Laureate Professor F. Sherwood Rowland on "Stratospheric Ozone Depletion: Theory, Measurements from Space and Ground"
August 7-24	TRMM satellite altitude boosted
August 30	Airborne SAR Observation Experiments at EOC
October 1-2	6 <sup>th</sup> GAME International Science Panel Meeting

October 3-5	5 <sup>th</sup> GAME International Study Conference on GEWEX in Asia and GAME
November 1-2	Joint TRMM Science Team Meeting
November 2	ADEOS-II Ground System Development Completion Review
November 6	Airborne SAR Observation Experiments at EOC
November 9	Global Precipitation Measurement (GPM) Symposium

**2002**

January 7-23	PEACE and Airborne OPUS Experiments at Nagoya and Kagoshima Airports
February 18-20	2 <sup>nd</sup> ALOS Data Node Technical Interface Meeting
February 27	EOS-PM1/AMSR-E Ground System Development Completion Review
March 11	EORC Head Office (former EOSD) moved and merged with EORC at Harumi
April 10-12	4 <sup>th</sup> ALOS Data Node Interagency Meeting
April 20-May 15	PEACE-B and Airborne OPUS Experiments at Nagoya Airport
May 4	AMSR-E Joint Science Team Meeting
May 5-10	CEOS Working Group on Information System and Service at ESA/ESRIN
May 13-17	Kyoto and Carbon Initiative, 2 <sup>nd</sup> Science advisory Panel Meeting
May 20-22	2 <sup>nd</sup> International Planning Workshop on GPM
June 11	Airborne SAR Observation Experiments
June 24-28	Sponsored IGARSS 2002 in Sydney
July 22-26	1 <sup>st</sup> TRMM International Science Conference
July 25	MODIS Image released
August 8-10	AMSR-E Joint Science Team Meeting
September 3-6	Pan Ocean Remote Sensing Conference 2002
October 14-15	The Kyoto and Carbon Initiative, 3 <sup>rd</sup> Science Advisory Panel Meeting
October 17	“What was found by ADEOS” Lecture
November 6	Airborne SAR Observation Experiments
November 6-7	7 <sup>th</sup> GAME International Science Panel (GISP) Meeting
November 8	MODIS data released
November 14	International Symposium Commemorating 5 <sup>th</sup> Anniversary of TRMM
November 29	Satellite Observing System for the Ecology of Marine and Fisheries Meeting
December 14	ADEOS-II was launched successfully.
December 24-25	2 <sup>nd</sup> Workshop for TRMM PI Interim Reports

**2003**

January 16-17	SAR Workshop 2003
January 18	First light image of AMSR successfully received and processed.

January 25	First light image of GLI successfully received and processed.
February 19	Workshop of Atmospheric Environment Monitoring Using Satellite
February 19-20	1 <sup>st</sup> Workshop of GPM Data Working Group
March 5-6	PEACE-B and ITCT 2002 Joint Science Team Meeting held at NOAA.
March 5-7	5 <sup>th</sup> ALOS Data Node Interagency Meeting
March 12-14	ADEOS-II AMSR Workshop 2003
May 20	ADEOS-II Routine Operation Readiness Review at Tsukuba Space Center
May 20-23	ALOS Kyoto & Carbon Initiative 4 <sup>th</sup> Science Advisory Panel Meeting
May 22-23	ADEOS-II NGN Mission Operation Meeting at Tsukuba Space Center
June 18	Release of AMSR-E Level-1 product
June 24	Operation Transfer Review of AMSR-E L1 processing system
June 24-26	3 <sup>rd</sup> GPM Workshop in Noordwijk, the Netherlands
July 21-25	ALOS special session at IGARSS 2003 in Toulouse, France
July 26-29	3 <sup>rd</sup> ALOS Data Node Technical Interface Meeting
August 24-30	16 <sup>th</sup> JAPAN Meeting-Earth Monitoring Workshop in Busan.
August 25	GPM/DPR Project Readiness Review #1
August 26-27	Polarimetric Interferometric SAR Workshop 2003 in Niigata
September 1	NASDA-CRL joint Pi-SAR AO issued.
September 14-19	Participation in CEOS Working Group on Information System and Service in Chiang Mai
September 16-19	ALOS International CAL/VAL Meeting #1
September 19	Release of AMSR-E physical parameter products
October 1	JAXA established. Institute of Space and Astronautical Science (ISAS), the National Aerospace Laboratory (NAL), and the National Space Development Agency of Japan (NASDA) merged into JAXA.
October 21-22	AMSR Science Workshop in Monterey
October 25	ADEOS-II ceased operating.
October 27-30	6 <sup>th</sup> ALOS Data Node Interagency Meeting in Sydney
November 18-21	ALOS Kyoto & Carbon Initiative 5 <sup>th</sup> Science Advisory Panel Meeting
November 25	GOSAT Project Readiness Review #1
December 7	NASDA-CRL joint Pi-SAR PIs selected.
December 11	Release of AMSR Level-1 products
December 24	Release of ADEOS-II GLI/AMSR Level-1 and physical parameter products
<b>2004</b>	
January 15	1 <sup>st</sup> PI meeting of Pi-SAR AO Program
January 19-23	ALOS 2 <sup>nd</sup> PI Meeting and Final Meeting of JERS-1 RI Program at Awaji Yumebutai Conference Center

February 2-3	GPM Asia Workshop in Tokyo
February 3-4	Water Cycle Asia Workshop in Tokyo
February 2-6	IGOS International Workshop in Tokyo
February 7-10	Pi-SAR 1 <sup>st</sup> AO observation flights
February 19-20	GPM Data Working Group Workshop
March 1-3	ADEOS-II Workshop in Tokyo
March 9-12	3 <sup>rd</sup> CEOP International Implementation Planning Meeting at UCI
March 9	Seminar on Pilot Project for ALOS Data Utilization in Bangkok
April 21	GOSAT Symposium
April 23	GEO-IV Plenary Meeting
April 25	Earth Observation Summit-II
May 17-19	7 <sup>th</sup> Interagency Meeting of the ALOS Data Node
May 17-21	3 <sup>rd</sup> ALOS Kyoto and Carbon Initiative Coordinators Meeting in Santa Barbara
June 28-30	10 <sup>th</sup> ICRS in Okinawa
July 22	EOS Direct Data Reception System Operational Phase Readiness Review
August 3	Pi-SAR 2 <sup>nd</sup> AO observation flights
August 23-24	Pi-SAR Workshop 2004
September 3	2 <sup>nd</sup> DAS/GOSAT/GPM Ground System Meeting
September 5-7	TRMM International Meeting
September 17	JAXA Symposium for Pilot Project in Indonesia
September 20-24	IGRASS 2004 in Anchorage
October 5	Satellite Remote Sensing Committee
October 7	3 <sup>rd</sup> DAS/GOSAT/GPM Ground System Meeting
October 19-22	4 <sup>th</sup> ALOS Kyoto and Carbon Initiative Coordinators Meeting
October 31-November 7	APRSAF-11
November 3-7	Pi-SAR 3 <sup>rd</sup> AO observation flight experiment
November 21-22	Training Workshop on Digital Asia at the 25 <sup>th</sup> ACRS in Chiang Mai
November 22-26	Exhibition at 25 <sup>th</sup> ACRS in Chiang Mai
December 7-10	FY16 ADEOS-II PI Workshop

**2005**

January 11	SAR Workshop 2005
January 20	Asian Workshop in Kobe
February 12-15	Pi-SAR 4 <sup>th</sup> AO observation flights
February 16	Earth Observation Summit III
February 16	Signing of International Charter on "Space and Major Disasters"
February 22	2 <sup>nd</sup> Seminar on Pilot Project for ALOS Data Utilization in Thailand
February 28-March 3	ALOS Kyoto and Carbon Initiative 6 <sup>th</sup> Advisory Panel/Science Team Meeting
February 28- March 4	CEOP/IGWCO Joint Meeting
July 25-29	IGARSS 2005, Seoul, Korea
September 12-16	Joint AMSR Science Team Meeting
October 11-13	APRSAF-12, Fukuoka, Japan

October 16-21	56 <sup>th</sup> Int. Astronautical Congress, Space Fair Exhibition, Fukuoka
October 25	Int. Arctic Research Center Seminar, Fairbanks, Alaska
November 7-9	5 <sup>th</sup> Global Precipitation Measurement (GPM) Int. Planning Workshop, Tokyo
November 7-11	ACRS 2005 26 <sup>th</sup> Asia Remote Sens. Conference, Hanoi, Vietnam
November 9	GPM Program Meeting, Tokyo
<b>2006</b>	
January 9-13	18 <sup>th</sup> GEWEX Science Steering Group Meeting, Dakar
January 23	Symposium on AMSR/GLI in Tokyo
January 24-26	AMSR Workshop in Tokyo
January 24	ALOS was launched successfully.
February 16-17	SCOSA in Hanoi, Vietnam
March 1-3	IGOS Water Theme Workshop, Paris
March 2-3	Workshop for 4 <sup>th</sup> Precipitation Measuring Mission Science PI Interim reports
March 6-10	EarthCare CPR JMAG Meeting
March 23	4 <sup>th</sup> GPM Science Team Meeting, Tokyo
May 1	Earth Observation Research and Application Center (EORC) reorganized into Earth Observation Research Center (EORC) and Satellite Applications and Promotion Center (SAPC).
May 17-29	4 <sup>th</sup> TRMM Latent Heating Workshop, Seattle
June 15	GCOM Symposium, Tokyo, Japan
June 26-29	ALOS Cal/Val & Science Team meeting
July 18	NASA-JAXA GPM Program Meeting/GPM Science Coordination Group Meeting, Tokyo
July 31-August 4	IGARSS 2006, Denver, U.S.A
July 31	IGARSS GPM special session
September 6-8	Joint AMSR-E Science Team Meeting, La Jolla, USA
September 12	SPIE GPM special session
September 26-28	Capacity Building in Asia, "Earth Observations in the service of water management," Bangkok
September 29	16 <sup>th</sup> UN/IAF Workshop on the use of space technology for water management, Spain
October 9-13	ACRS 2006 27 <sup>th</sup> Asia Remote Sens. Conference, Ulaanbaatar, Mongolia
October 12-13, 16-17	ALOS Cal/Val & Science Team Meeting #5
October 29	EORC move from Harumi to Tsukuba Space Center completed.
November 3	NASA-JAXA GPM Program Meeting, NASA HQ
November 6-8	6 <sup>th</sup> GPM International Planning Workshop, Annapolis
November 28	GPM/DPR Preliminary Design Review (Baseline Document Review)
December 4-8	APRSAF-13, Jakarta, Indonesia
December 19	GPM/DPR Preliminary Design Review

**2007**

January 16-19	Kyoto & Carbon Initiative Science Team Meeting #7
January 22-26	19 <sup>th</sup> GEWEX Science Steering Group Meeting, Hawaii
January 29	AMSR/GLI Workshop, Tsukuba, Japan
January 30	GLI PI Workshop, Tsukuba, Japan
January 30-31	AMSR PI Workshop, Tsukuba, Japan
February 1	Special lecture on TRMM data handling/training in Asia Mini-project participants, AIT
February 16	5 <sup>th</sup> Precipitation Measuring Mission Science Research Announcement issued.
February 19-20	7th International Conference on Global Change: Connection to the Arctic (GCCA-7), Fairbanks, Alaska
March 2	Release of Precipitation Measuring Mission (PMM) Science 5 <sup>th</sup> Research Announcement
March 5-6	Workshop for 4 <sup>th</sup> Precipitation Measuring Mission Science PI final reports
March 6-7	SAR Workshop 2007
March 17	Symposium on Alaskan Wild Fire and Global Change, Tokyo, Japan
March 20	5 <sup>th</sup> GPM Science Team Meeting, Tokyo, Japan
August 16	Precipitation Measuring Mission (PMM) Science Team 1 <sup>st</sup> meeting
December 2-4	The 3 <sup>rd</sup> Asian Water Cycle Symposium
December 5-7	The 7 <sup>th</sup> GPM International Planning Workshop, Tokyo, Japan
December 8	“Rain in a Changing Earth” Symposium of 10-year Anniversary of TRMM, Tokyo, Japan

**2008**

January 18	Release of GPM 1 <sup>st</sup> Research Announcement
January 21	ALOS Kyoto & Carbon Initiative 9 <sup>th</sup> Science Team meeting, Tokyo, Japan
January 22-24	AMSR/GLI PI Workshop 2008, Atami, Japan
February 4-8	The 3 <sup>rd</sup> NASA/JAXA International TRMM Science Conference, Las Vegas, Nevada, USA
April 7	Release of GOSAT Research Announcement
June 2	The Second Global Precipitation Measurement (GPM) Asia Workshop, Hamamatsu, Japan
June 23	ALOS Kyoto & Carbon Initiative 10 <sup>th</sup> Science Team meeting, Tokyo, Japan
July 5-7	Symposium Sentinel Earth, Detection of Environmental Change, Sapporo, Japan
October 15	'IBUKI' chosen as nickname of GOSAT
November 3-7	ALOS PI Symposium 2008, Rhodes, Greece
December 9-12	The 15 <sup>th</sup> Session of the Asia-Pacific Regional Space Agency Forum (APRSF-15), Hanoi & Ha Long Bay, Vietnam

**2009**

- January 7 Release of GCOM 2<sup>nd</sup> Research Announcement (GCOM-C1 1<sup>st</sup> RA)
- January 13 Global Change Observation Mission (GCOM) Symposium 2009, Yokohama, Japan
- January 13 ALOS Kyoto & Carbon Initiative Final Science Team meeting - Phase 1, Tsukuba, Japan
- January 23 GOSAT was launched successfully.

## 6.8 Acronyms and Abbreviations

### (1) Institutes & Organizations

AIST	National Institute of Advanced Industrial Science and Technology (Japan)
ASF	Alaska Satellite Facility
CEOS	Committee of Earth Observation Satellites (International)
CNES	Centre National d'Etudes Spatiales (France)
ECMWF	European Center for Medium-Range Weather Forecast
EOC	Earth Observation Center (JAXA/EORC, Japan)
EORC	Earth Observation Research Center (JAXA, Japan)
ERSDAC	Earth Remote Sensing Data Analysis Center (Japan)
ESA	European Space Agency
ESRIN	European Space Research Institute
GA	Geoscience Australia
GEO	Group on Earth Observation
GISTDA	Geo-Informatics and Space Technology Development Agency (Thailand)
GPCC	WMO's Global Precipitation Climatology Center (International, in Germany)
GSFC	Goddard Space Flight Center (NASA, USA)
GSI	Geographical Survey Institute (Japan)
GSJ	Geological Survey of Japan (AIST, Japan)
HEEIC	Hiroshima Earth Environmental Information Center (Hiroshima, Japan)
IARC	International Arctic Research Center (at University of Alaska Fairbanks , USA)
INPA	Brazilian National Institute of the Amazon
IGOS	Integrated Global Observing Strategy
INPE	Brazilian National Institute for Space Research
IOCCG	International Ocean Color Coordinating Group (International)
JAFIC	Japan Fisheries Information Service Center
JAMSTEC	Japan Marine Science and Technology Center
JAROS	Japan Resources Observation System Organization
JAXA	Japan Aerospace Exploration Agency
JCG	Japan Coast Guard
JHD	Hydrographic Department of Japan
JICA	Japan International Cooperation Agency
JMA	Japan Meteorological Agency
JPL	Jet Propulsion Laboratory (NASA, USA)
JRC	Joint Research Center of European Commission
JWA	Japan Weather Association
LAPAN	National Institute of Aeronautics and Space of Indonesia
LIPAP	Lanzhou Institute of Plateau Atmospheric Physics (China)
MAFF	Ministry of Agriculture, Forestry and Fisheries (Japan)
METI	Ministry of Economy, Trade and Industry (Japan)
MEXT	Ministry of Education, Culture, Sports, Science and Technology (Japan)

MOE	Ministry of Environment (Japan)
MRI	Meteorological Research Institute (JMA, Japan)
MSFC	Marshall Space Flight Center (NASA, USA)
MWR	Ministry of Water Resources (India)
NASA	National Aeronautics and Space Administration (NASA, USA)
NASDA	National Space Development Agency of Japan
NCEP	National Center for Environmental Prediction (NOAA/NWS, USA)
NIAES	National Institute of Agro-Environmental Sciences (Japan)
NICT	National Institute of Information and Communications Technology (Japan)
NIED	National Research Institute for Earth Science and Disaster Prevention (Japan)
NIES	National Institute for Environmental Studies (Japan)
NOAA	National Oceanic and Atmospheric Administration (DOC, USA)
NWS	National Weather Service (NOAA, USA)
PWRI	Public Works Research Institute (Japan)
RAL	Rutherford Appleton Laboratory (UK)
RESTEC	Remote Sensing Technology Center (Japan)
SAC	Space Activity Commission (Japan)
SAPC	Satellite Applications and Promotion Center (JAXA, Japan)
SSC	Swedish Space Corporation
TKSC	Tsukuba Space Center (JAXA, Japan)
TMD	Meteorological Department of Thailand
UCSB	University of California, Santa Barbara (USA)
UKMO	UK Met Office
WMO	UN's World Meteorological Organization (International, in Switzerland)

**(2) Projects**

CEOP	Coordinated Enhanced Observing Period
GAME	GEWEX Asian Monsoon Experiment
GBFM	Global Boreal Forest Mapping Project
GCMAPS	Global Carbon Cycle and Related Mapping based on Satellite Imagery Program
GEWEX	Global Energy and Water Cycle Experiment
GOIN	Global Observing Information Network
GFM	Global Rain Forest Mapping Project
PEACE	Pacific Exploration of Asian Continental Emission
SPF	Stratospheric Platform
WCRP	World Climate Research Program
WOCE	World Ocean Circulation Experiment

**(3) Satellites and spacecraft**

ADEOS	Advanced Earth-Observing Satellite (“Midori”, Japan)
ADEOS-II	Advanced Earth-Observing Satellite-II (“Midori-2”, Japan)
ALOS	Advanced Land-Observing Satellite (“Daichi”, Japan)
Aqua	Earth-Observing System PM-1 (USA)
DMSP	Defense Meteorological Satellite Program (USA)
DRTS	Data Relay Test Satellite (“Kodama”, Japan)
ENVISAT	Environment Satellite (Europe)
ERS-1,2	ESA Remote Sensing Satellite-1, 2
GCOM	Global Change Observation Mission
GOSAT	Greenhouse Gasses Observing Satellite (“Ibuki”, Japan)
GPM	Global Precipitation Measurement
GOES	Geostationary Operational Environmental Satellite (USA)
ISS	International Space Station
JEM	Japanese Experiment Module (in ISS, “Kibo”)
JERS-1	Japanese Earth Resources Satellite-1 (Fuyo-1)
LANDSAT	Land Remote Sensing Satellite (USA)
MOS	Marine Observation Satellite
NOAA	National Oceanic and Atmospheric Administration (USA)
SPOT	Satellite Pour d’Observation de la Terre (France)
Terra	Earth Observing System AM-1 (USA)
TRMM	Tropical Rainfall Measuring Mission (USA)

**(4) Instruments**

AMSR	Advanced Microwave Scanning Radiometer ( in ADEOS-II)
AMSR-E	Advanced Microwave Scanning Radiometer for EOS (in Aqua)
AVHRR	Advanced Very-High-Resolution Radiometer (NOAA)
AVNIR	Advanced Visible and Near-Infrared Radiometer (in ADEOS)
AVNIR-2	Advanced Visible and Near-Infrared Radiometer-2 (in ALOS)
CERES	Clouds and the Earth’s Radiant Energy System (in EO-1, TRMM, Terra, Aqua)
DPR	Dual-frequency Precipitation Radar (in GPM)
GLI	Global Imager (in ADEOS-II)
GMI	GPM Microwave Imager (in GPM)
ILAS	Improved Limb Atmospheric Spectrometer (in ADEOS)
ILAS-II	Improved Limb Atmospheric Spectrometer-II (in ADEOS-II)
IMG	Interferometric Monitor for Greenhouse gases (in ADEOS)
LIS	Lightning Imaging Sensor (in TRMM)
MODIS	Moderate-Resolution Imaging Spectroradiometer (in Terra, Aqua)
MSS	Multi-Spectral Scanner (in LANDSAT)
OCTS	Ocean Color and Temperature Scanner (in ADEOS)
OPS	Optical Sensor (in JERS-1)
PALSAR	Phased-Array L-band Synthetic-Aperture Radar (in ALOS)

Pi-SAR	Polarimetric Interferometric Synthetic-Aperture Radar
POLDER	Polarization and Directionality of the Earth's Reflectances (in ADEOS-II)
PR	Precipitation Radar (in TRMM)
SAR	Synthetic-Aperture Radar (in JERS-1 etc.)
SeaWiFS	Sea-viewing Wide Field-of-view Sensor (in Orb View-2, SeaStar)
SMMR	Scanning Multispectral Microwave Radiometer (in Nimbus-7)
SMILES	Superconducting Submillimeter-wave Limb Emission Sounder (in ISS/JEM)
SSM/I	Special Sensor Microwave/Imager (in DMSP)
SWIR	Short-Wave Infrared Radiometer (in JERS-1/OPS)
TMI	TRMM Microwave Imager (in TRMM)
VIRS	Visible Infrared Scanner (in TRMM)
VNIR	Visible and Near-Infrared Radiometer (JERS-1/OPS)

**(5) Computers and information**

DCW	Digital Chart of the World
DEM	Digital Elevation Model
DSM	Digital Surface Model
DTM	Digital Terrain Model
EOIS	Earth-Observation Information System
EOSDIS	Earth-Observation Satellite Data Information System
GIS	Geographic Information System
GMT	Generic Mapping Tool
HDF	Hierarchical Data Format
ISS	Information-Service System

**(6) Conferences and Meetings**

APRSAF	Asia-Pacific Regional Space Agency Forum
IAGA	International Association of Geomagnetism and Aeronomy
IGARSS	International Geosciences And Remote Sensing Symposium
JPTM	Joint Project Team Meeting (of Sentinel Asia)
PIERS	Progress In Electromagnetics Research Symposium
SPIE	International Society for Photo-optical Instrumentation Engineers

**(7) Others**

DAS	Data-Analysis System
DCS	Data-Collection System
DT	Direct Transmission (system)
GCM	General Circulation Model
GCP	Ground Control Point
MDR	Mission Data Recorder
MOU	Memorandum of Understanding
RA	Research Announcement
SST	Sea-Surface Temperature

# ***Earth Observation Research Center (EORC)***



Tsukuba Space Center  
2-1-1 Sengen, Tsukuba-shi, Ibaraki, 305-8505 Japan  
Tel. +81-50-3362-3064 Fax. +81-29-868-5987